Density Model for Spinner Dolphin (*Stenella longirostris*) for the U.S. East Coast: Supplementary Report

Model Version 2.1

Duke University Marine Geospatial Ecology Laboratory*

2023-05-27

Citation

When citing our methodology or results generally, please cite Roberts et al. (2016, 2023). The complete references appear at the end of this document. We are preparing a new article for a peer-reviewed journal that will eventually replace those. Until that is published, those are the best general citations.

When citing this model specifically, please use this reference:

Roberts JJ, Yack TM, Cañadas A, Fujioka E, Halpin PN, Barco SG, Boisseau O, Chavez-Rosales S, Cole TVN, Cotter MP, Cummings EW, Davis GE, DiGiovanni Jr. RA, Garrison LP, Gowan TA, Jackson KA, Kenney RD, Khan CB, Lockhart GG, Lomac-MacNair KS, McAlarney RJ, McLellan WA, Mullin KD, Nowacek DP, O'Brien O, Pabst DA, Palka DL, Quintana-Rizzo E, Redfern JV, Rickard ME, White M, Whitt AD, Zoidis AM (2022) Density Model for Spinner Dolphin (*Stenella longirostris*) for the U.S. East Coast, Version 2.1, 2023-05-27, and Supplementary Report. Marine Geospatial Ecology Laboratory, Duke University, Durham, North Carolina.

Copyright and License

Model Version History

Version	Date	Description
1	2015-01-31	Initial version.
1.1	2015-05-14	Updated calculation of CVs. Switched density rasters to logarithmic breaks. No changes to the model. Model files released as supplementary information to Roberts et al. (2016).

*For questions or to offer feedback please contact Jason Roberts (jason.roberts@duke.edu) and Tina Yack (tina.yack@duke.edu)

(continued)

Version	Date	Description
2	2022-06-20	This model is a major update over the prior version, with substantial additional data, improved statistical methods, and an increased spatial resolution. It was released as part of the final delivery of the U.S. Navy Marine Species Density Database (NMSDD) for the Atlantic Fleet Testing and Training (AFTT) Phase IV Environmental Impact Statement. Several new collaborators joined and contributed survey data: New York State Department of Environmental Conservation, TetraTech, HDR, and Marine Conservation Research. We incorporated additional surveys from all continuing and new collaborators through the end of 2020. (Because some environmental covariates were only available through 2019, certain models only extend through 2019.) We increased the spatial resolution to 5 km and, at NOAA's request, we extended the model further inshore from New York through Maine. We reformulated and refitted all detection functions and spatial models. We updated all enviromental covariates to newer products, when available, and added several covariates to the set of candidates. For models that incorporated dynamic covariates, we estimated model uncertainty using a new method that accounts for both model parameter error and temporal variability.
2.1	2023-05-27	Completed the supplementary report documenting the details of this model. Corrected the 5 and 95 percent rasters so that they contain the value 0 where the taxon was asssumed absent, rather than NoData. Nothing else was changed.

1 Survey Data

We built this model from data collected between 1998-2020 (Table 1, Figure 1). We excluded surveys that did not target small cetaceans or were otherwise problematic for modeling them. To maintain consistency with the other models developed during the 2022 modeling cycle, most of which excluded data prior to 1998 in order to utilize biological covariates derived from satellite ocean color observations, we also excluded data prior to 1998 from this model. We restricted the model to aerial survey transects with sea states of Beaufort 4 or less (for a few surveys we used Beaufort 3 or less) and shipboard transects with Beaufort 5 or less (for a few we used Beaufort 4 or less). We also excluded transects with poor weather or visibility for surveys that reported those conditions.

Table 1: Survey effort and observations considered for this model. Effort is tallied as the cumulative length of on-effort transects. Observations are the number of groups and individuals encountered while on effort. Off effort observations and those lacking an estimate of group size or distance to the group were excluded.

			Effort	Observations		
Institution	Program	Period	1000s km	Groups	Individuals	Mean Group Size
Aerial Surveys						
HDR	Navy Norfolk Canyon	2018-2019	10	0	0	
NEFSC	AMAPPS	2010-2019	83	0	0	
NEFSC	NARWSS	2003-2016	380	0	0	
NEFSC	Pre-AMAPPS	1999-2008	45	0	0	
SEFSC	AMAPPS	2010-2020	112	0	0	
SEFSC	MATS	2002-2005	27	0	0	
UNCW	MidA Bottlenose	2002-2002	15	0	0	
UNCW	Navy Cape Hatteras	2011-2017	34	1	70	70.0
UNCW	Navy Jacksonville	2009-2017	92	0	0	
UNCW	Navy Norfolk Canyon	2015-2017	14	0	0	
UNCW	Navy Onslow Bay	2007-2011	49	0	0	
UNCW	SEUS NARW EWS	2005-2008	106	0	0	
VAMSC	MD DNR WEA	2013-2015	15	0	0	
VAMSC	Navy VACAPES	2016-2017	18	0	0	
VAMSC	VA CZM WEA	2012-2015	19	0	0	
		Total	**1,020**	**1**	**70**	**70.0**
Shipboard Surveys						
MCR	SOTW Visual	2012-2019	9	0	0	
NEFSC	AMAPPS	2011-2016	15	0	0	
NEFSC	Pre-AMAPPS	1998-2007	13	1	6	6.0
NJDEP	NJEBS	2008-2009	14	0	0	
SEFSC	AMAPPS	2011-2016	16	1	169	169.0
SEFSC	Pre-AMAPPS	1998-2006	30	2	195	97.5
		Total	**96**	**4**	**370**	**92.5**
		Grand Total	**1,115**	**5**	**440**	**88.0**

Table 2: Institutions that contributed surveys used in this model.

Institution	Full Name
HDR	HDR, Inc.
MCR	Marine Conservation Research
NEFSC	NOAA Northeast Fisheries Science Center
NJDEP	New Jersey Department of Environmental Protection
SEFSC	NOAA Southeast Fisheries Science Center
UNCW	University of North Carolina Wilmington
VAMSC	Virginia Aquarium & Marine Science Center

Table 3: Descriptions and references for survey programs used in this model.

Program	Description	References
AMAPPS	Atlantic Marine Assessment Program for Protected Species	Palka et al. (2017), Palka et al. (2021)
MATS	Mid-Atlantic Tursiops Surveys	
MD DNR WEA	Aerial Surveys of the Maryland Wind Energy Area	Barco et al. (2015)
MidA Bottlenose	Mid-Atlantic Onshore/Offshore Bottlenose Dolphin Surveys	Torres et al. (2005)
NARWSS	North Atlantic Right Whale Sighting Surveys	Cole et al. (2007)
Navy Cape Hatteras	Aerial Surveys of the Navy's Cape Hatteras Study Area	McLellan et al. (2018)
Navy Jacksonville	Aerial Surveys of the Navy's Jacksonville Study Area	Foley et al. (2019)
Navy Norfolk Canyon	Aerial Surveys of the Navy's Norfolk Canyon Study Area	Cotter (2019), McAlarney et al. (2018)
Navy Onslow Bay	Aerial Surveys of the Navy's Onslow Bay Study Area	Read et al. (2014)
Navy VACAPES	Aerial Survey Baseline Monitoring in the Continental Shelf Region of the VACAPES OPAREA	Mallette et al. (2017)
NJEBS	New Jersey Ecological Baseline Study	Geo-Marine, Inc. (2010), Whitt et al. (2015)
Pre-AMAPPS	Pre-AMAPPS Marine Mammal Abundance Surveys	Mullin and Fulling (2003), Garrison et al. (2010), Palka (2006)
SEUS NARW EWS	Southeast U.S. Right Whale Early Warning System Surveys	
SOTW Visual	R/V Song of the Whale Visual Surveys	Ryan et al. (2013)
VA CZM WEA	Virginia CZM Wind Energy Area Surveys	Mallette et al. (2014), Mallette et al. (2015)

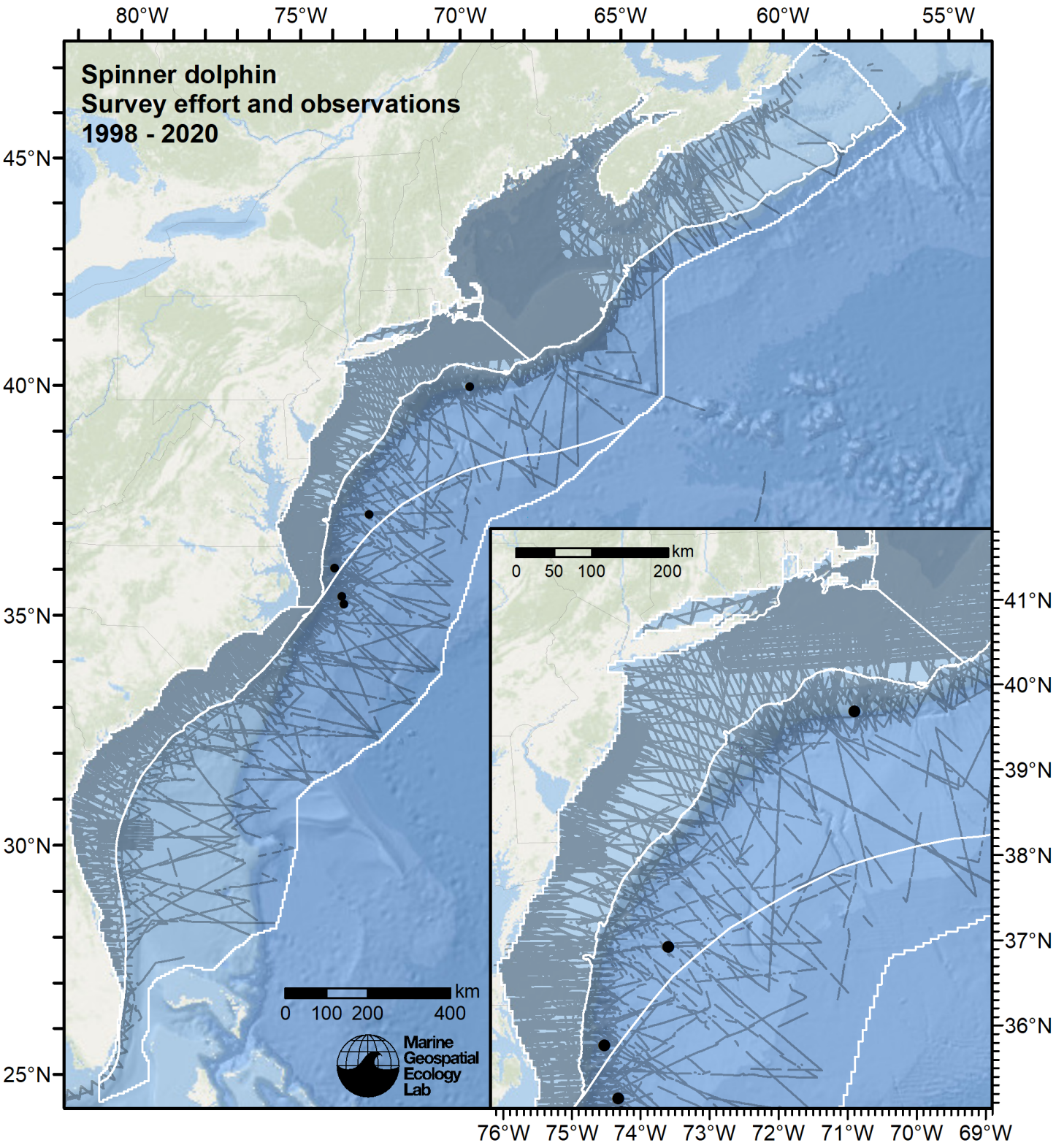

Figure 1: Survey effort and spinner dolphin observations available for density modeling, after detection functions were applied, and excluded segments and truncated observations were removed. White outlines show the strata for which density estimates were derived.

2 Detection Functions

2.1 With a Taxonomic Covariate

We fitted the detection functions in this section to pools of species with similar detectability characteristics and used the taxonomic identification as a covariate (ScientificName) to account for differences between them. We consulted the literature and observer teams to determine appropriate poolings. We usually employed this approach to boost the counts of observations in the detection functions, which increased the chance that other covariates such as Beaufort sea state could be used to account for differences in observing conditions. When defining the taxonomic covariate, we sometimes had too few observations of species to allocate each of them their own level of the covariate and had to group them together, again consulting the literature and observers for advice on species similarity. Also, when species were observed frequently enough to be allocated their own levels but statistical tests indicated no significant difference between the levels, we usually grouped them together into a single level.

2.1.1 Aerial Surveys

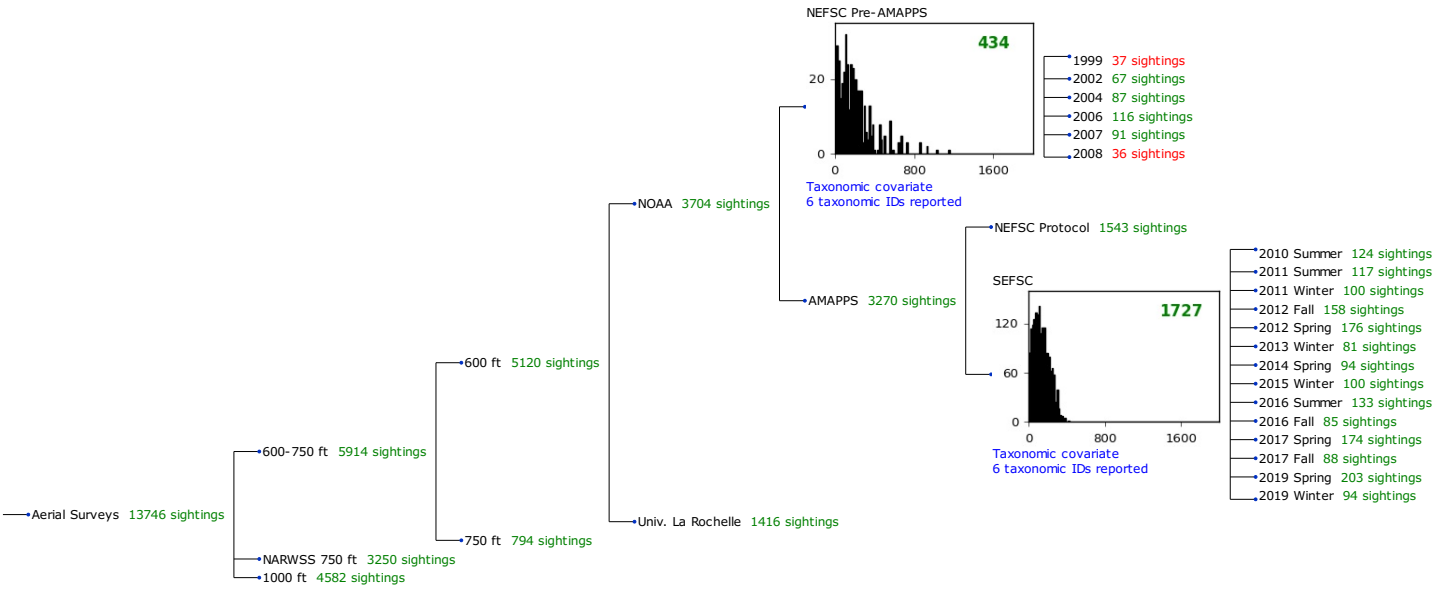

Figure 2: Detection hierarchy for aerial surveys, showing how they were pooled during detectability modeling, for detection functions that pooled multiple taxa and used used a taxonomic covariate to account for differences between them. Each histogram represents a detection function and summarizes the perpendicular distances of observations that were pooled to fit it, prior to truncation. Observation counts, also prior to truncation, are shown in green when they met the recommendation of Buckland et al. (2001) that detection functions utilize at least 60 sightings, and red otherwise. For rare taxa, it was not always possible to meet this recommendation, yielding higher statistical uncertainty. During the spatial modeling stage of the analysis, effective strip widths were computed for each survey using the closest detection function above it in the hierarchy (i.e. moving from right to left in the figure). Surveys that do not have a detection function above them in this figure were either addressed by a detection function presented in a different section of this report, or were omitted from the analysis.

2.1.1.1 NEFSC Pre-AMAPPS

After right-truncating observations greater than 600 m, we fitted the detection function to the 413 observations that remained (Table 4). The selected detection function (Figure 3) used a hazard rate key function with Beaufort (Figure 4) and ScientificName (Figure 5) as covariates.

Table 4: Observations used to fit the NEFSC Pre-AMAPPS detection function.

ScientificName	n
Delphinus, Lagenodelphis, Stenella	239
Lagenorhynchus	128
Tursiops, Steno	46
Total	**413**

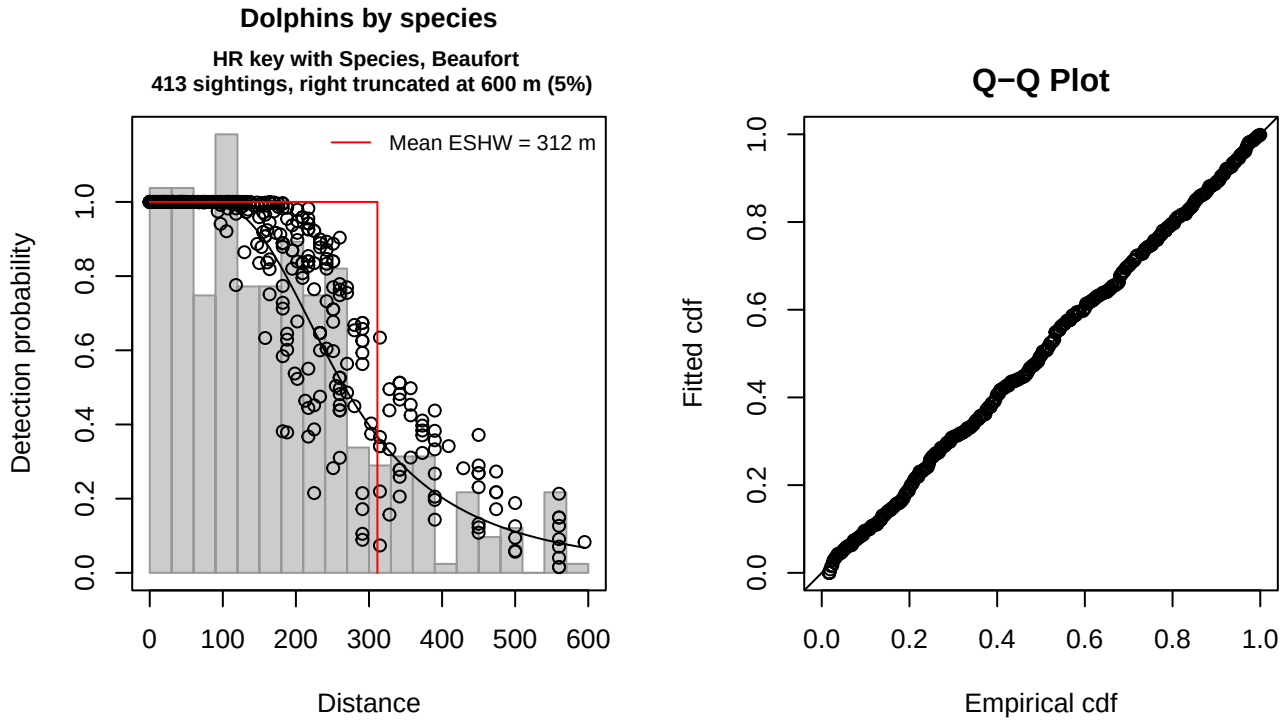

Figure 3: NEFSC Pre-AMAPPS detection function and Q-Q plot showing its goodness of fit.

Statistical output for this detection function:

```
Summary for ds object
Number of observations :  413
Distance range         :  0  -  600
AIC                    :  5043.994

Detection function:
 Hazard-rate key function

Detection function parameters
Scale coefficient(s):
                                estimate         se
(Intercept)                    5.3188665 0.15126469
ScientificNameLagenorhynchus  -0.1872175 0.11165678
ScientificNameTursiops, Steno -0.5457529 0.14785313
Beaufort                       0.1451869 0.05844944

Shape coefficient(s):
            estimate        se
(Intercept) 1.107015 0.1176733

                     Estimate          SE         CV
```

```
Average p             0.4982478  0.02373666 0.04764026
N in covered region 828.9047438 49.28440455 0.05945726

Distance sampling Cramer-von Mises test (unweighted)
Test statistic = 0.023324  p = 0.992716
```

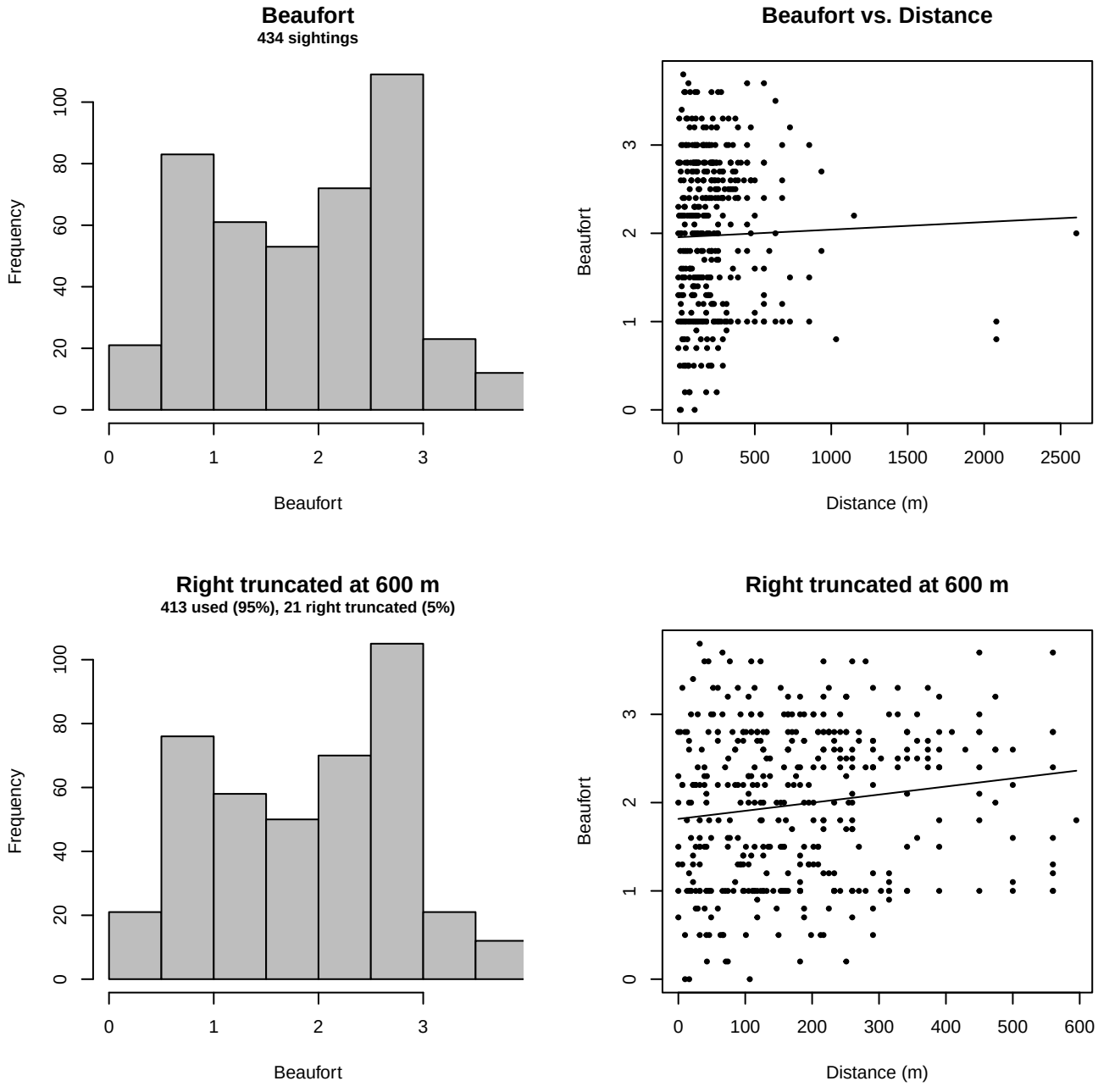

Figure 4: Distribution of the Beaufort covariate before (top row) and after (bottom row) observations were truncated to fit the NEFSC Pre-AMAPPS detection function.

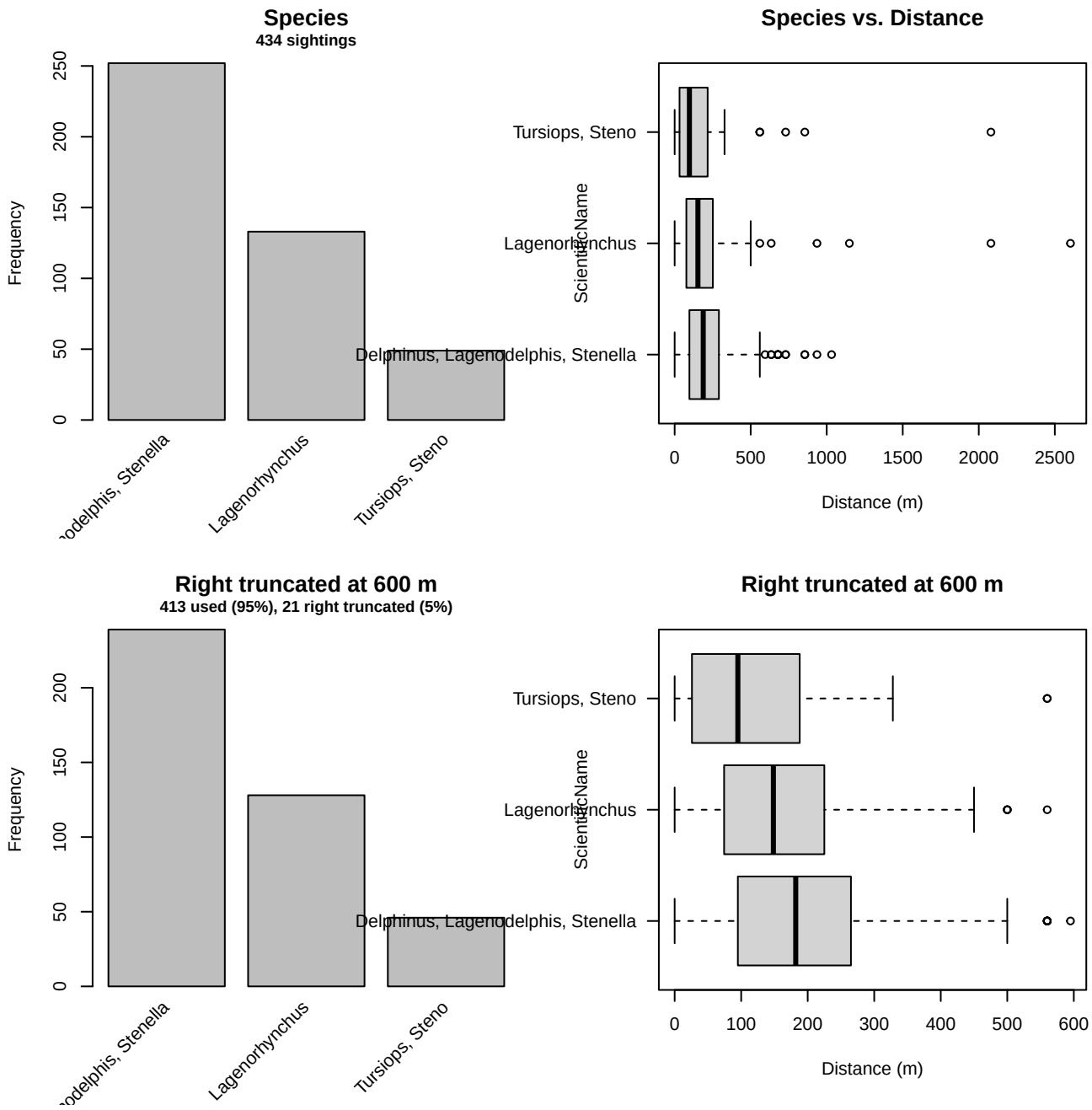

Figure 5: Distribution of the ScientificName covariate before (top row) and after (bottom row) observations were truncated to fit the NEFSC Pre-AMAPPS detection function.

2.1.1.2 SEFSC AMAPPS

After right-truncating observations greater than 325 m and left-truncating observations less than 15 m (Figure 7), we fitted the detection function to the 1628 observations that remained (Table 5). The selected detection function (Figure 6) used a hazard rate key function with Beaufort (Figure 8), ScientificName (Figure 9) and Season (Figure 10) as covariates.

Table 5: Observations used to fit the SEFSC AMAPPS detection function.

ScientificName	n
Delphinus, Tursiops, Lagenorhynchus, Steno	1422
Stenella, Lagenodelphis	206
Total	**1628**

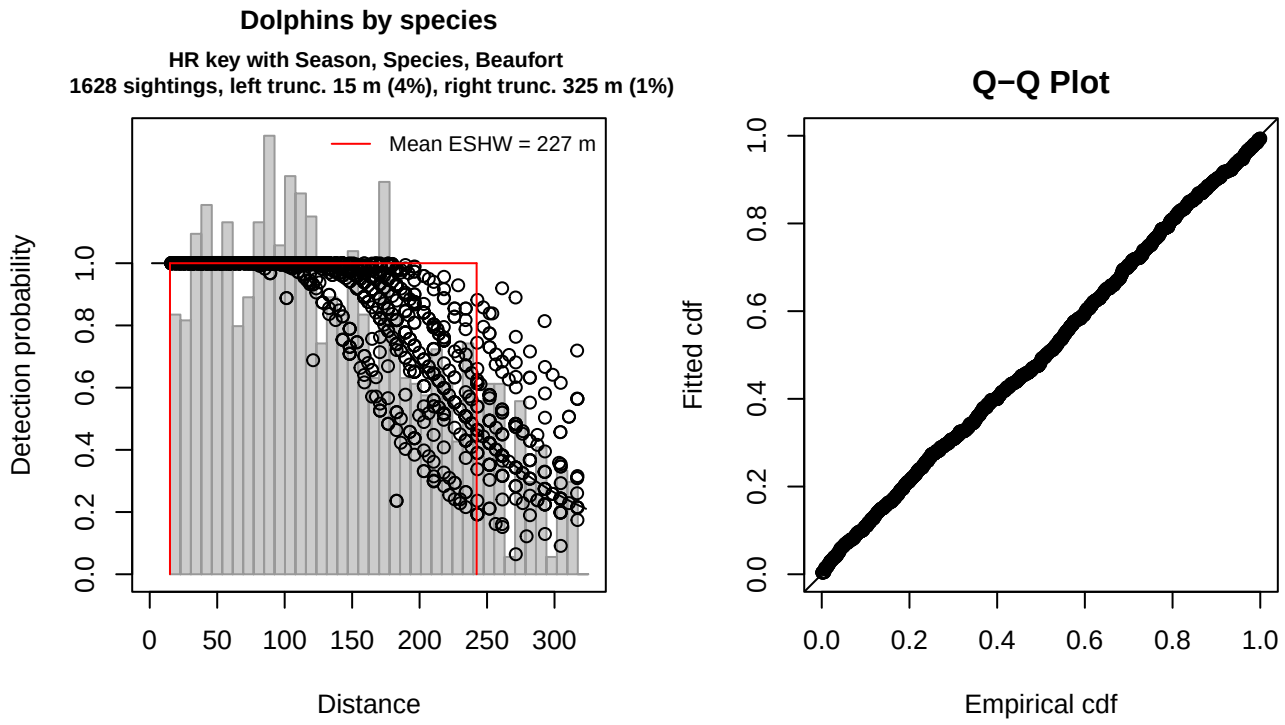

Figure 6: SEFSC AMAPPS detection function and Q-Q plot showing its goodness of fit.

Statistical output for this detection function:

```
Summary for ds object
Number of observations :  1628
Distance range         :  15  -  325
AIC                    :  18351.39

Detection function:
 Hazard-rate key function

Detection function parameters
Scale coefficient(s):
                                      estimate         se
(Intercept)                          5.4780735 0.08251975
SeasonSummer                         0.1269645 0.06172358
SeasonWinter                        -0.2356803 0.06102237
ScientificNameStenella, Lagenodelphis  0.2204074 0.08699872
Beaufort2                           -0.1192230 0.08713320
Beaufort3                           -0.1846083 0.08971655
Beaufort4                           -0.4027356 0.12330363

Shape coefficient(s):
            estimate        se
(Intercept) 1.266688 0.1150367

                       Estimate          SE         CV
Average p              0.720161  0.01522909 0.02114679
N in covered region 2260.605761 56.60731047 0.02504077

Distance sampling Cramer-von Mises test (unweighted)
Test statistic = 0.138923  p = 0.425167
```

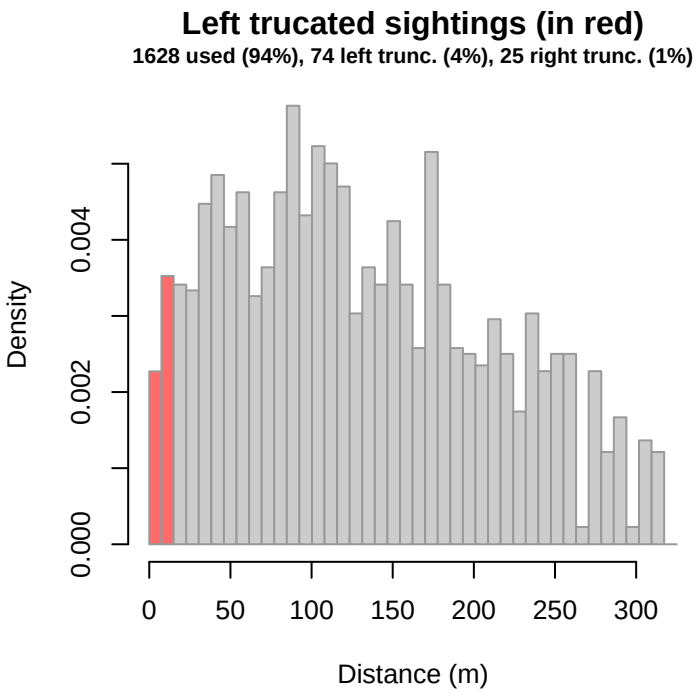

Figure 7: Density histogram of observations used to fit the SEFSC AMAPPS detection function, with the left-most bar showing observations at distances less than 15 m, which were left-truncated and excluded from the analysis [Buckland et al. (2001)]. (This bar may be very short if there were very few left-truncated sightings, or very narrow if the left truncation distance was very small; in either case it may not appear red.)

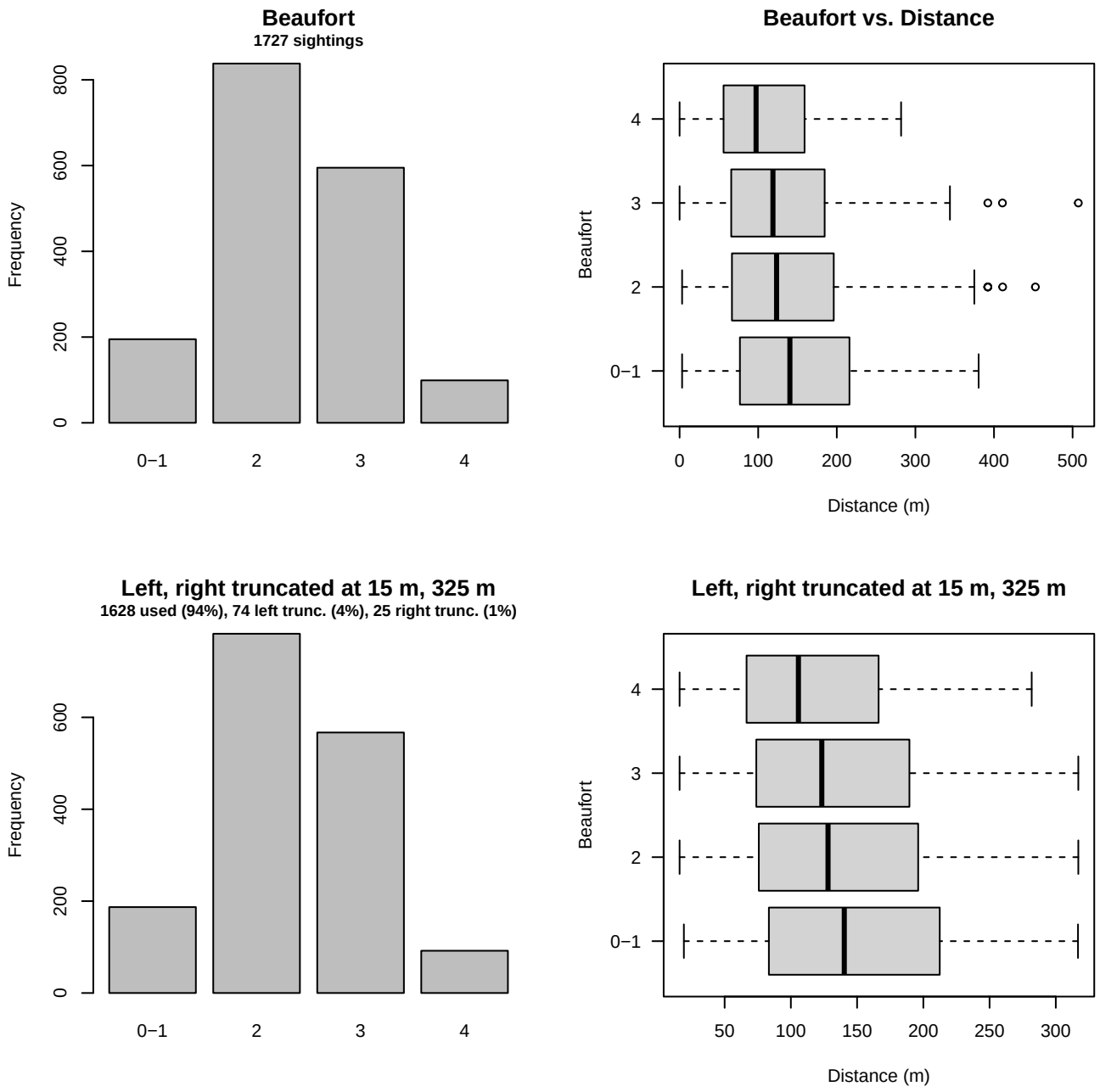

Figure 8: Distribution of the Beaufort covariate before (top row) and after (bottom row) observations were truncated to fit the SEFSC AMAPPS detection function.

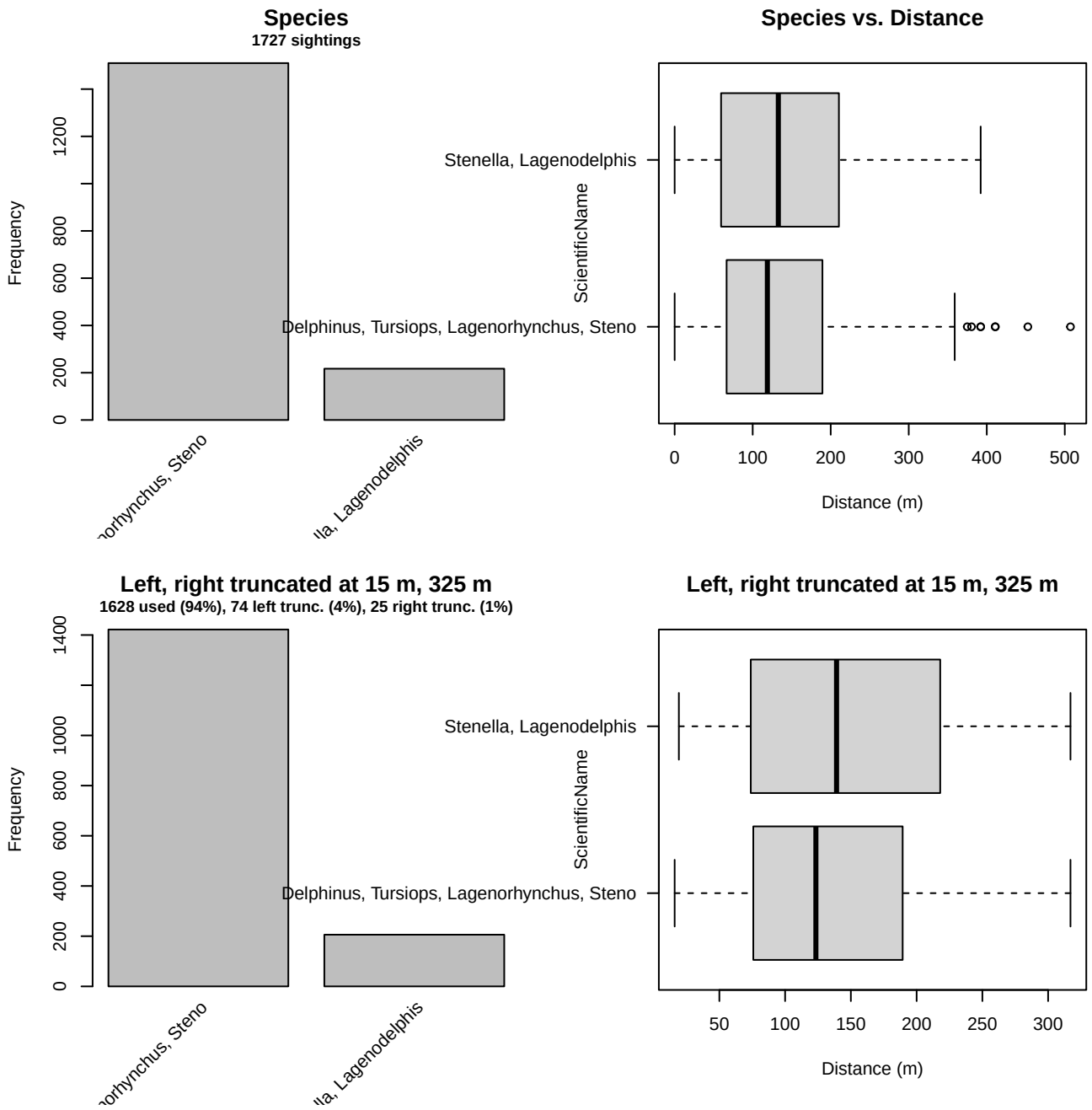

Figure 9: Distribution of the ScientificName covariate before (top row) and after (bottom row) observations were truncated to fit the SEFSC AMAPPS detection function.

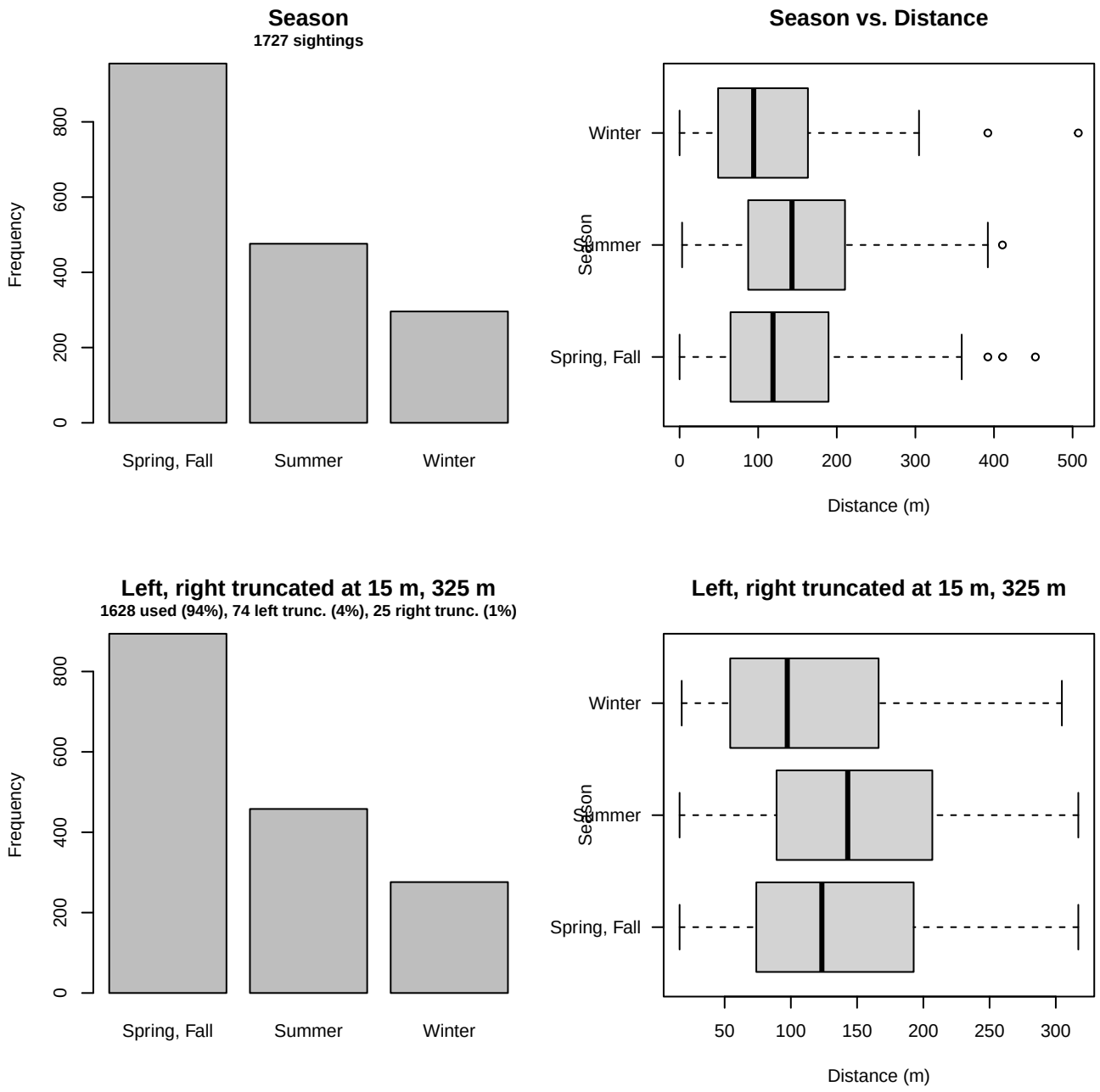

Figure 10: Distribution of the Season covariate before (top row) and after (bottom row) observations were truncated to fit the SEFSC AMAPPS detection function.

2.1.2 Shipboard Surveys

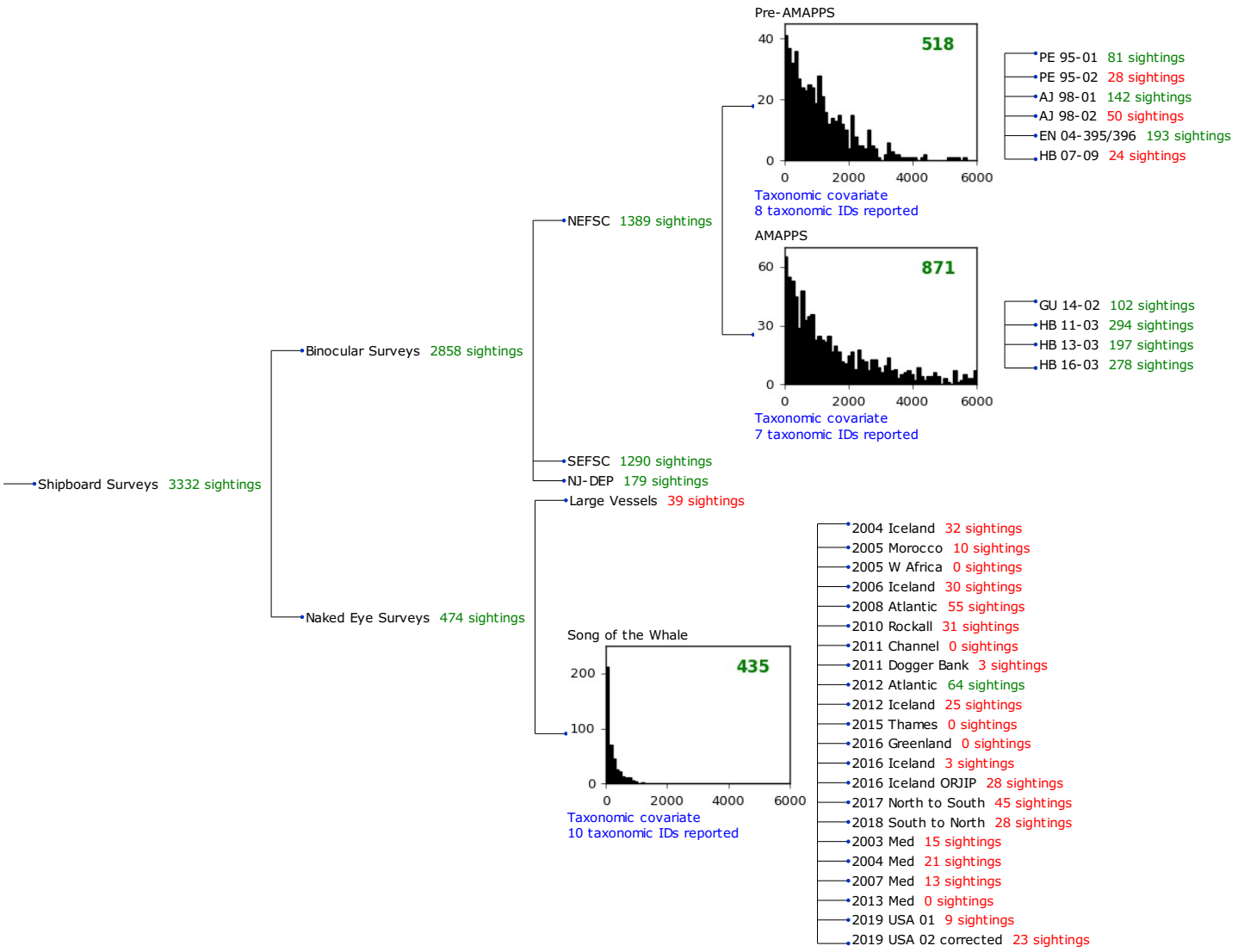

Figure 11: Detection hierarchy for shipboard surveys, showing how they were pooled during detectability modeling, for detection functions that pooled multiple taxa and used used a taxonomic covariate to account for differences between them. Each histogram represents a detection function and summarizes the perpendicular distances of observations that were pooled to fit it, prior to truncation. Observation counts, also prior to truncation, are shown in green when they met the recommendation of Buckland et al. (2001) that detection functions utilize at least 60 sightings, and red otherwise. For rare taxa, it was not always possible to meet this recommendation, yielding higher statistical uncertainty. During the spatial modeling stage of the analysis, effective strip widths were computed for each survey using the closest detection function above it in the hierarchy (i.e. moving from right to left in the figure). Surveys that do not have a detection function above them in this figure were either addressed by a detection function presented in a different section of this report, or were omitted from the analysis.

2.1.2.1 NEFSC Pre-AMAPPS

After right-truncating observations greater than 4000 m, we fitted the detection function to the 508 observations that remained (Table 6). The selected detection function (Figure 12) used a hazard rate key function with Beaufort (Figure 13), ScientificName (Figure 14) and VesselName (Figure 15) as covariates.

Table 6: Observations used to fit the NEFSC Pre-AMAPPS detection function.

ScientificName	n
Delphinus, Lagenorhynchus, Tursiops, Steno	365
Other Stenella, Lagenodelphis	130
Stenella frontalis	13
Total	**508**

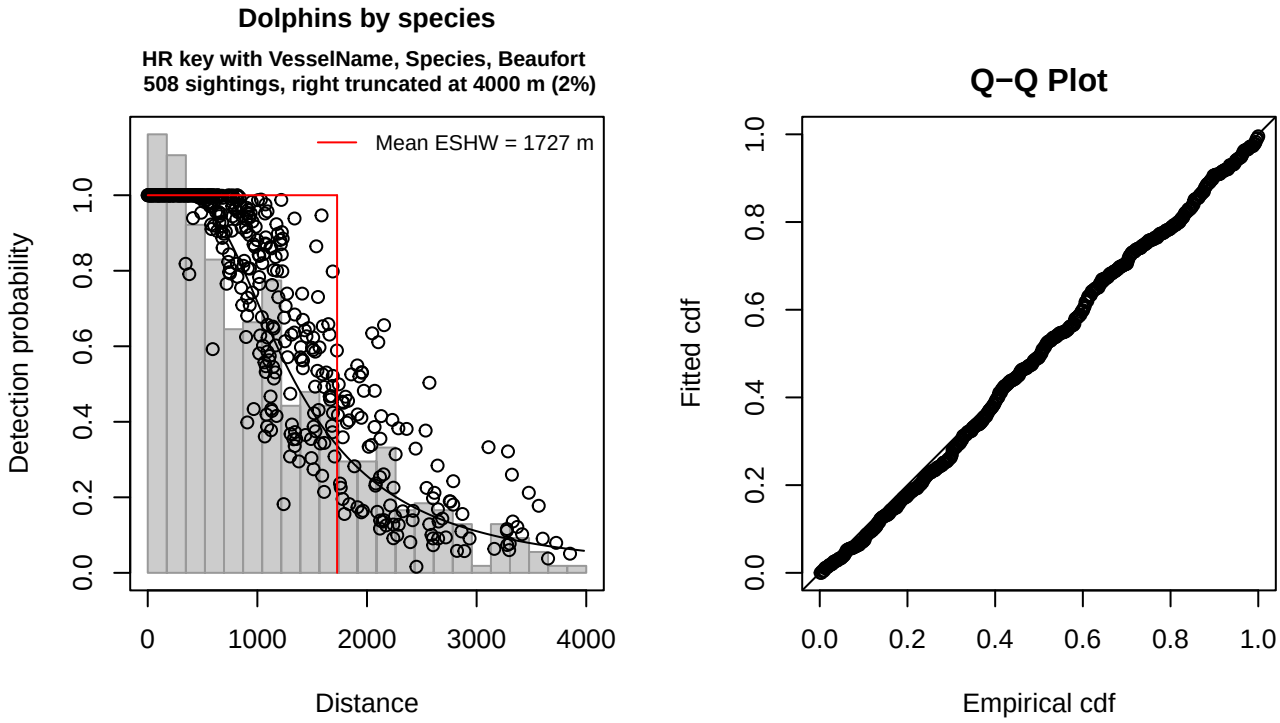

Figure 12: NEFSC Pre-AMAPPS detection function and Q-Q plot showing its goodness of fit.

Statistical output for this detection function:

```
Summary for ds object
Number of observations :  508
Distance range         :  0  -  4000
AIC                    :  8058.614

Detection function:
 Hazard-rate key function

Detection function parameters
Scale coefficient(s):
                                          estimate        se
(Intercept)                              7.3979634 0.1986065
VesselNameEndeavor, Bigelow              0.2529041 0.1095209
ScientificNameOther Stenella, Lagenodelphis  0.3555978 0.1258179
ScientificNameStenella frontalis        -0.8556981 0.3078540
Beaufort                                -0.1897812 0.0694737

Shape coefficient(s):
             estimate        se
(Intercept) 0.8752144 0.1006522
```

```
                        Estimate          SE         CV
Average p               0.4071518  0.02118698 0.05203705
N in covered region 1247.6919609 78.15195776 0.06263722

Distance sampling Cramer-von Mises test (unweighted)
Test statistic = 0.120847  p = 0.492001
```

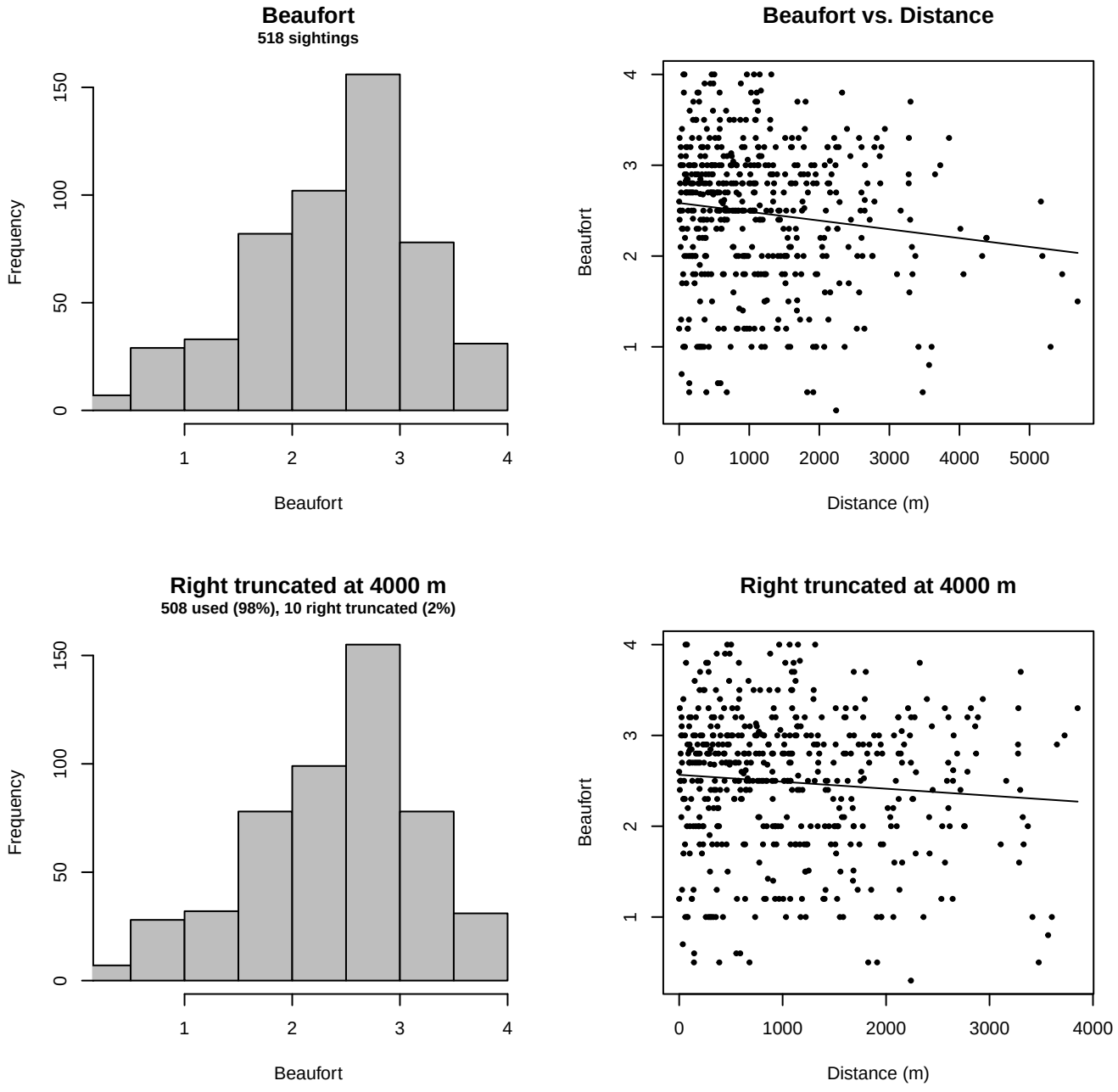

Figure 13: Distribution of the Beaufort covariate before (top row) and after (bottom row) observations were truncated to fit the NEFSC Pre-AMAPPS detection function.

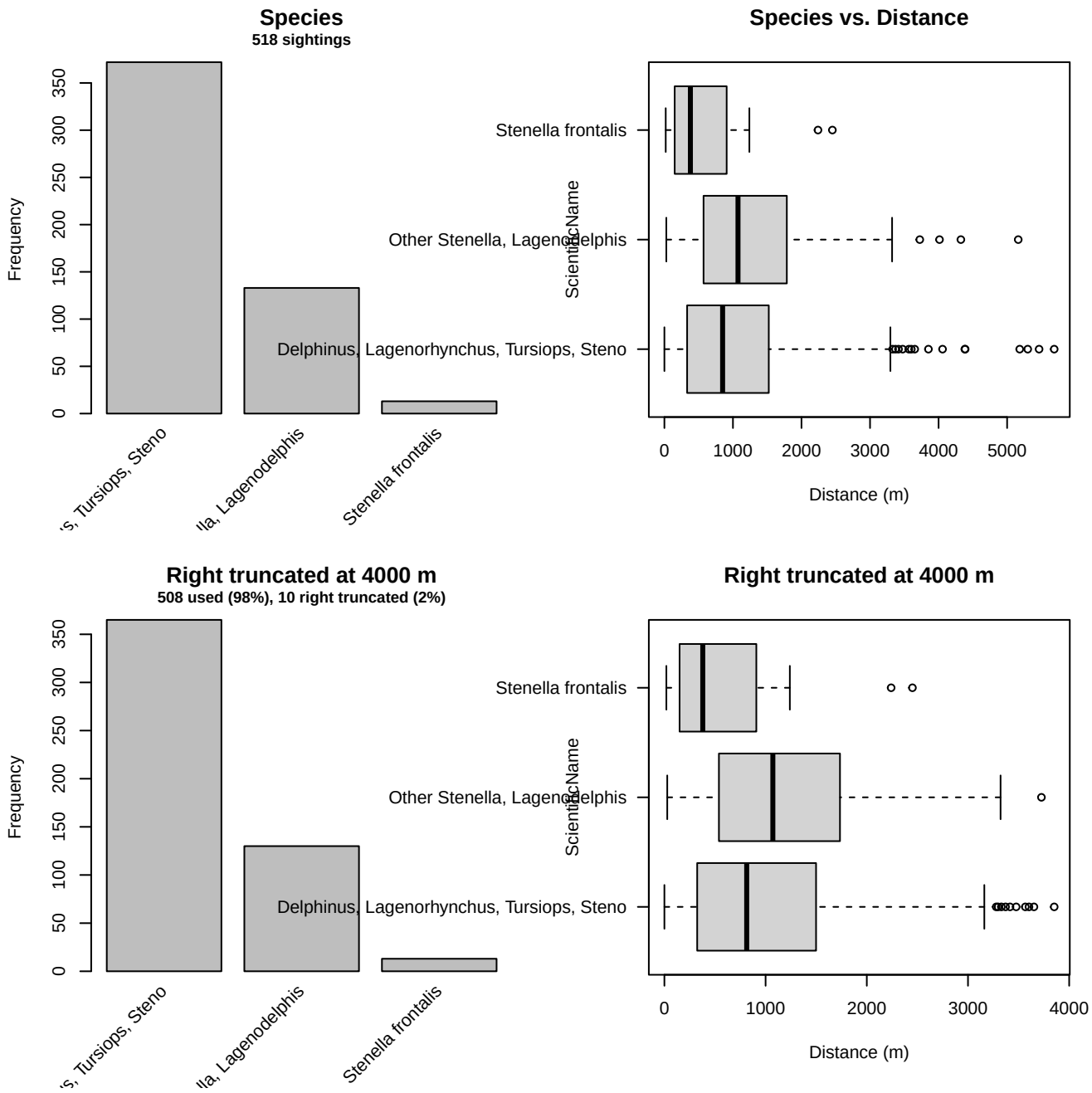

Figure 14: Distribution of the ScientificName covariate before (top row) and after (bottom row) observations were truncated to fit the NEFSC Pre-AMAPPS detection function.

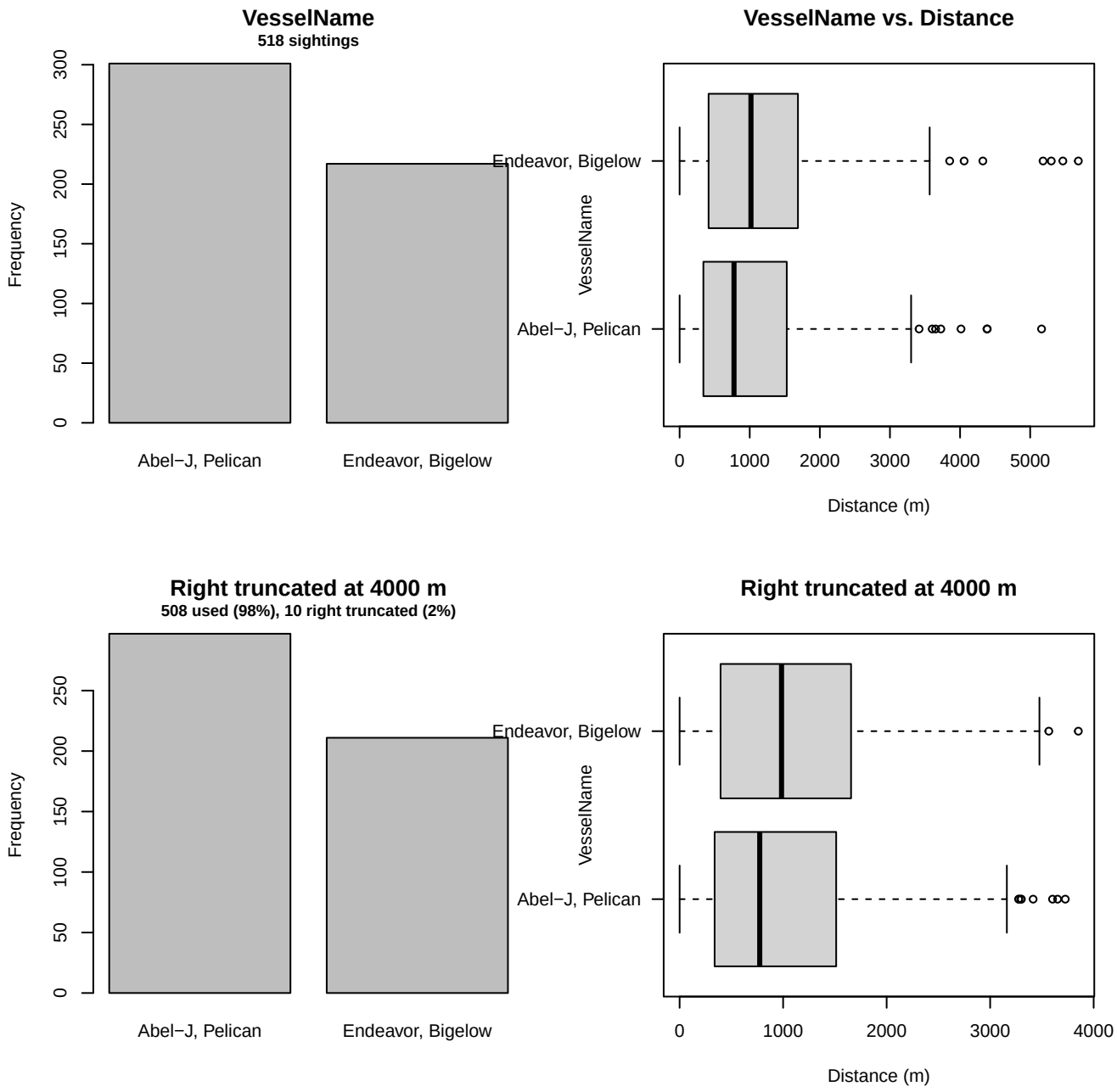

Figure 15: Distribution of the VesselName covariate before (top row) and after (bottom row) observations were truncated to fit the NEFSC Pre-AMAPPS detection function.

2.1.2.2 NEFSC AMAPPS

After right-truncating observations greater than 6000 m, we fitted the detection function to the 857 observations that remained (Table 7). The selected detection function (Figure 16) used a hazard rate key function with Beaufort (Figure 17) and ScientificName (Figure 18) as covariates.

Table 7: Observations used to fit the NEFSC AMAPPS detection function.

ScientificName	n
Delphinus, Lagenorhynchus	358
Other Stenella, Lagenodelphis	175
Stenella frontalis	53
Tursiops, Steno	271
Total	**857**

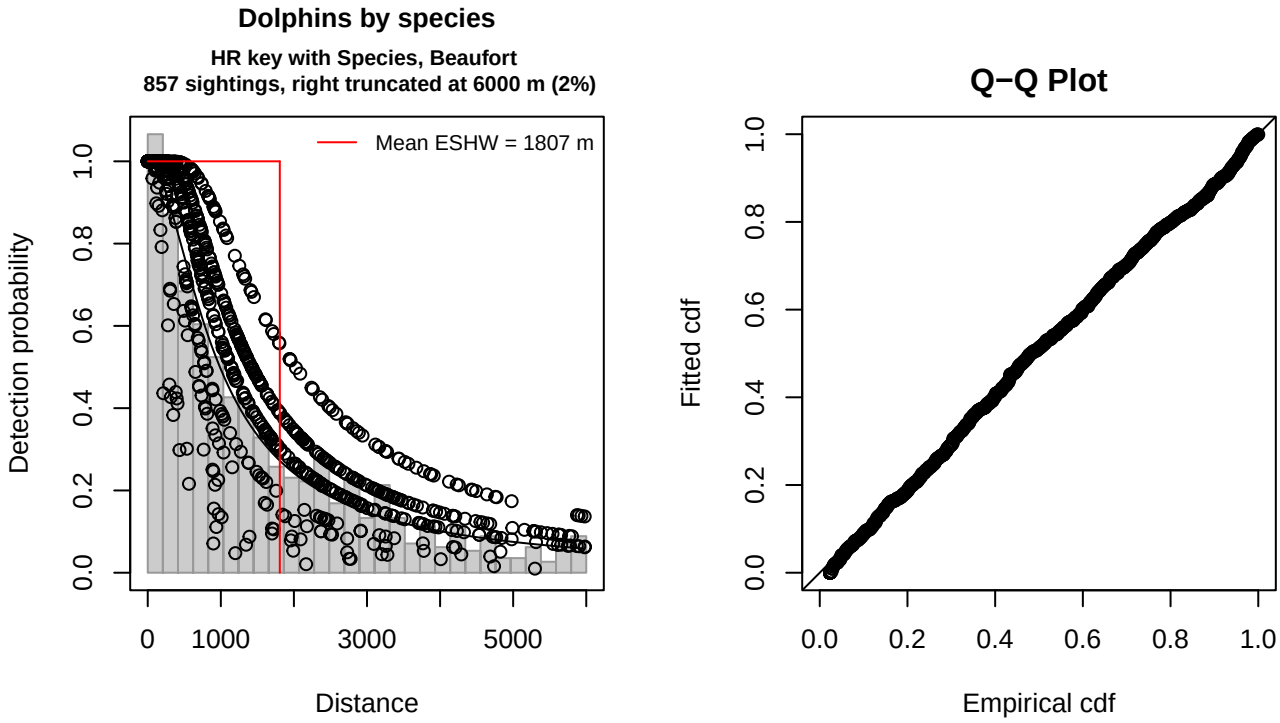

Figure 16: NEFSC AMAPPS detection function and Q-Q plot showing its goodness of fit.

Statistical output for this detection function:

```
Summary for ds object
Number of observations :  857
Distance range         :  0  -  6000
AIC                    :  14222.66

Detection function:
 Hazard-rate key function

Detection function parameters
Scale coefficient(s):
                                           estimate        se
(Intercept)                               7.0022801 0.1342692
ScientificNameOther Stenella, Lagenodelphis  0.3515378 0.1854896
ScientificNameStenella frontalis           -0.5910499 0.3033455
ScientificNameTursiops, Steno              -0.2176361 0.1602756
Beaufort3-4                                -0.5842019 0.1839783
Beaufort4-5                                -1.4374209 0.2667762

Shape coefficient(s):
            estimate        se
```

```
(Intercept) 0.356339 0.0663051

                         Estimate           SE         CV
Average p                0.2624967   0.01868208 0.07117073
N in covered region 3264.8026106 252.27662296 0.07727163

Distance sampling Cramer-von Mises test (unweighted)
Test statistic = 0.089267  p = 0.640081
```

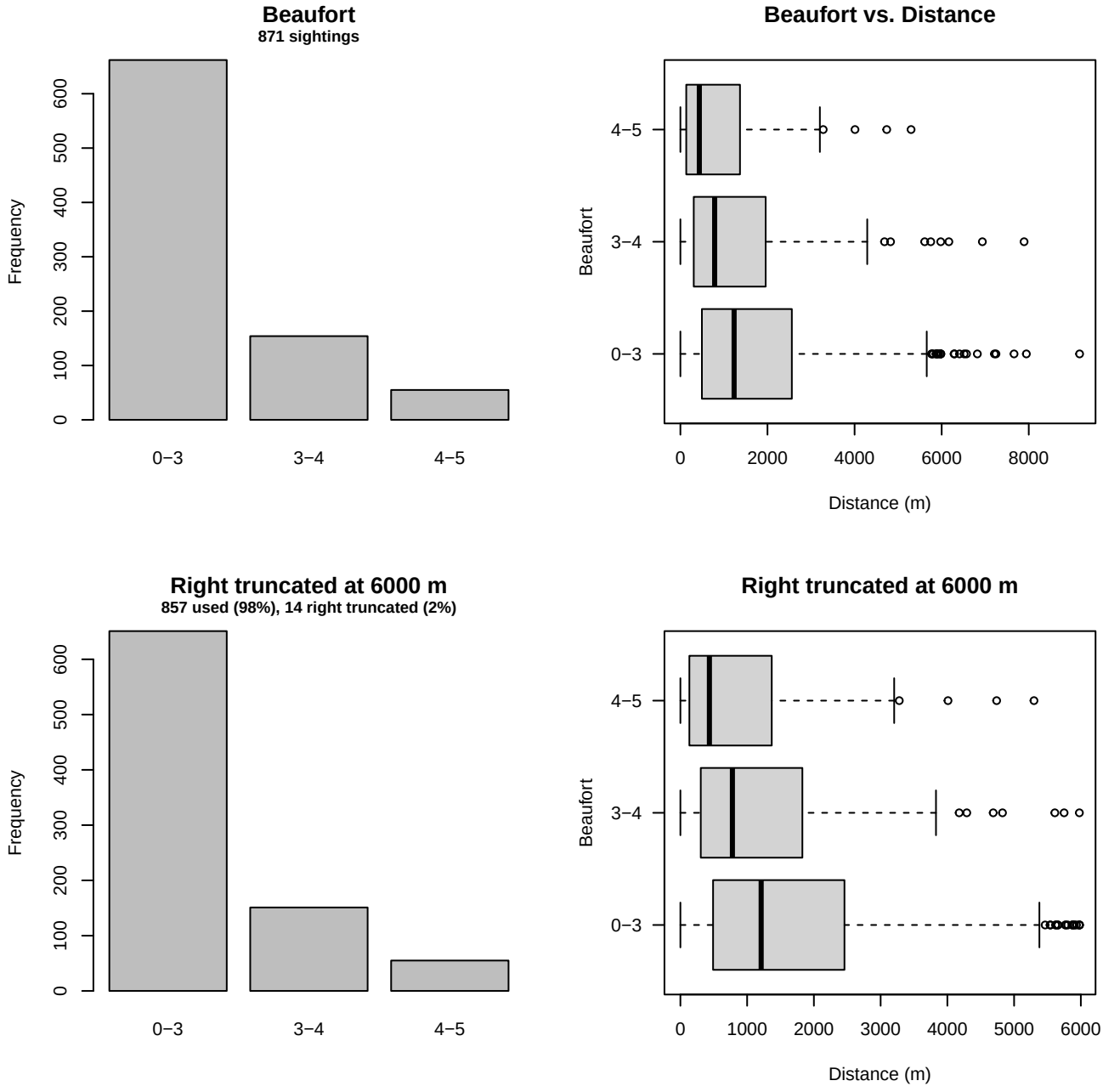

Figure 17: Distribution of the Beaufort covariate before (top row) and after (bottom row) observations were truncated to fit the NEFSC AMAPPS detection function.

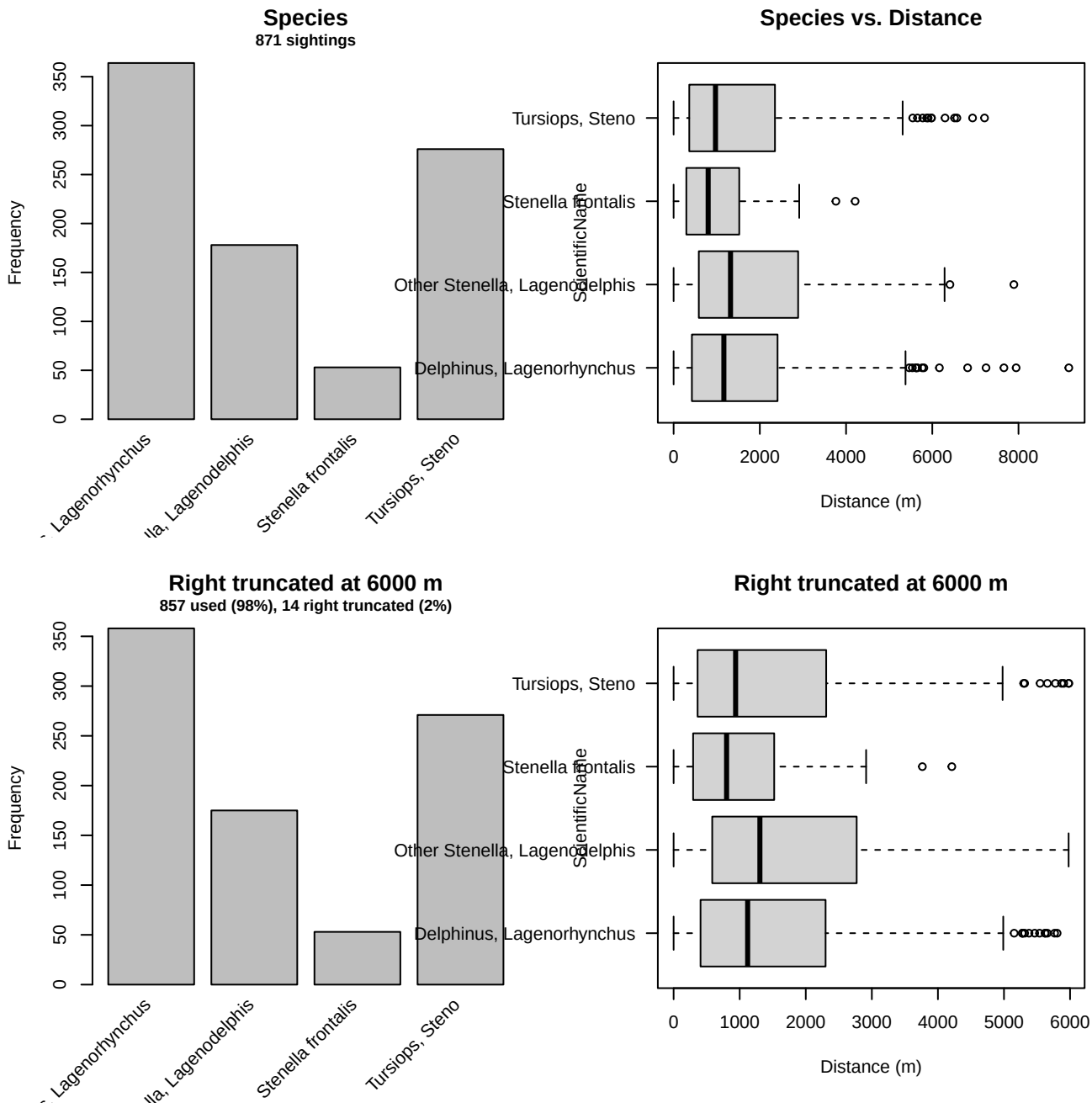

Figure 18: Distribution of the ScientificName covariate before (top row) and after (bottom row) observations were truncated to fit the NEFSC AMAPPS detection function.

2.1.2.3 Song of the Whale

After right-truncating observations greater than 700 m and left-truncating observations less than 1 m (Figure 20), we fitted the detection function to the 360 observations that remained (Table 8). The selected detection function (Figure 19) used a hazard rate key function with Beaufort (Figure 21), ScientificName (Figure 22) and Visibility (Figure 23) as covariates.

Table 8: Observations used to fit the Song of the Whale detection function.

ScientificName	n
All others	211
Delphinus	149
Total	**360**

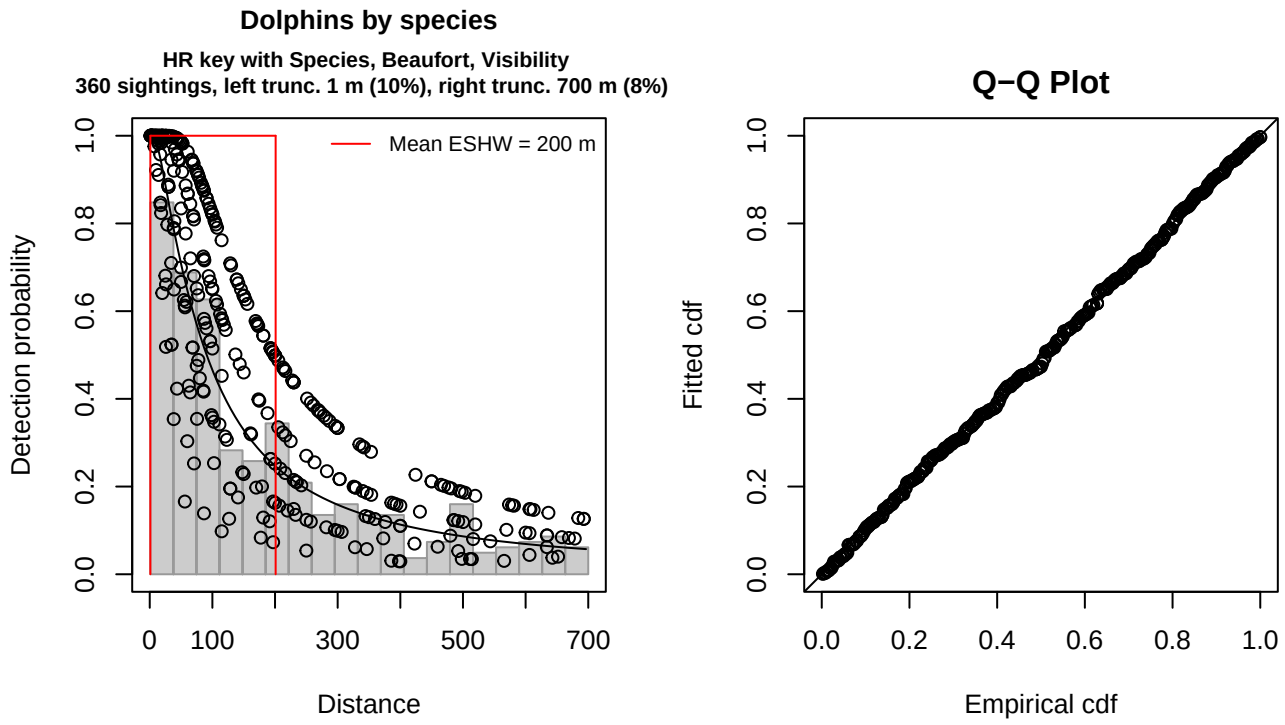

Figure 19: Song of the Whale detection function and Q-Q plot showing its goodness of fit.

Statistical output for this detection function:

```
Summary for ds object
Number of observations :  360
Distance range         :  1  -  700
AIC                    :  4434.06

Detection function:
 Hazard-rate key function

Detection function parameters
Scale coefficient(s):
                             estimate        se
(Intercept)                 5.0168382 0.2118228
ScientificNameDelphinus    -0.3746003 0.2526245
Beaufort3                  -0.6586604 0.2922112
Beaufort3.5-4              -1.3223280 0.3841776
VisibilityModerate (2-5nmi) -0.9687696 0.4363084

Shape coefficient(s):
             estimate         se
(Intercept) 0.2728327 0.09542948

                      Estimate          SE        CV
Average p             0.232512   0.02944422 0.1266352
N in covered region 1548.306965 209.54903632 0.1353408

Distance sampling Cramer-von Mises test (unweighted)
Test statistic = 0.019198  p = 0.997687
```

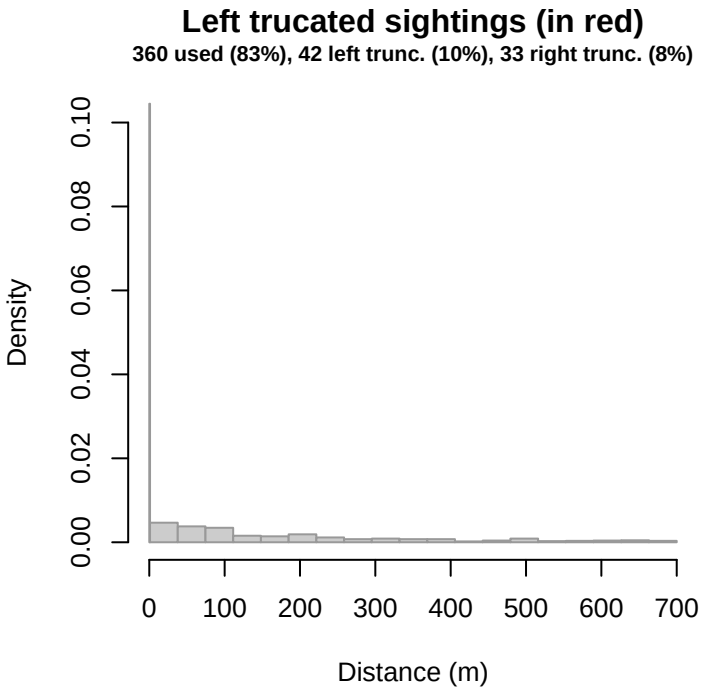

Figure 20: Density histogram of observations used to fit the Song of the Whale detection function, with the left-most bar showing observations at distances less than 1 m, which were left-truncated and not used to fit the detection function. (This bar may be very short if there were very few left-truncated sightings, or very narrow if the left truncation distance was very small; in either case it may not appear red.) These were excluded because they formed a problematic "spike" in detections close to the trackline, suggesting that animals approached the vessel (e.g. to bow-ride) prior to being detected. To address this, we fitted the detection function to the observations beyond the spike and assumed that within it, detection probability was 1, effectively treating it like a strip transect. We then added the left-truncated observations back into the analysis as if they occurred in this strip. This treatment may have resulted in an underestimation of detection probability.

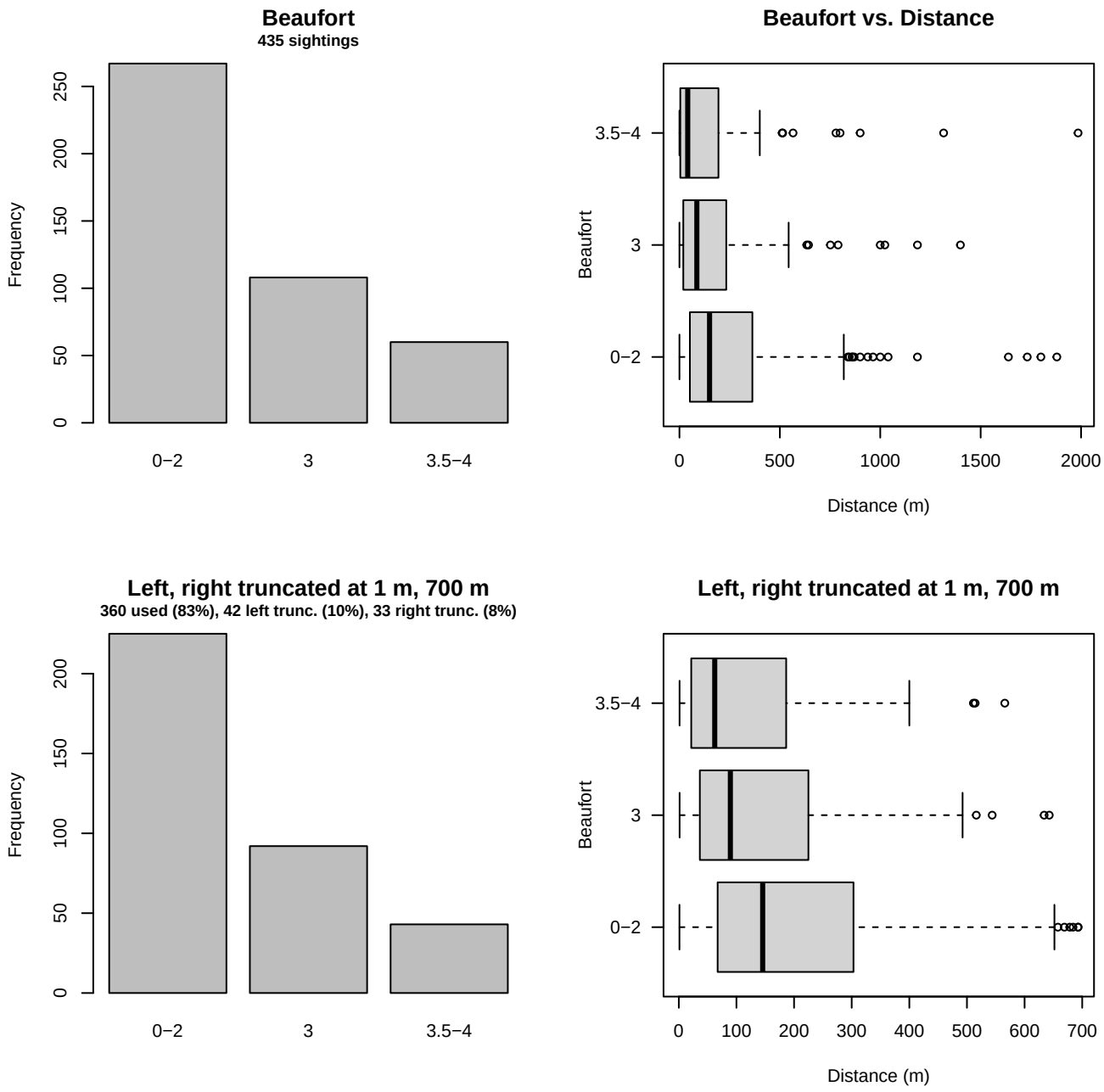

Figure 21: Distribution of the Beaufort covariate before (top row) and after (bottom row) observations were truncated to fit the Song of the Whale detection function.

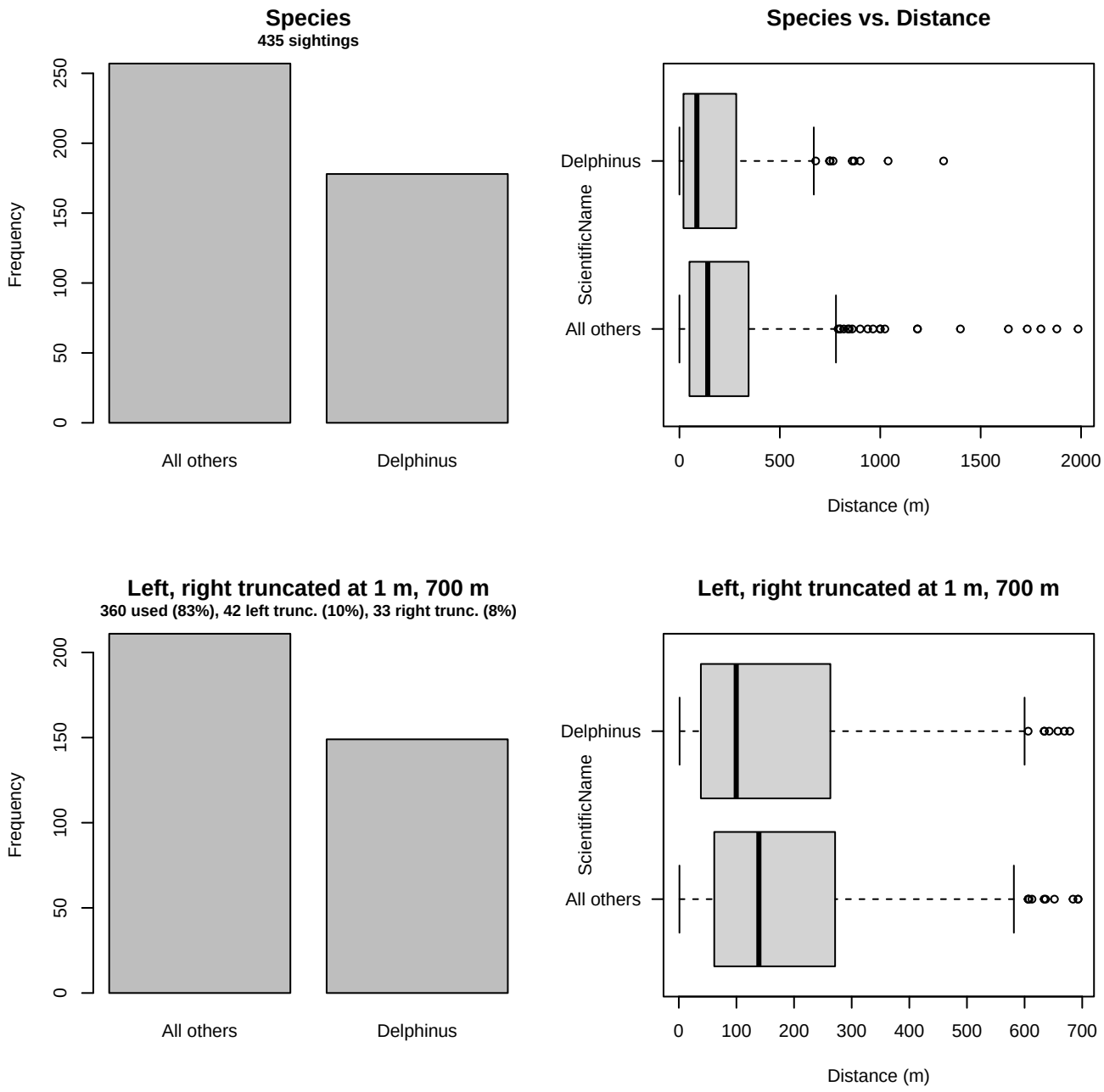

Figure 22: Distribution of the ScientificName covariate before (top row) and after (bottom row) observations were truncated to fit the Song of the Whale detection function.

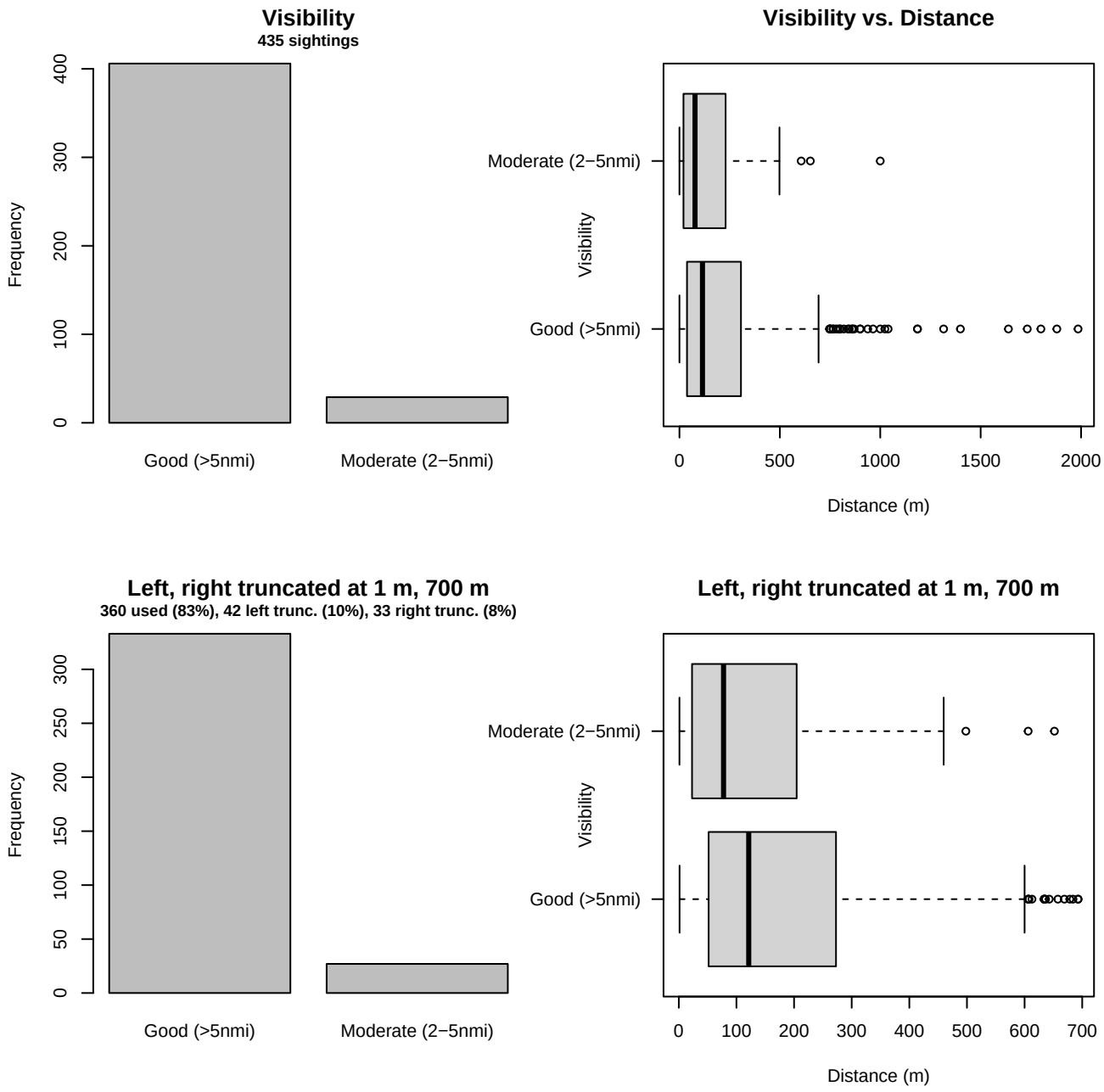

Figure 23: Distribution of the Visibility covariate before (top row) and after (bottom row) observations were truncated to fit the Song of the Whale detection function.

2.2 Without a Taxonomic Covariate

We fitted the detection functions in this section to pools of species with similar detectability characteristics but could not use a taxonomic identification as a covariate to account for differences between them. We usually took this approach after trying the taxonomic covariate and finding it had insufficient statistical power to be retained. We also resorted to it when the focal taxon being modeled had too few observations to be allocated its own taxonomic covariate level and was too poorly known for us to confidently determine which other taxa we could group it with.

2.2.1 Aerial Surveys

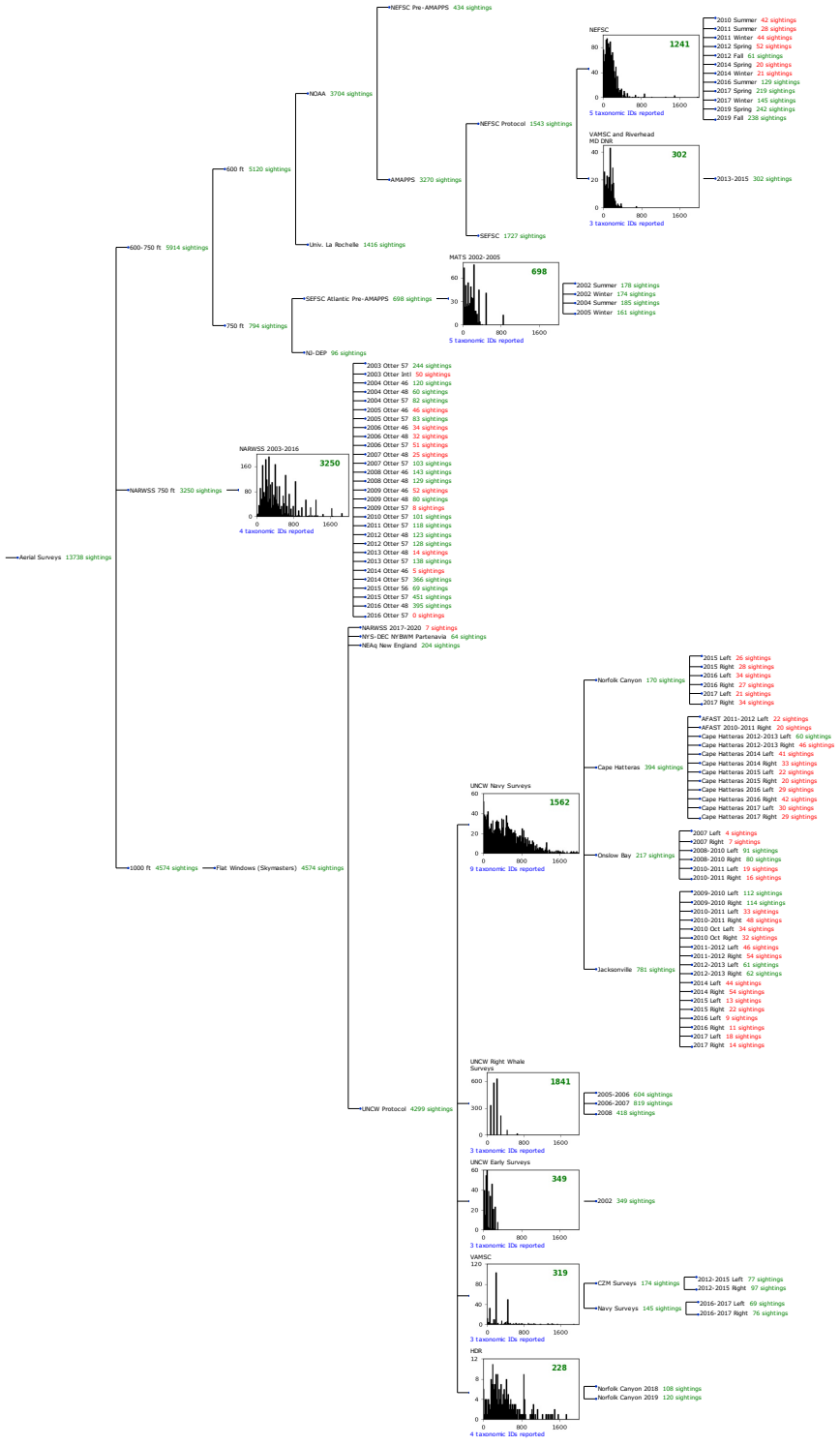

Figure 24: Detection hierarchy for aerial surveys, showing how they were pooled during detectability modeling, for detection functions that pooled multiple taxa but could not use a taxonomic covariate to account for differences between them. Each histogram represents a detection function and summarizes the perpendicular distances of observations that were pooled to fit it, prior to truncation. Observation counts, also prior to truncation, are shown in green when they met the recommendation of Buckland et al. (2001) that detection functions utilize at least 60 sightings, and red otherwise. For rare taxa, it was not always possible to meet this recommendation, yielding higher statistical uncertainty. During the spatial modeling stage of the analysis, effective strip widths were computed for each survey using the closest detection function above it in the hierarchy (i.e. moving from right to left in the figure). Surveys that do not have a detection function above them in this figure were either addressed by a detection function presented in a different section of this report, or were omitted from the analysis.

2.2.1.1 NEFSC AMAPPS

After right-truncating observations greater than 600 m, we fitted the detection function to the 1218 observations that remained (Table 9). The selected detection function (Figure 25) used a hazard rate key function with Season (Figure 26) as a covariate.

Table 9: Observations used to fit the NEFSC AMAPPS detection function.

ScientificName	n
Delphinus delphis	817
Lagenorhynchus acutus	280
Lagenorhynchus albirostris	3
Stenella coeruleoalba	13
Tursiops truncatus	105
Total	**1218**

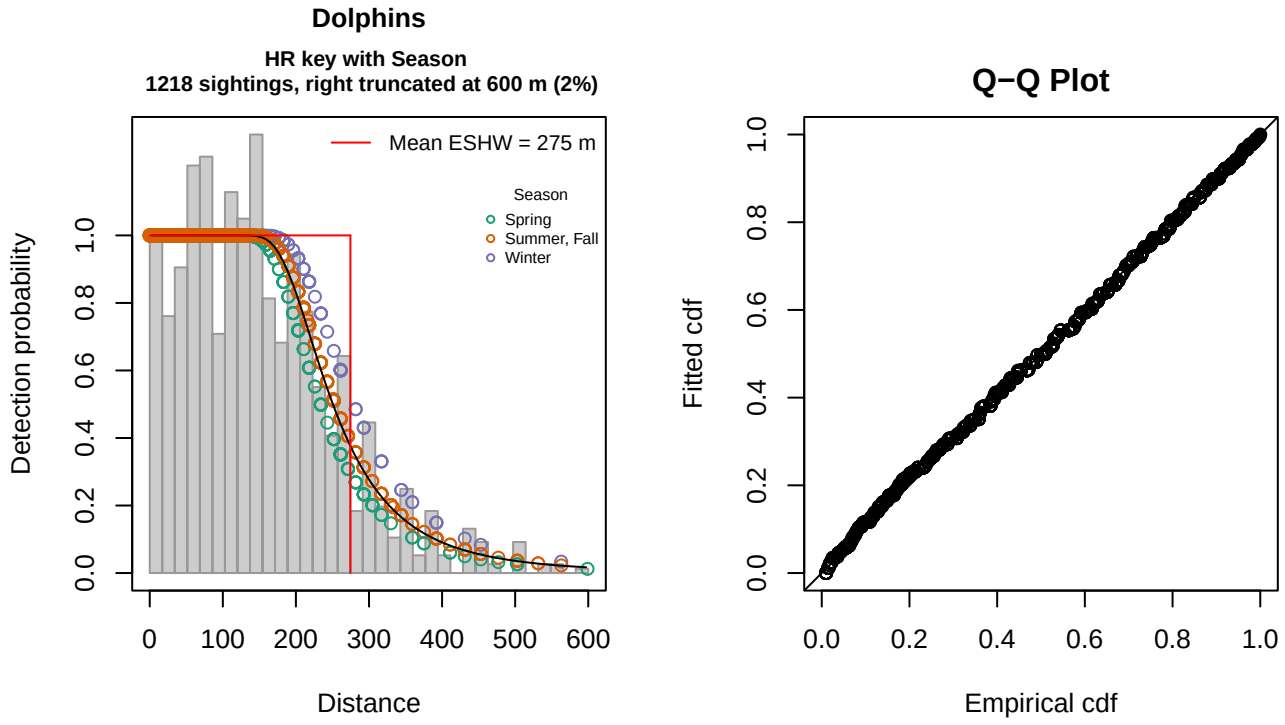

Figure 25: NEFSC AMAPPS detection function and Q-Q plot showing its goodness of fit.

Statistical output for this detection function:

```
Summary for ds object
Number of observations :  1218
Distance range         :  0  -  600
AIC                    :  14460.69

Detection function:
 Hazard-rate key function

Detection function parameters
Scale coefficient(s):
                     estimate         se
(Intercept)        5.36944749 0.04422696
SeasonSummer, Fall 0.08083579 0.04638562
SeasonWinter       0.17600218 0.07702020
```

```
Shape coefficient(s):
            estimate       se
(Intercept) 1.452854 0.065484

                        Estimate          SE         CV
Average p               0.456561  0.00970389 0.02125431
N in covered region 2667.770370 79.97999993 0.02998009

Distance sampling Cramer-von Mises test (unweighted)
Test statistic = 0.126854  p = 0.468488
```

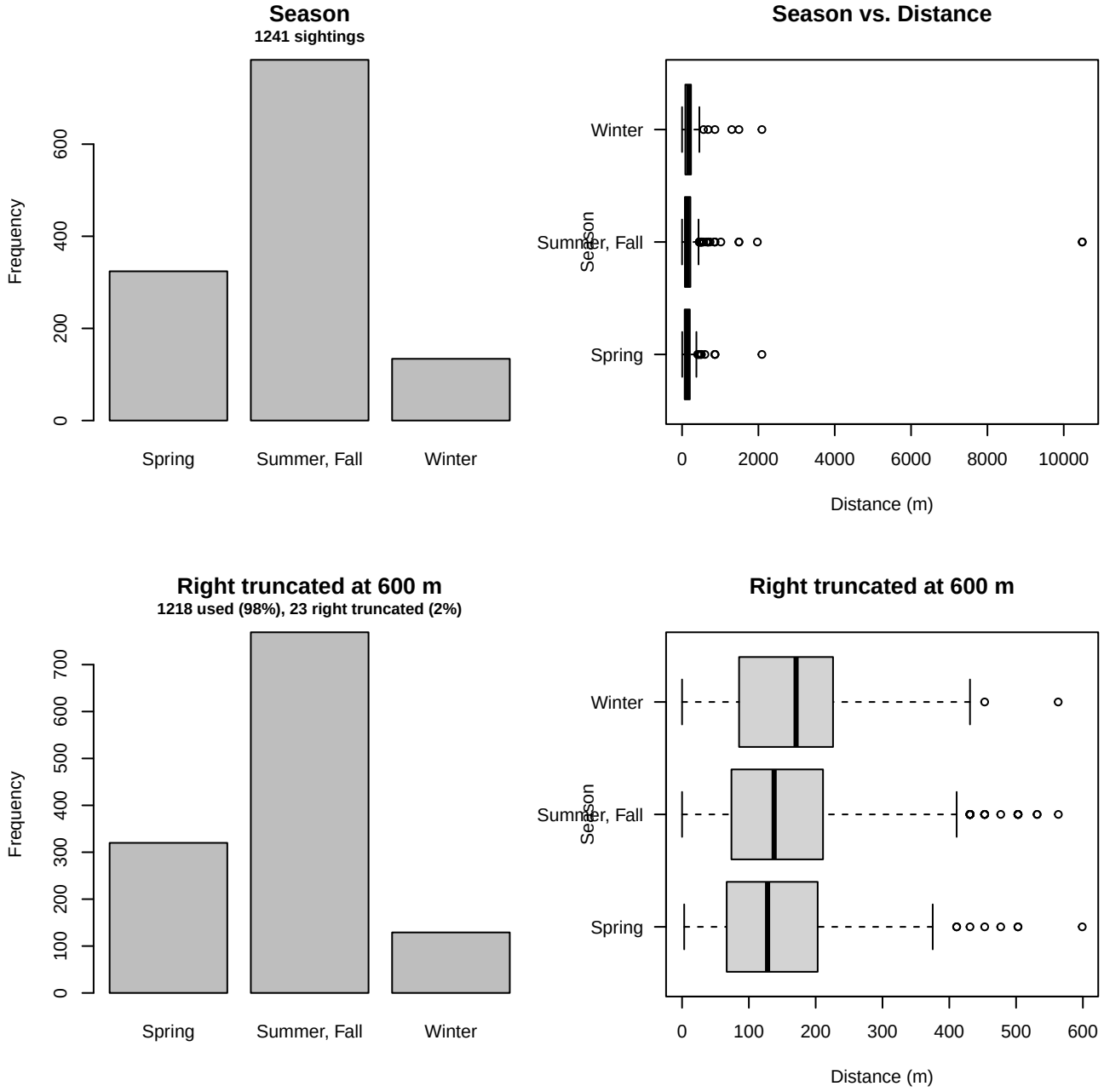

Figure 26: Distribution of the Season covariate before (top row) and after (bottom row) observations were truncated to fit the NEFSC AMAPPS detection function.

2.2.1.2 VAMSC and Riverhead MD DNR

After right-truncating observations greater than 400 m, we fitted the detection function to the 301 observations that remained (Table 10). The selected detection function (Figure 27) used a hazard rate key function with no covariates.

Table 10: Observations used to fit the VAMSC and Riverhead MD DNR detection function.

ScientificName	n
Delphinus delphis	22
Stenella frontalis	1
Tursiops truncatus	278
Total	**301**

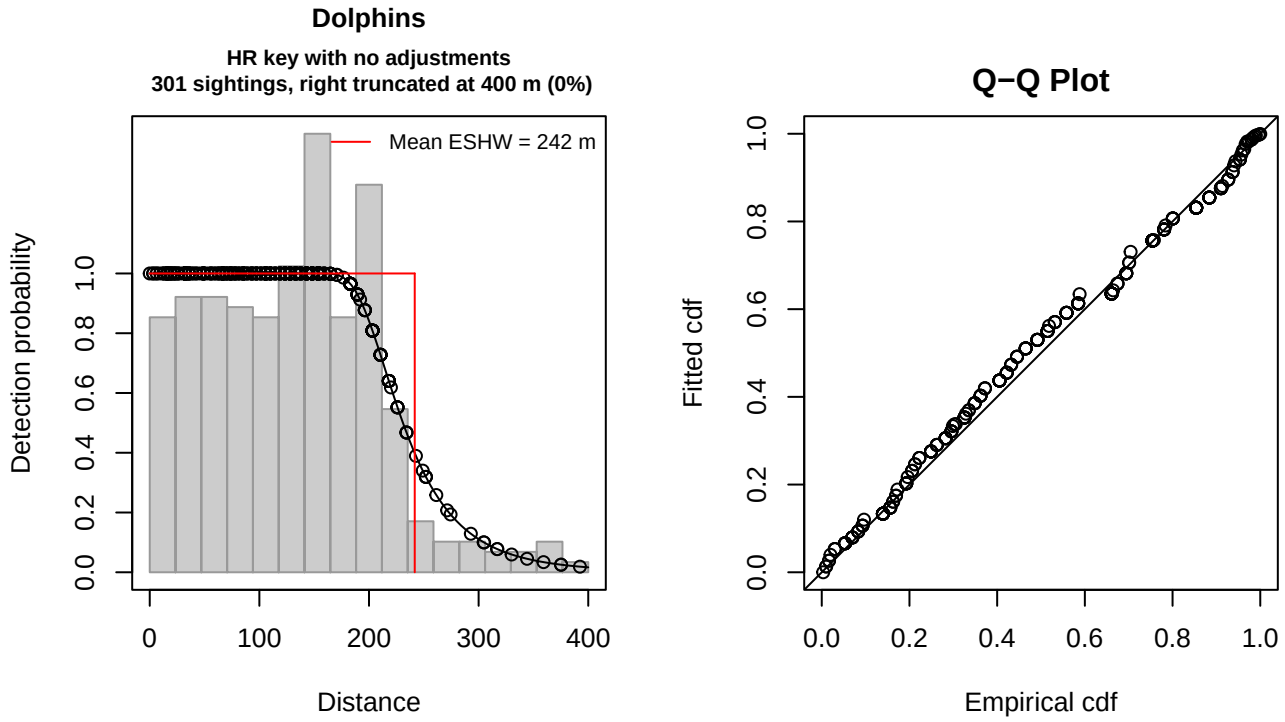

Figure 27: VAMSC and Riverhead MD DNR detection function and Q-Q plot showing its goodness of fit.

Statistical output for this detection function:

```
Summary for ds object
Number of observations :  301
Distance range         :  0  -  400
AIC                    :  3426.124

Detection function:
 Hazard-rate key function

Detection function parameters
Scale coefficient(s):
            estimate         se
(Intercept) 5.388208 0.04209556

Shape coefficient(s):
            estimate        se
(Intercept)  1.91525 0.1331166
```

```
                        Estimate         SE         CV
Average p               0.6042969  0.0203517 0.03367831
N in covered region 498.0995265 24.6489147 0.04948592

Distance sampling Cramer-von Mises test (unweighted)
Test statistic = 0.302011  p = 0.133421
```

2.2.1.3 MATS 2002-2005

After right-truncating observations greater than 629 m, we fitted the detection function to the 684 observations that remained (Table 11). The selected detection function (Figure 28) used a hazard rate key function with Beaufort (Figure 29) as a covariate.

Table 11: Observations used to fit the MATS 2002-2005 detection function.

ScientificName	n
Delphinus delphis	2
Stenella attenuata	2
Stenella frontalis	104
Tursiops truncatus	576
Total	**684**

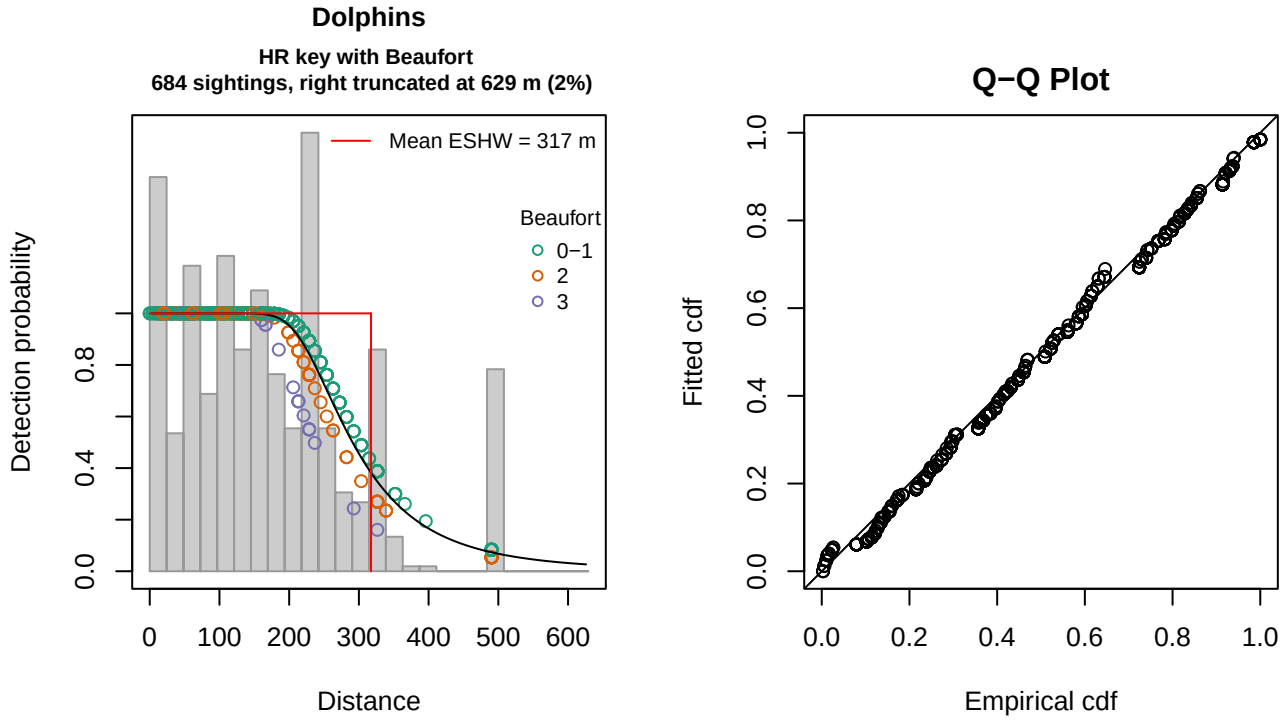

Figure 28: MATS 2002-2005 detection function and Q-Q plot showing its goodness of fit.

Statistical output for this detection function:

```
Summary for ds object
Number of observations :  684
Distance range         :  0  -  629
AIC                    :  8306.088

Detection function:
```

```
 Hazard-rate key function

Detection function parameters
Scale coefficient(s):
              estimate         se
(Intercept)  5.6213531 0.04325709
Beaufort2   -0.1046854 0.06814971
Beaufort3   -0.2421057 0.13060115

Shape coefficient(s):
            estimate         se
(Intercept) 1.449025 0.08965229

                        Estimate         SE         CV
Average p              0.5026836  0.0147185 0.02927984
N in covered region 1360.6968013 54.2106880 0.03984039

Distance sampling Cramer-von Mises test (unweighted)
Test statistic = 0.194502  p = 0.278380
```

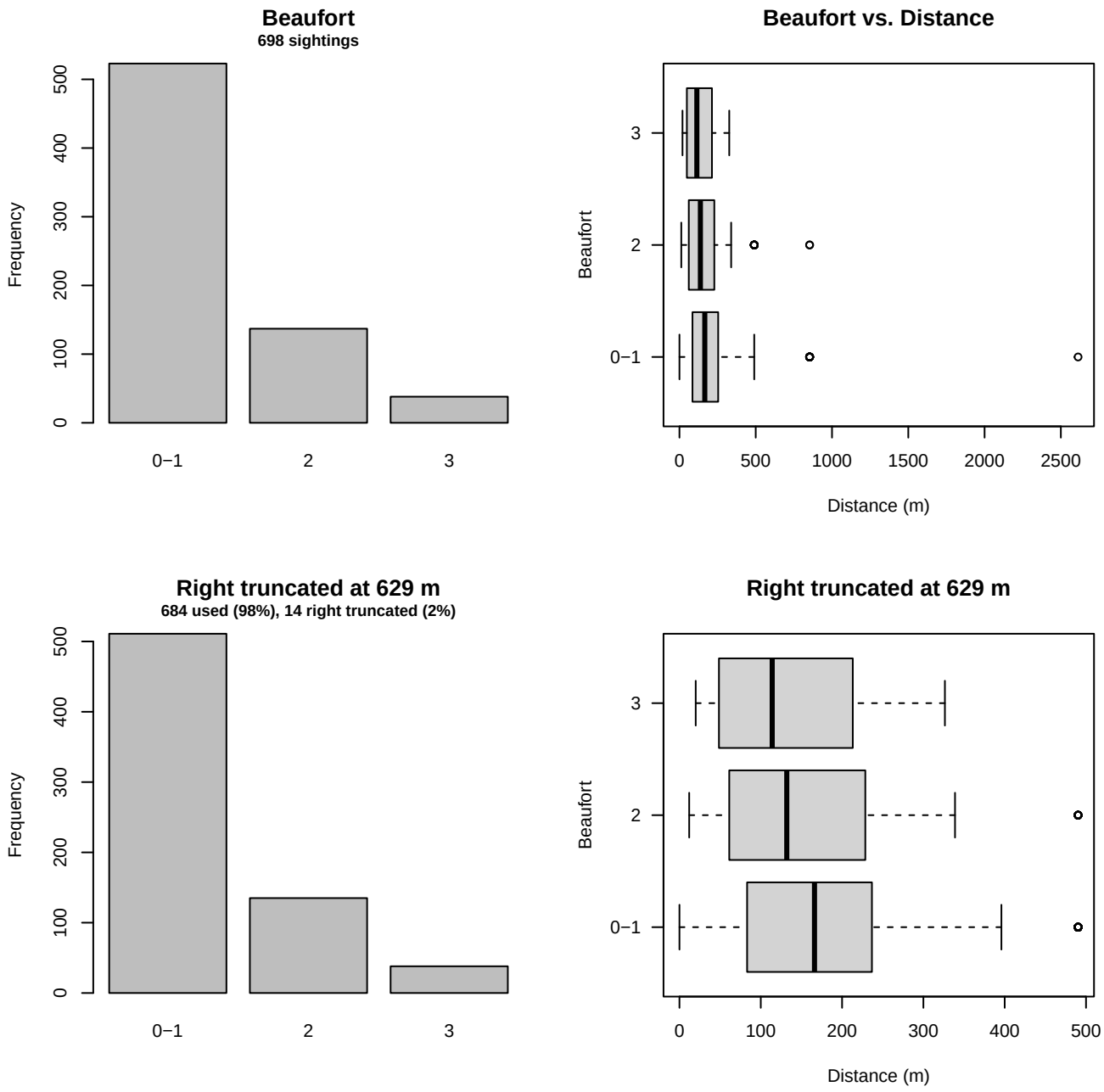

Figure 29: Distribution of the Beaufort covariate before (top row) and after (bottom row) observations were truncated to fit the MATS 2002-2005 detection function.

2.2.1.4 NARWSS 2003-2016

After right-truncating observations greater than 1367 m and left-truncating observations less than 61 m (Figure 31), we fitted the detection function to the 3073 observations that remained (Table 12). The selected detection function (Figure 30) used a hazard rate key function with Beaufort (Figure 32) and Season (Figure 33) as covariates.

Table 12: Observations used to fit the NARWSS 2003-2016 detection function.

ScientificName	n
Delphinus delphis	607
Lagenorhynchus acutus	2404
Lagenorhynchus albirostris	6
Tursiops truncatus	56
Total	**3073**

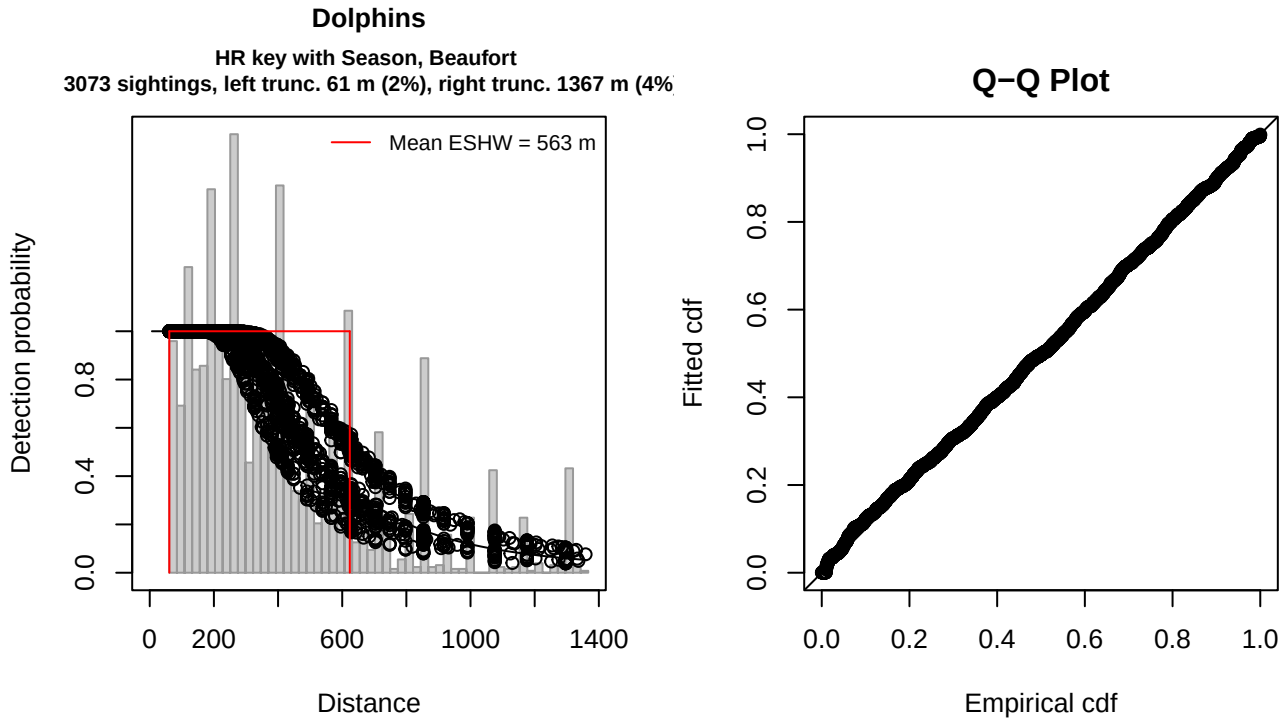

Figure 30: NARWSS 2003-2016 detection function and Q-Q plot showing its goodness of fit.

Statistical output for this detection function:

```
Summary for ds object
Number of observations :  3073
Distance range         :  61  -  1367
AIC                    :  41850.8

Detection function:
 Hazard-rate key function

Detection function parameters
Scale coefficient(s):
               estimate         se
(Intercept)   6.10469263 0.07579397
SeasonSpring  0.06689438 0.05622050
SeasonSummer  0.29278056 0.05383279
SeasonWinter -0.15259970 0.06804643
Beaufort     -0.03572691 0.02383833

Shape coefficient(s):
            estimate        se
(Intercept) 1.009361 0.0398862
```

```
                         Estimate           SE         CV
Average p              0.4196247 8.827249e-03 0.02103606
N in covered region 7323.2113220 1.845410e+02 0.02519946

Distance sampling Cramer-von Mises test (unweighted)
Test statistic = 0.246036  p = 0.193531
```

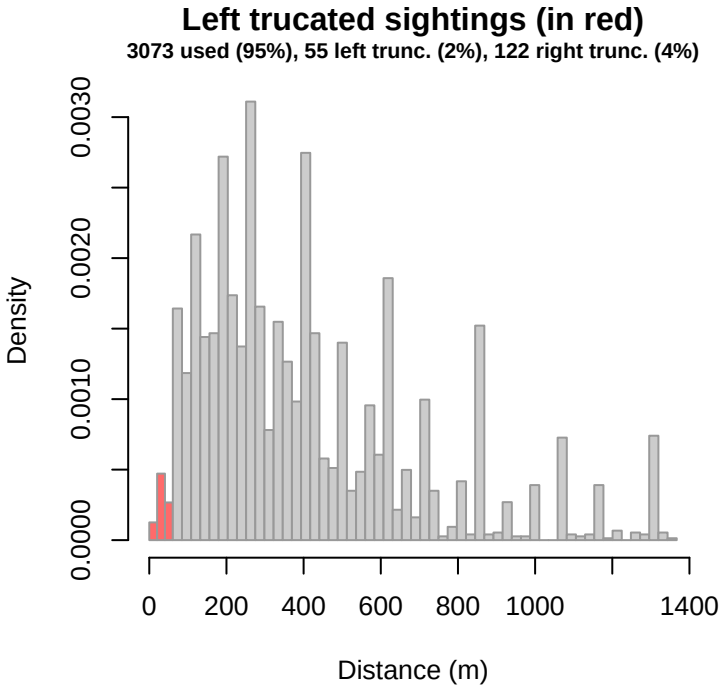

Figure 31: Density histogram of observations used to fit the NARWSS 2003-2016 detection function, with the left-most bar showing observations at distances less than 61 m, which were left-truncated and excluded from the analysis [Buckland et al. (2001)]. (This bar may be very short if there were very few left-truncated sightings, or very narrow if the left truncation distance was very small; in either case it may not appear red.)

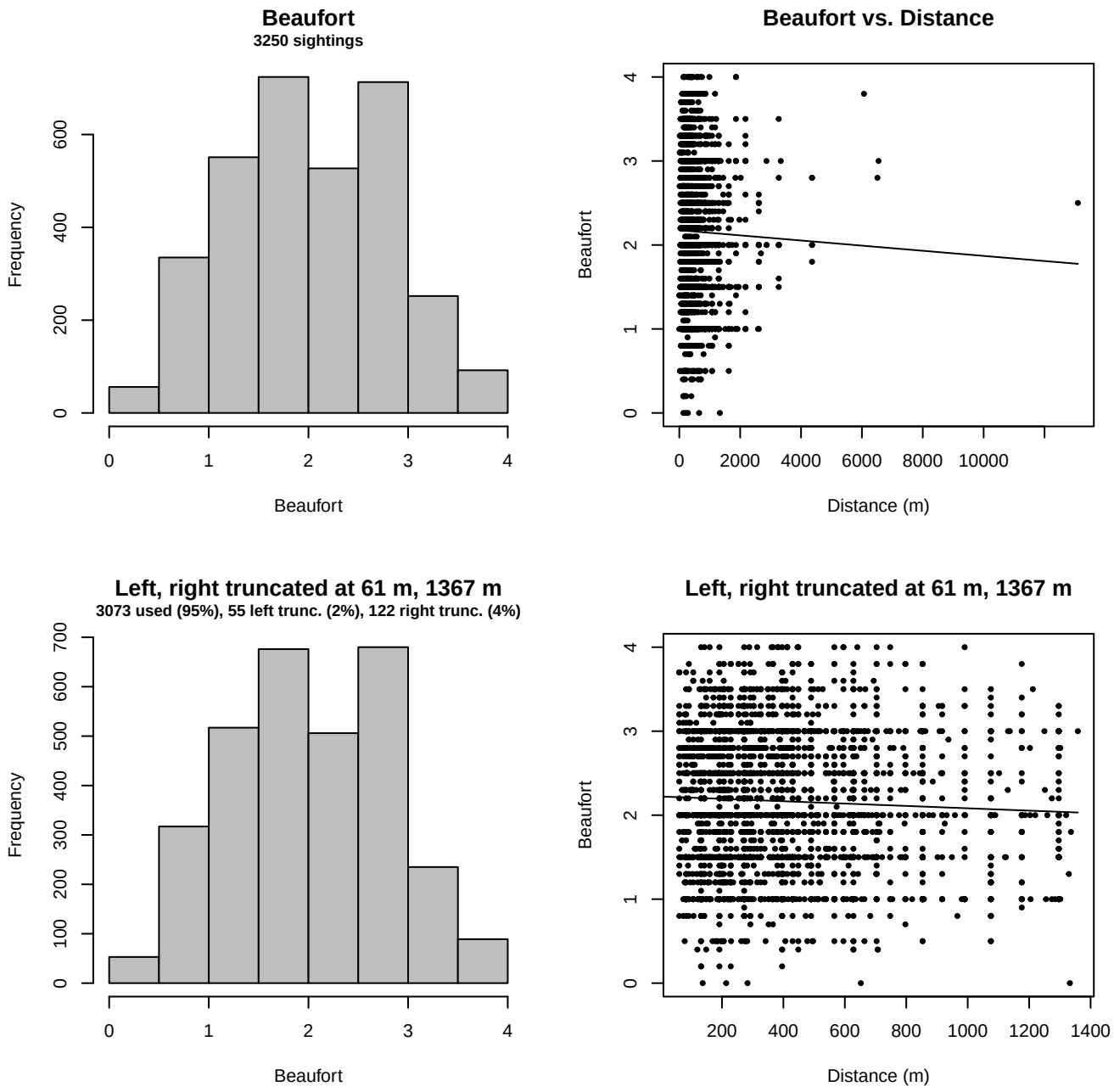

Figure 32: Distribution of the Beaufort covariate before (top row) and after (bottom row) observations were truncated to fit the NARWSS 2003-2016 detection function.

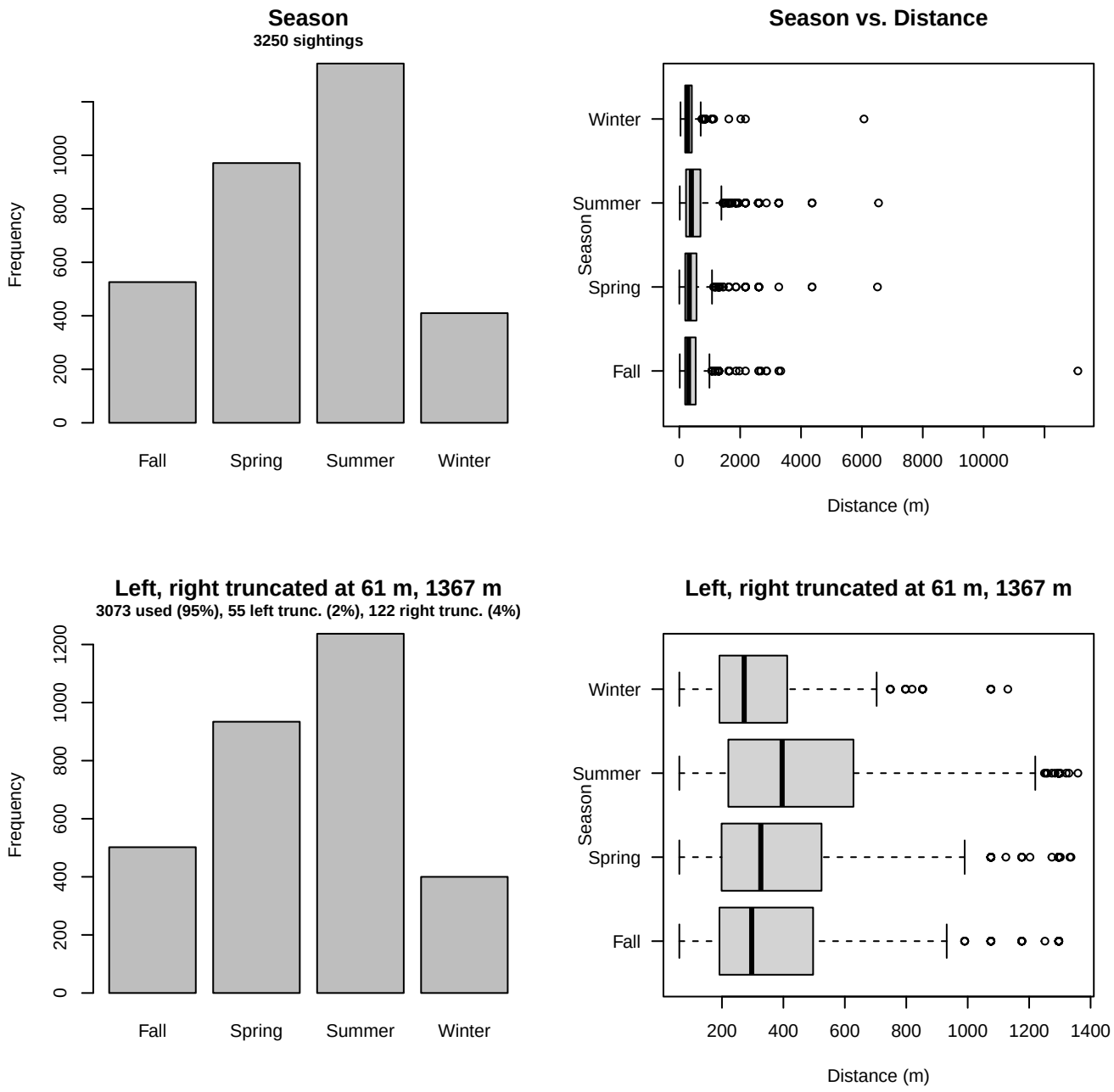

Figure 33: Distribution of the Season covariate before (top row) and after (bottom row) observations were truncated to fit the NARWSS 2003-2016 detection function.

2.2.1.5 UNCW Navy Surveys

After right-truncating observations greater than 1600 m, we fitted the detection function to the 1523 observations that remained (Table 13). The selected detection function (Figure 34) used a half normal key function with Glare (Figure 35) and Visibility (Figure 36) as covariates.

Table 13: Observations used to fit the UNCW Navy Surveys detection function.

ScientificName	n
Delphinus delphis	77
Lagenodelphis hosei	1
Stenella attenuata	2
Stenella clymene	11
Stenella coeruleoalba	19
Stenella frontalis	480
Stenella longirostris	1
Steno bredanensis	14
Tursiops truncatus	918
Total	**1523**

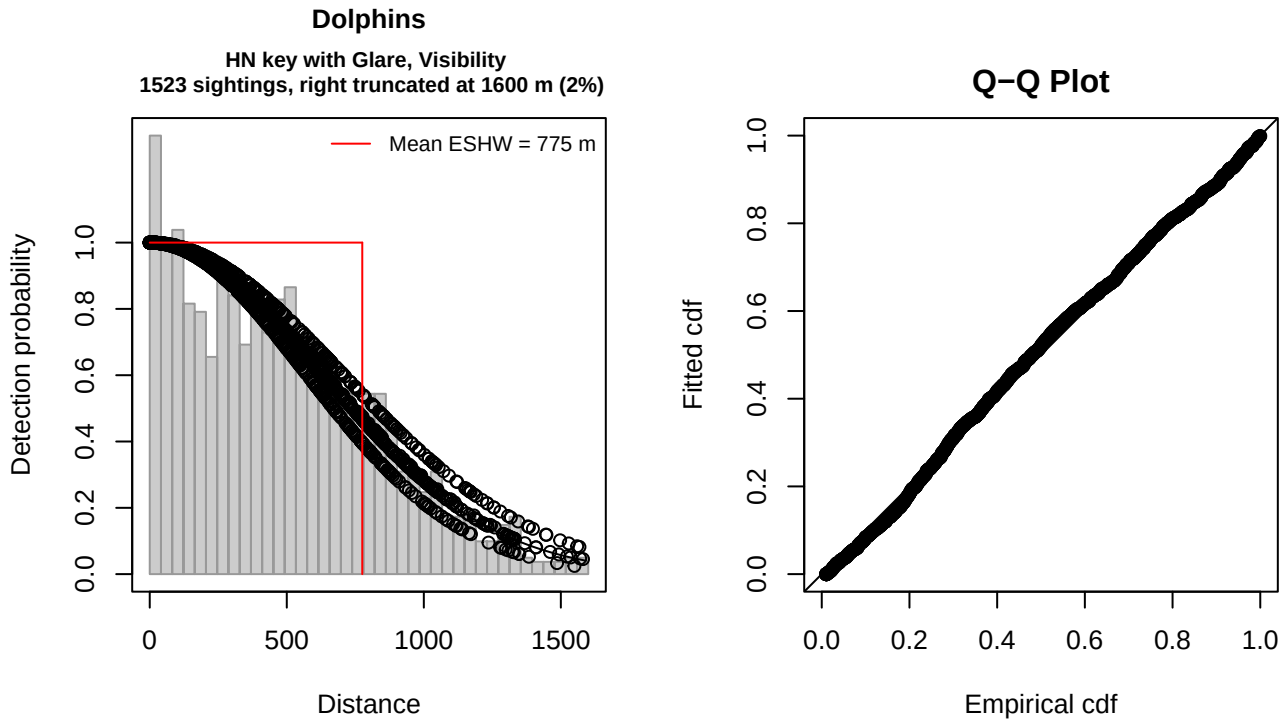

Figure 34: UNCW Navy Surveys detection function and Q-Q plot showing its goodness of fit.

Statistical output for this detection function:

```
Summary for ds object
Number of observations :  1523
Distance range         :  0  -  1600
AIC                    :  21665.78

Detection function:
 Half-normal key function

Detection function parameters
Scale coefficient(s):
                          estimate         se
(Intercept)             6.55223233 0.04798577
GlareNone, 0-25%, Unk. -0.10934970 0.05247015
VisibilityHalf         -0.09759271 0.04601702
```

```
                        Estimate          SE         CV
Average p               0.4827398  0.01003395 0.02078542
N in covered region 3154.9084328 87.71221948 0.02780183

Distance sampling Cramer-von Mises test (unweighted)
Test statistic = 0.331909  p = 0.110182
```

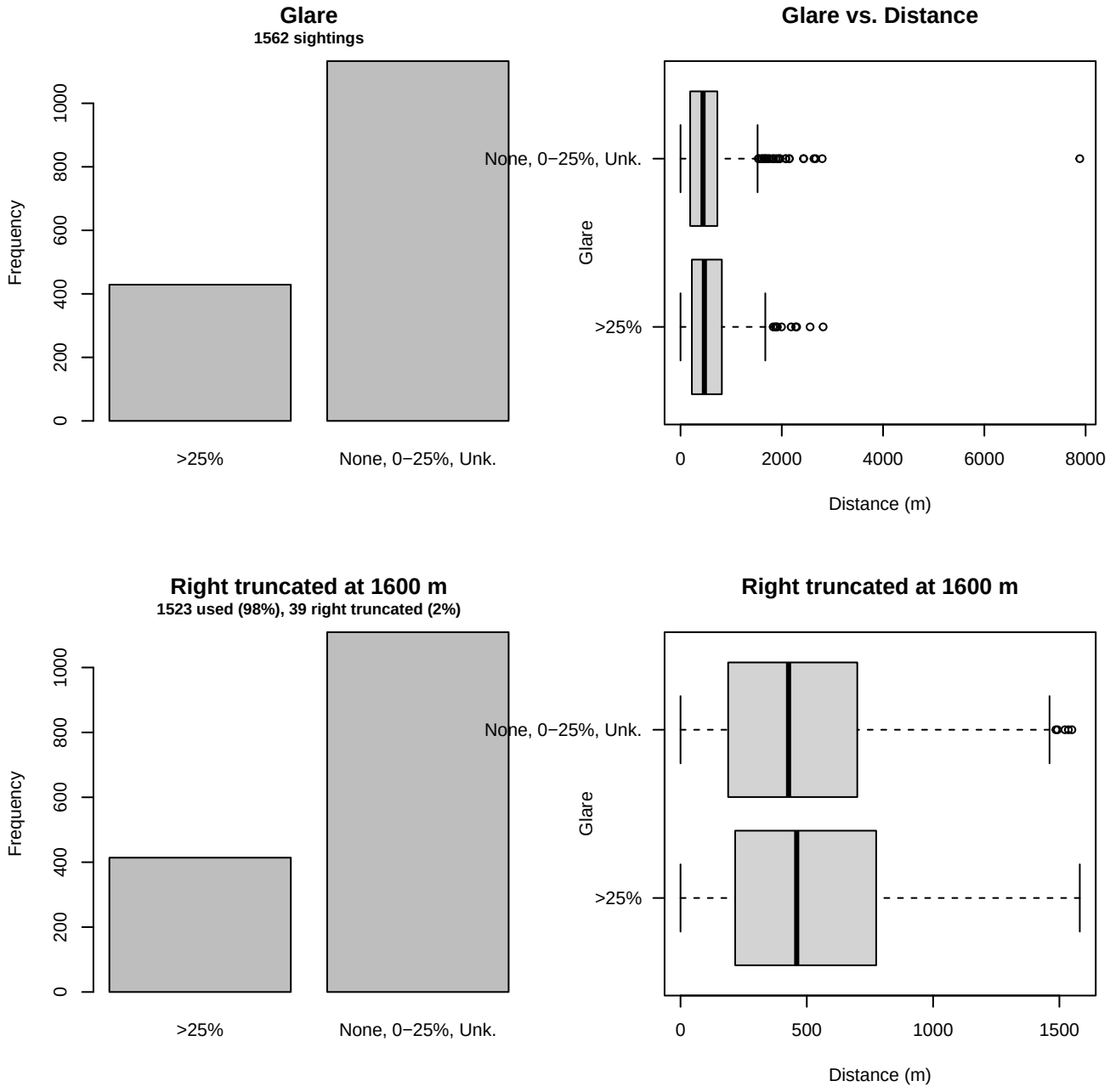

Figure 35: Distribution of the Glare covariate before (top row) and after (bottom row) observations were truncated to fit the UNCW Navy Surveys detection function.

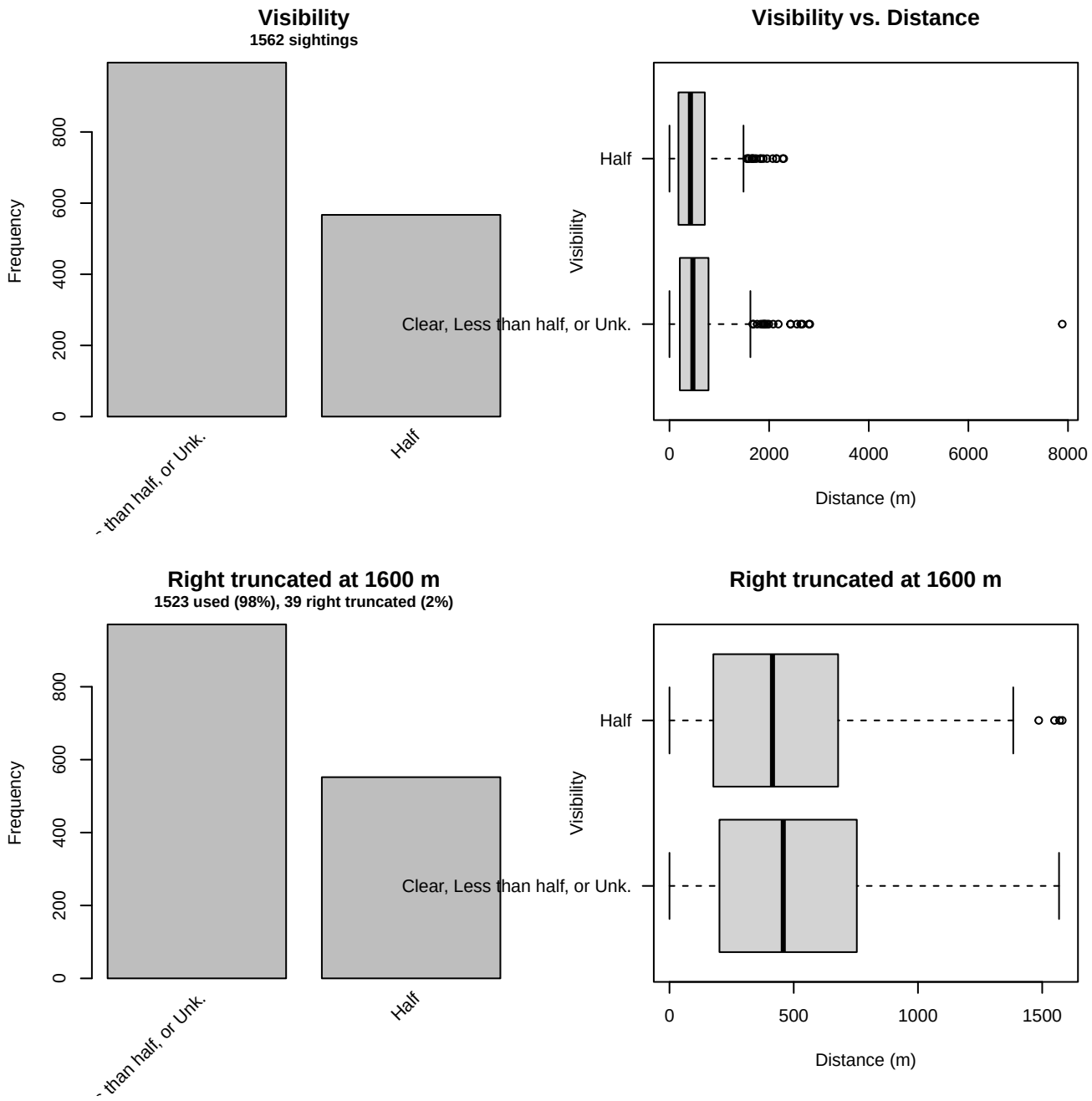

Figure 36: Distribution of the Visibility covariate before (top row) and after (bottom row) observations were truncated to fit the UNCW Navy Surveys detection function.

2.2.1.6 UNCW Right Whale Surveys

After right-truncating observations greater than 528 m and left-truncating observations less than 54 m (Figure 38), we fitted the detection function to the 1821 observations that remained (Table 14). The selected detection function (Figure 37) used a hazard rate key function with no covariates.

Table 14: Observations used to fit the UNCW Right Whale Surveys detection function.

ScientificName	n
Delphinus delphis	26
Stenella frontalis	4
Tursiops truncatus	1791
Total	**1821**

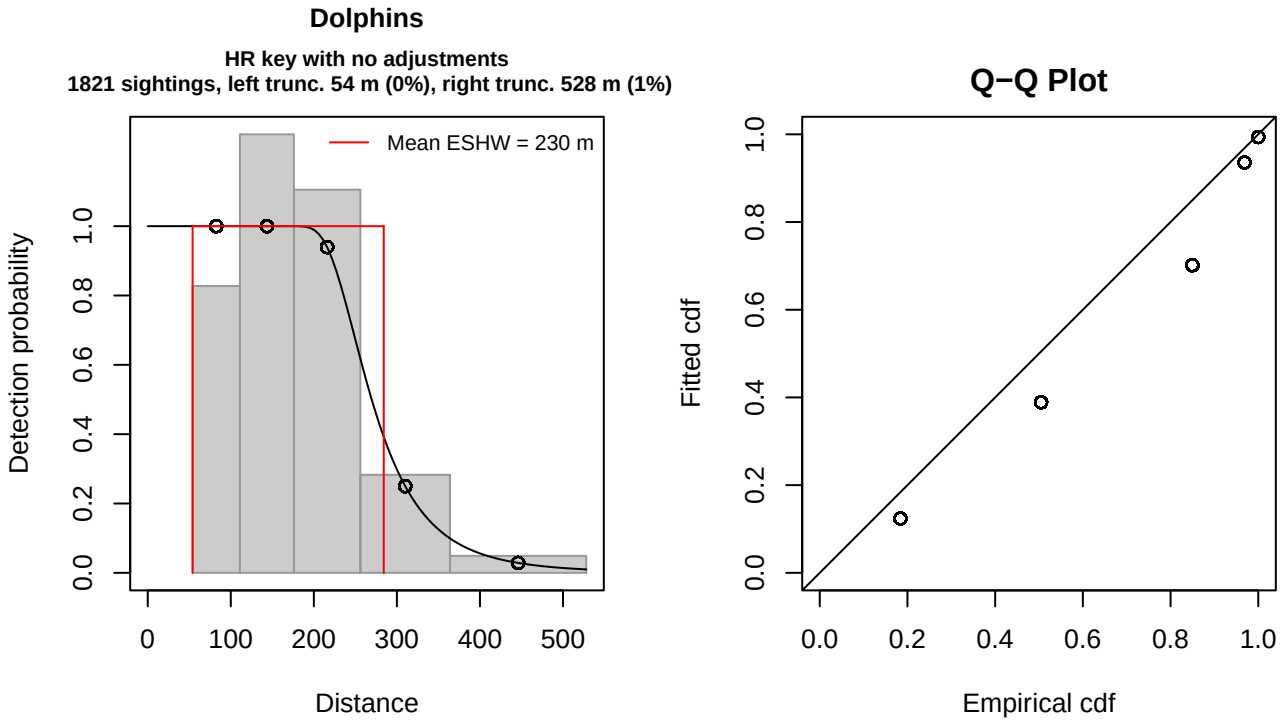

Figure 37: UNCW Right Whale Surveys detection function and Q-Q plot showing its goodness of fit.

Statistical output for this detection function:

```
Summary for ds object
Number of observations :  1821
Distance range         :  54  -  528
AIC                    :  5176.116

Detection function:
 Hazard-rate key function

Detection function parameters
Scale coefficient(s):
            estimate         se
(Intercept) 5.538954 0.02098751

Shape coefficient(s):
            estimate         se
(Intercept) 1.841299 0.06464608

                         Estimate           SE         CV
Average p                0.4855453  0.009233858 0.01901750
N in covered region 3750.4226341 95.188173832 0.02538065
```

```
Distance sampling Cramer-von Mises test (unweighted)
Test statistic = 14.468539  p = 0.010416
```

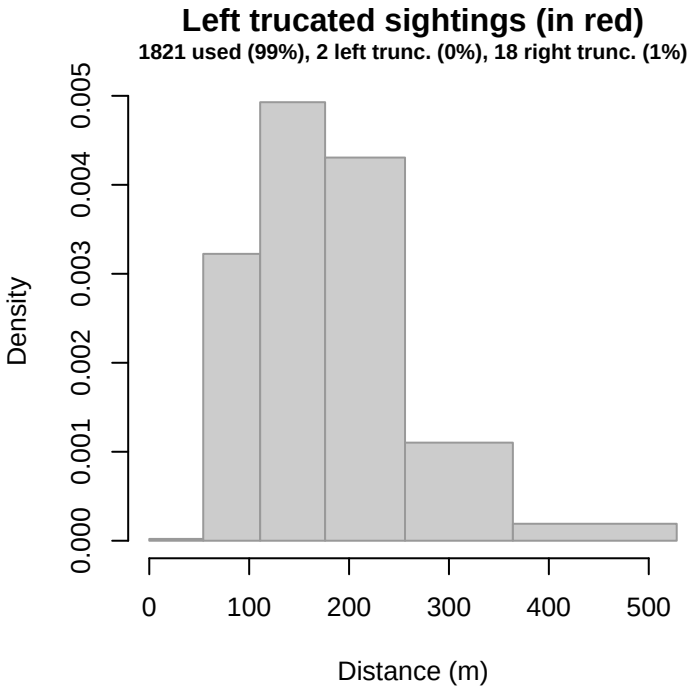

Figure 38: Density histogram of observations used to fit the UNCW Right Whale Surveys detection function, with the left-most bar showing observations at distances less than 54 m, which were left-truncated and excluded from the analysis [Buckland et al. (2001)]. (This bar may be very short if there were very few left-truncated sightings, or very narrow if the left truncation distance was very small; in either case it may not appear red.)

2.2.1.7 UNCW Early Surveys

After right-truncating observations greater than 333 m and left-truncating observations less than 14 m (Figure 40), we fitted the detection function to the 349 observations that remained (Table 15). The selected detection function (Figure 39) used a half normal key function with Beaufort (Figure 41) as a covariate.

Table 15: Observations used to fit the UNCW Early Surveys detection function.

ScientificName	n
Delphinus delphis	5
Stenella frontalis	1
Tursiops truncatus	343
Total	**349**

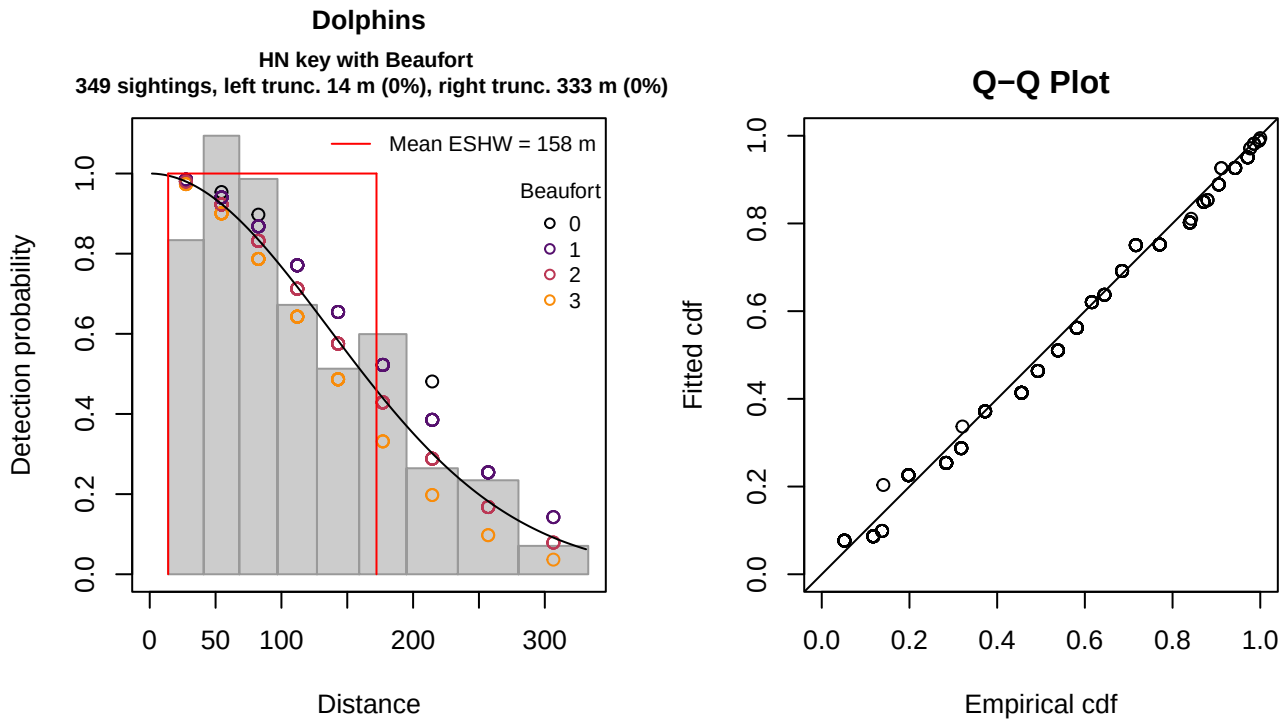

Figure 39: UNCW Early Surveys detection function and Q-Q plot showing its goodness of fit.

Statistical output for this detection function:

```
Summary for ds object
Number of observations :  349
Distance range         :  14  -  333
AIC                    :  1464.597

Detection function:
 Half-normal key function

Detection function parameters
Scale coefficient(s):
             estimate         se
(Intercept)  5.1778911 0.14575211
Beaufort    -0.1325498 0.07066838

                       Estimate          SE         CV
Average p              0.4915207  0.02352103 0.04785360
N in covered region 710.0413079 43.53534195 0.06131382

Distance sampling Cramer-von Mises test (unweighted)
Test statistic = 0.278162  p = 0.155953
```

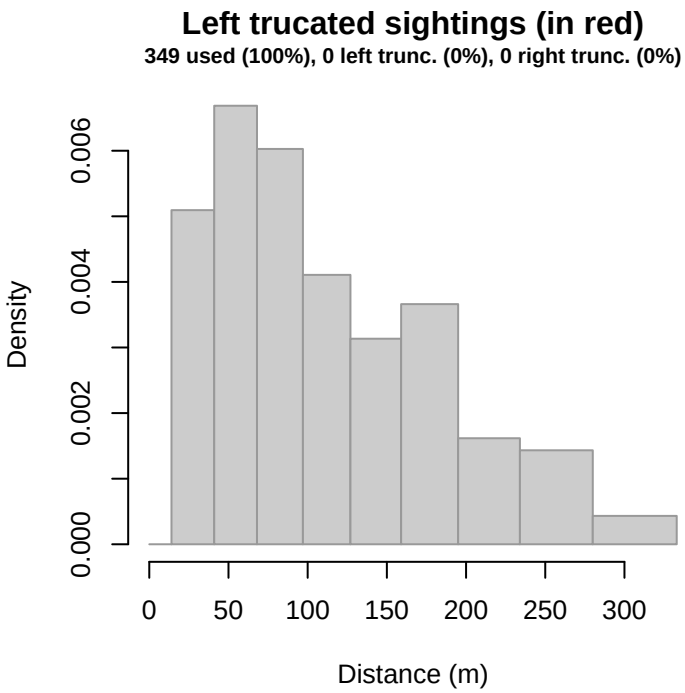

Figure 40: Density histogram of observations used to fit the UNCW Early Surveys detection function, with the left-most bar showing observations at distances less than 14 m, which were left-truncated and excluded from the analysis [Buckland et al. (2001)]. (This bar may be very short if there were very few left-truncated sightings, or very narrow if the left truncation distance was very small; in either case it may not appear red.)

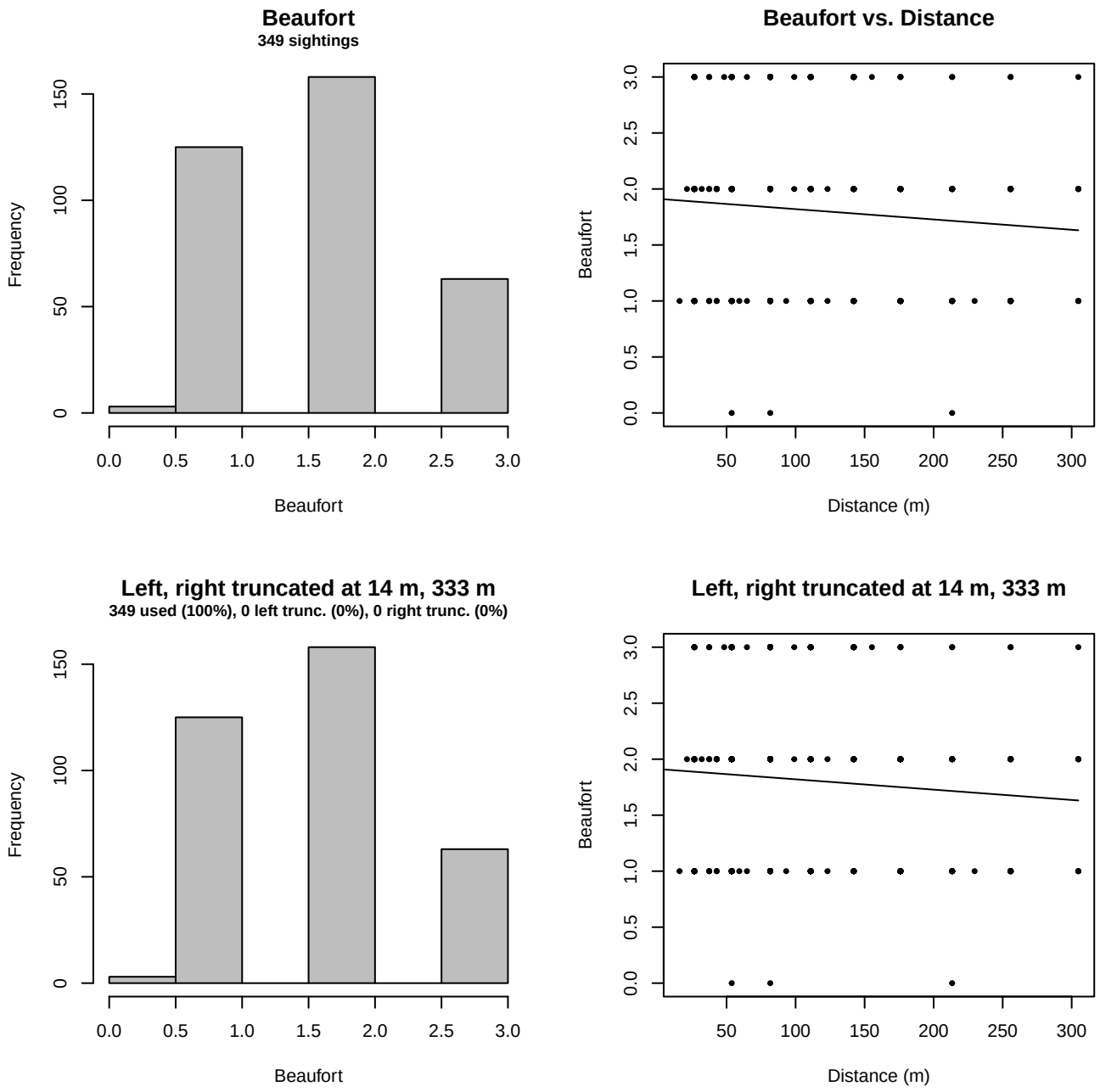

Figure 41: Distribution of the Beaufort covariate before (top row) and after (bottom row) observations were truncated to fit the UNCW Early Surveys detection function.

2.2.1.8 VAMSC

After right-truncating observations greater than 1000 m, we fitted the detection function to the 303 observations that remained (Table 16). The selected detection function (Figure 42) used a hazard rate key function with no covariates.

Table 16: Observations used to fit the VAMSC detection function.

ScientificName	n
Delphinus delphis	30
Stenella frontalis	4
Tursiops truncatus	269
Total	**303**

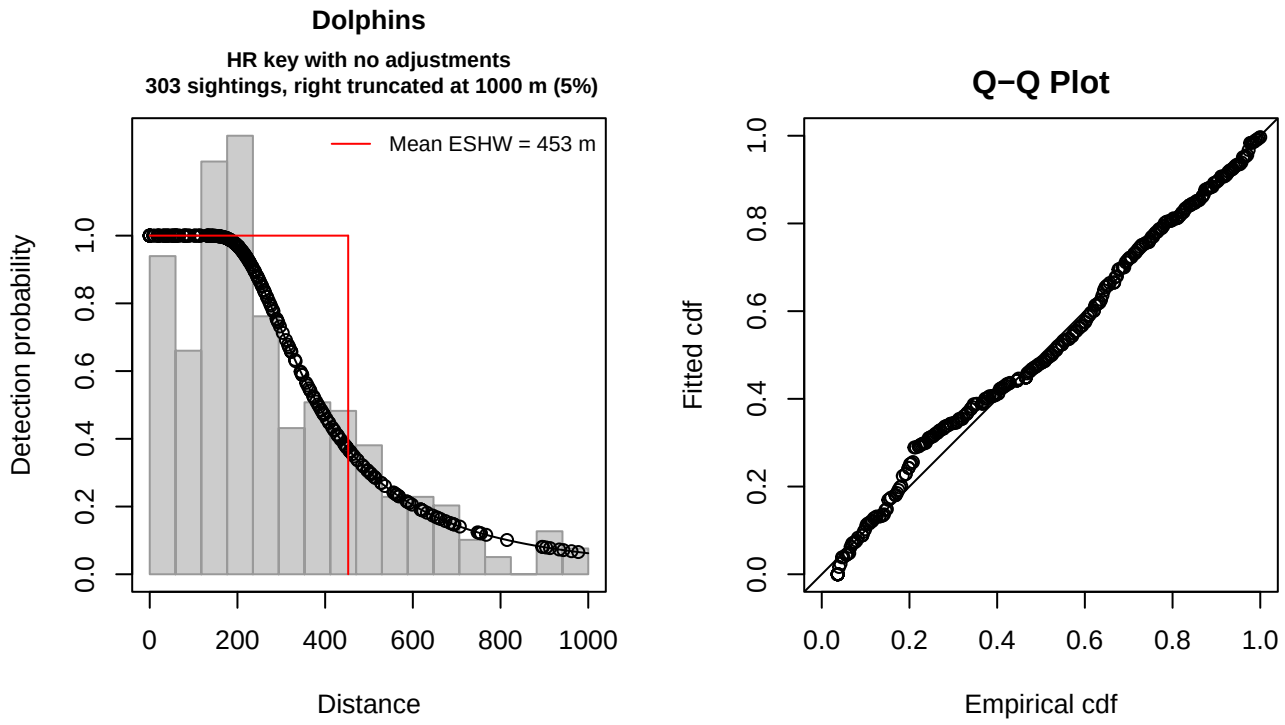

Figure 42: VAMSC detection function and Q-Q plot showing its goodness of fit.

Statistical output for this detection function:

```
Summary for ds object
Number of observations :  303
Distance range         :  0  -  1000
AIC                    :  3992.632

Detection function:
 Hazard-rate key function

Detection function parameters
Scale coefficient(s):
            estimate        se
(Intercept) 5.803823 0.1019737

Shape coefficient(s):
             estimate        se
(Intercept) 0.9119562 0.1438459

                       Estimate          SE         CV
Average p             0.4525805  0.02853931 0.06305908
N in covered region 669.4942067 50.91287837 0.07604678

Distance sampling Cramer-von Mises test (unweighted)
Test statistic = 0.212402  p = 0.244680
```

2.2.1.9 HDR

After right-truncating observations greater than 1500 m and left-truncating observations less than 111 m (Figure 44), we fitted the detection function to the 203 observations that remained (Table 17). The selected detection function (Figure 43) used a hazard rate key function with Season (Figure 45) and Swell (Figure 46) as covariates.

Table 17: Observations used to fit the HDR detection function.

ScientificName	n
Delphinus delphis	47
Stenella coeruleoalba	14
Stenella frontalis	19
Tursiops truncatus	123
Total	**203**

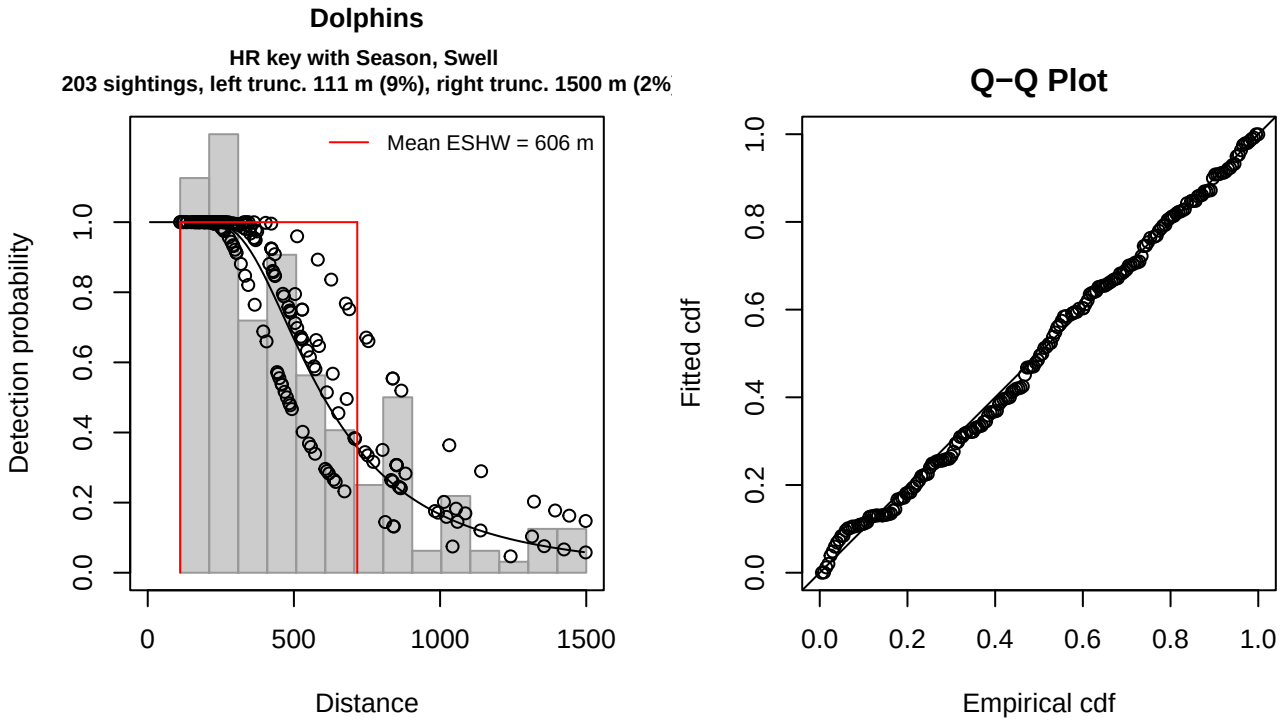

Figure 43: HDR detection function and Q-Q plot showing its goodness of fit.

Statistical output for this detection function:

```
Summary for ds object
Number of observations :  203
Distance range         :  111  -  1500
AIC                    :  2802.845

Detection function:
 Hazard-rate key function

Detection function parameters
Scale coefficient(s):
                       estimate        se
(Intercept)           6.3015171 0.1328018
SeasonWinter, Spring -0.2671651 0.1458664
Swell3-4              0.3527933 0.1530784

Shape coefficient(s):
            estimate        se
(Intercept) 1.026101 0.1620057

                     Estimate          SE         CV
```

```
Average p             0.419883  0.03654238 0.08702991
N in covered region 483.467993 49.56848062 0.10252691

Distance sampling Cramer-von Mises test (unweighted)
Test statistic = 0.059652  p = 0.816171
```

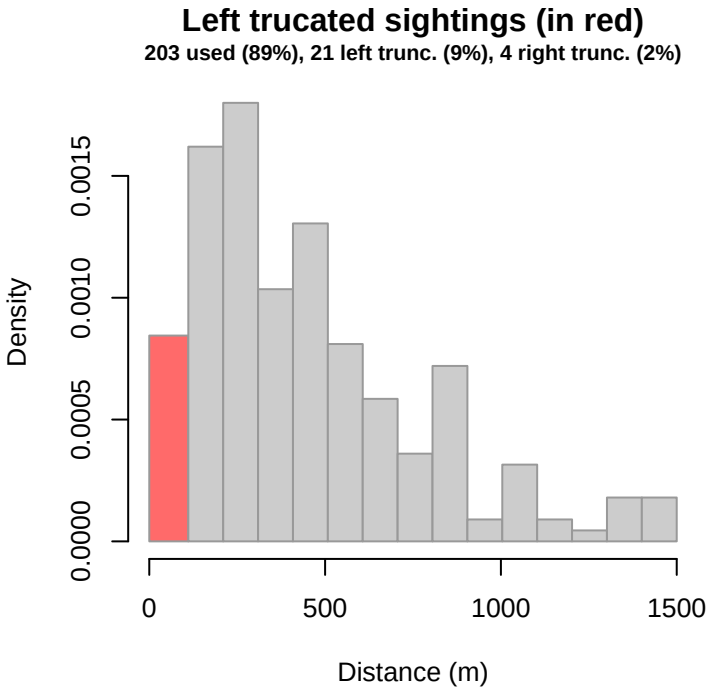

Figure 44: Density histogram of observations used to fit the HDR detection function, with the left-most bar showing observations at distances less than 111 m, which were left-truncated and excluded from the analysis [Buckland et al. (2001)]. (This bar may be very short if there were very few left-truncated sightings, or very narrow if the left truncation distance was very small; in either case it may not appear red.)

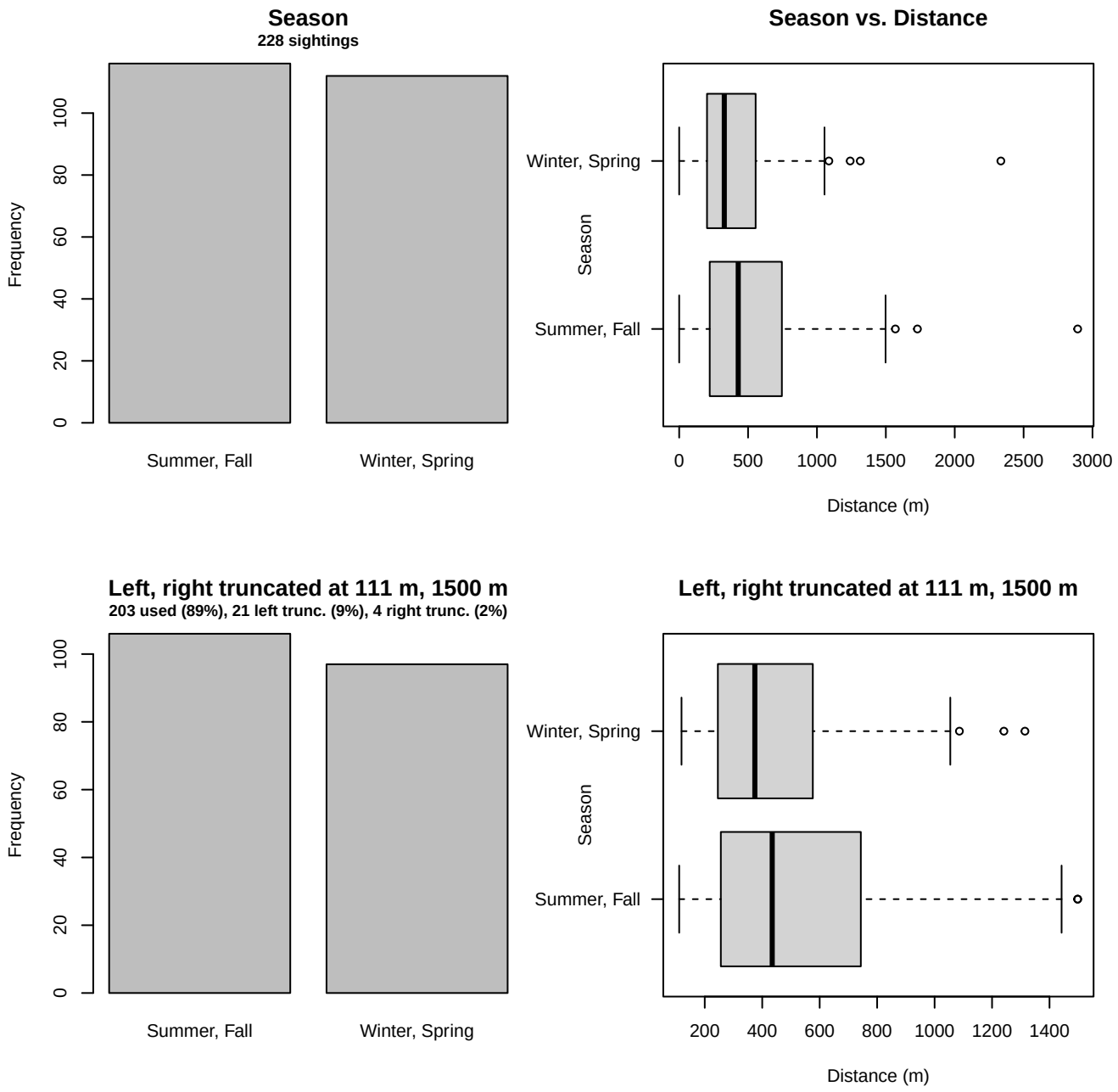

Figure 45: Distribution of the Season covariate before (top row) and after (bottom row) observations were truncated to fit the HDR detection function.

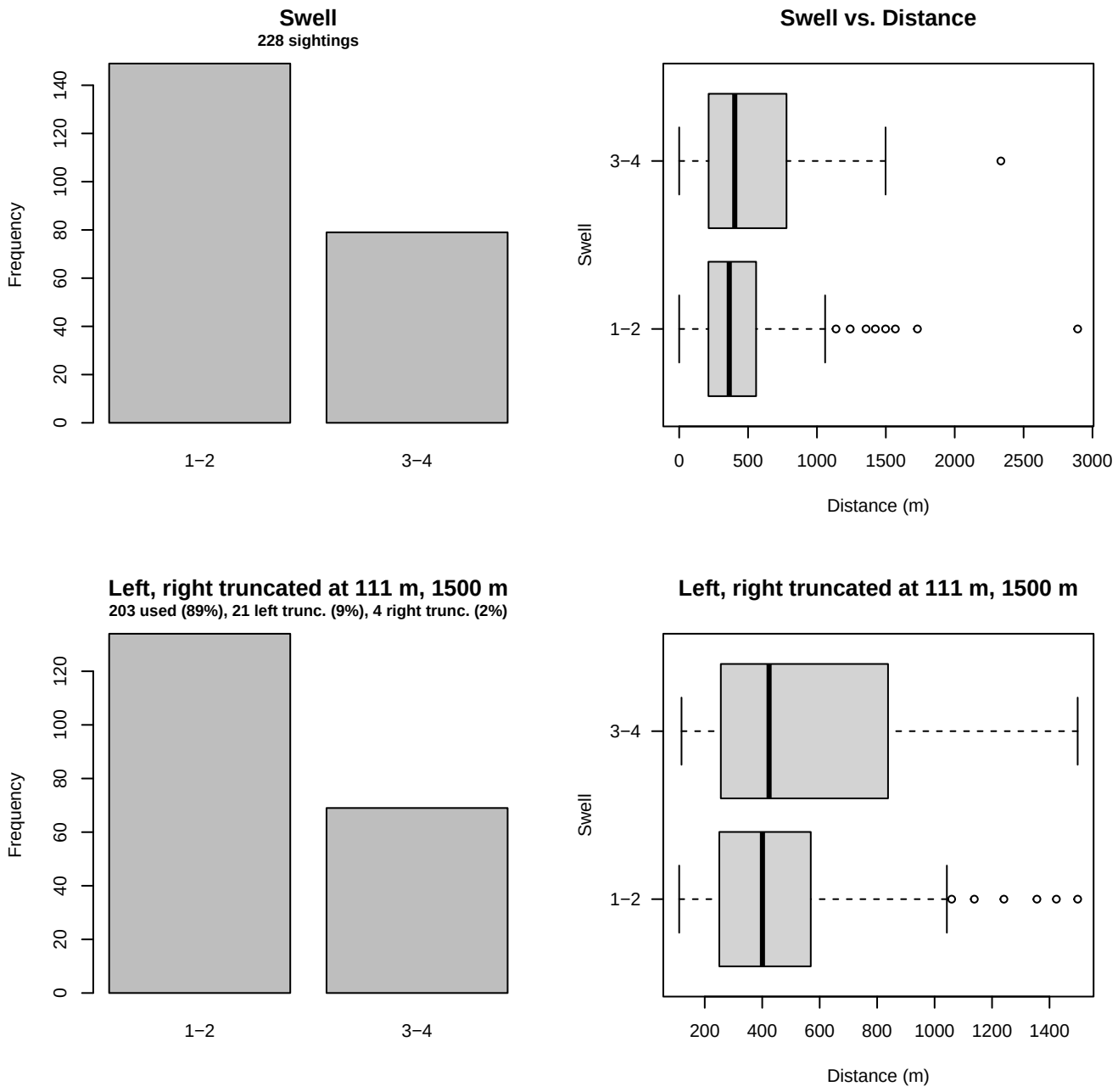

Figure 46: Distribution of the Swell covariate before (top row) and after (bottom row) observations were truncated to fit the HDR detection function.

2.2.2 Shipboard Surveys

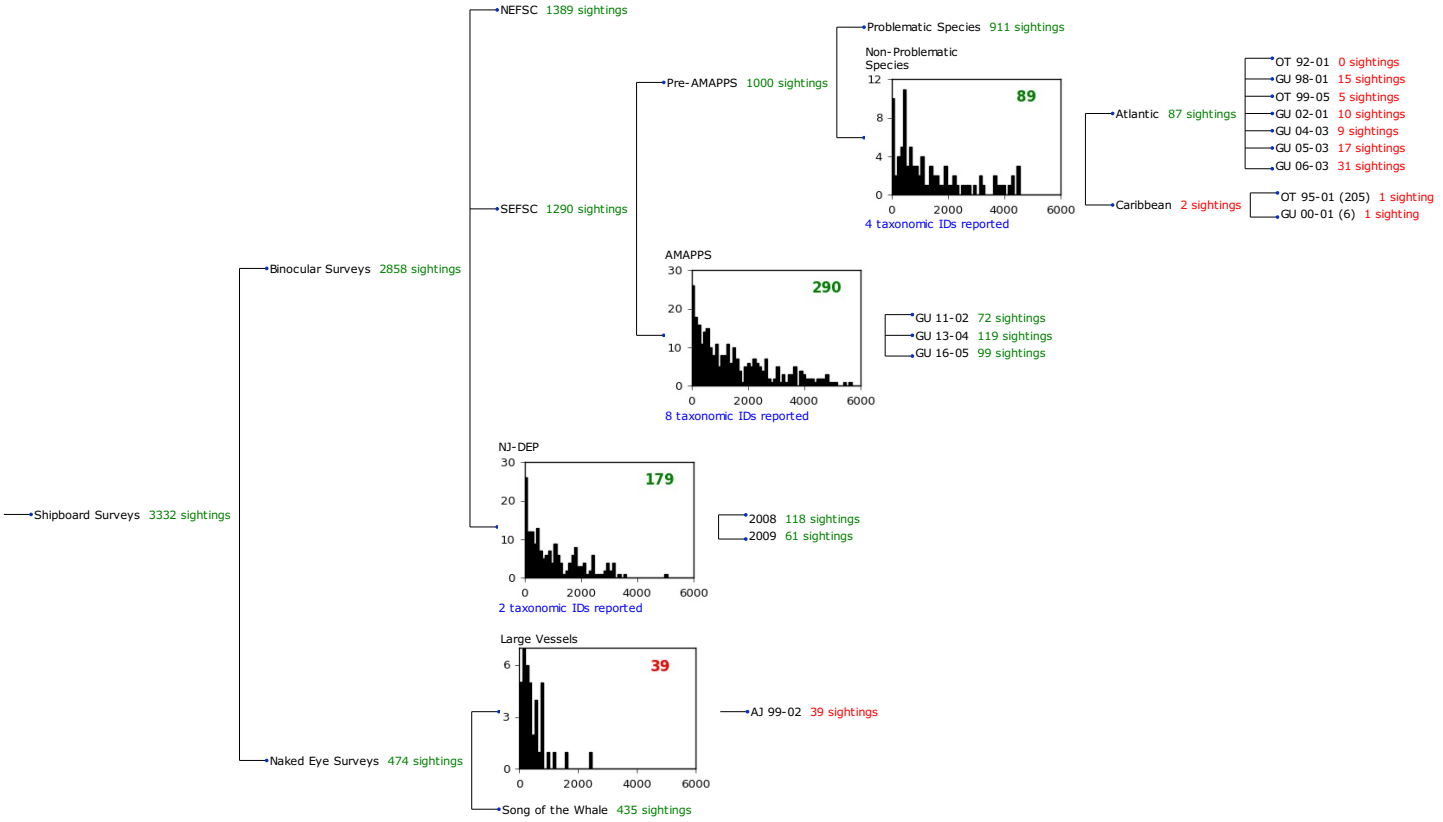

Figure 47: Detection hierarchy for shipboard surveys, showing how they were pooled during detectability modeling, for detection functions that pooled multiple taxa but could not use a taxonomic covariate to account for differences between them. Each histogram represents a detection function and summarizes the perpendicular distances of observations that were pooled to fit it, prior to truncation. Observation counts, also prior to truncation, are shown in green when they met the recommendation of Buckland et al. (2001) that detection functions utilize at least 60 sightings, and red otherwise. For rare taxa, it was not always possible to meet this recommendation, yielding higher statistical uncertainty. During the spatial modeling stage of the analysis, effective strip widths were computed for each survey using the closest detection function above it in the hierarchy (i.e. moving from right to left in the figure). Surveys that do not have a detection function above them in this figure were either addressed by a detection function presented in a different section of this report, or were omitted from the analysis.

2.2.2.1 SEFSC Pre-AMAPPS Non-Problematic Species

After right-truncating observations greater than 4700 m, we fitted the detection function to the 89 observations that remained (Table 18). The selected detection function (Figure 48) used a hazard rate key function with no covariates.

Table 18: Observations used to fit the SEFSC Pre-AMAPPS Non-Problematic Species detection function.

ScientificName	n
Lagenodelphis hosei	1
Stenella clymene	10
Stenella coeruleoalba	75
Stenella longirostris	3
Total	**89**

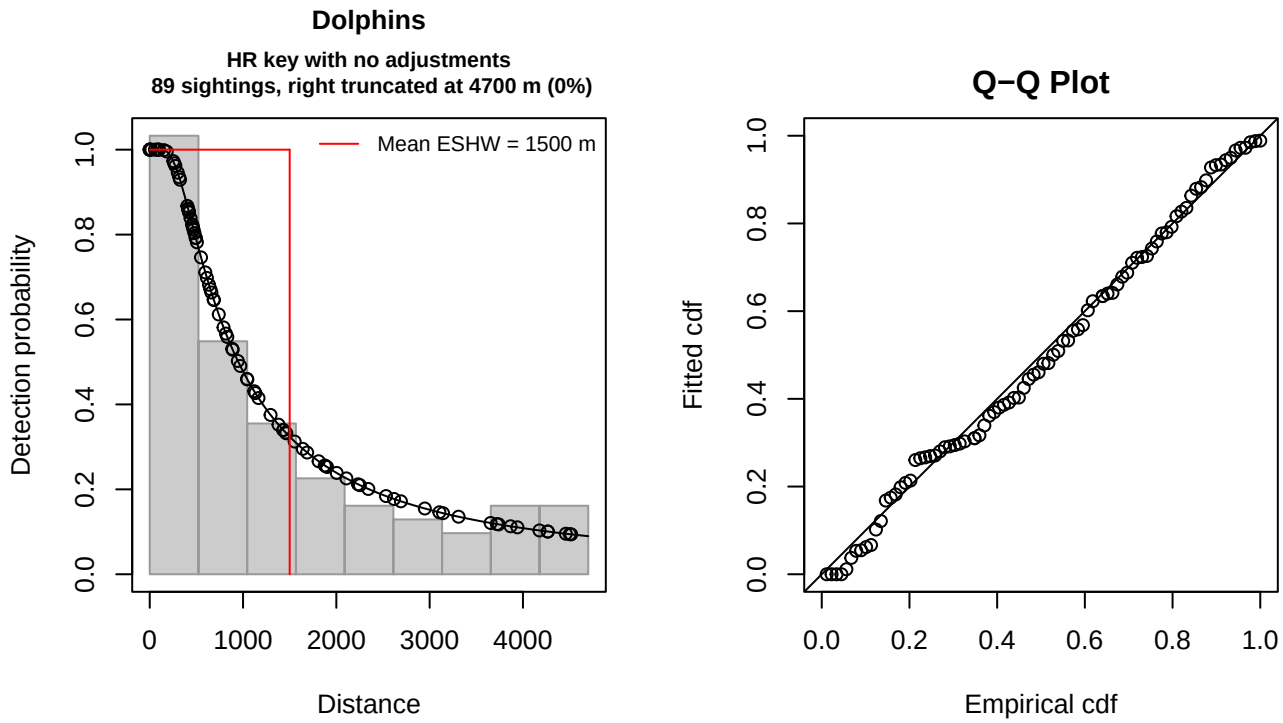

Figure 48: SEFSC Pre-AMAPPS Non-Problematic Species detection function and Q-Q plot showing its goodness of fit.

Statistical output for this detection function:

```
Summary for ds object
Number of observations :  89
Distance range         :  0  -  4700
AIC                    :  1457.185

Detection function:
 Hazard-rate key function

Detection function parameters
Scale coefficient(s):
            estimate        se
(Intercept) 6.562458 0.4314852

Shape coefficient(s):
             estimate        se
(Intercept) 0.2225386 0.2209014

                     Estimate          SE        CV
Average p             0.319168  0.07146324 0.2239048
N in covered region 278.850035 67.03032811 0.2403813

Distance sampling Cramer-von Mises test (unweighted)
Test statistic = 0.048231  p = 0.886935
```

2.2.2.2 SEFSC AMAPPS

After right-truncating observations greater than 5000 m, we fitted the detection function to the 284 observations that remained (Table 19). The selected detection function (Figure 49) used a hazard rate key function with Beaufort (Figure 50) as a covariate.

Table 19: Observations used to fit the SEFSC AMAPPS detection function.

ScientificName	n
Delphinus delphis	2
Stenella attenuata	10
Stenella clymene	3
Stenella coeruleoalba	11
Stenella frontalis	84
Stenella longirostris	1
Steno bredanensis	2
Tursiops truncatus	171
Total	**284**

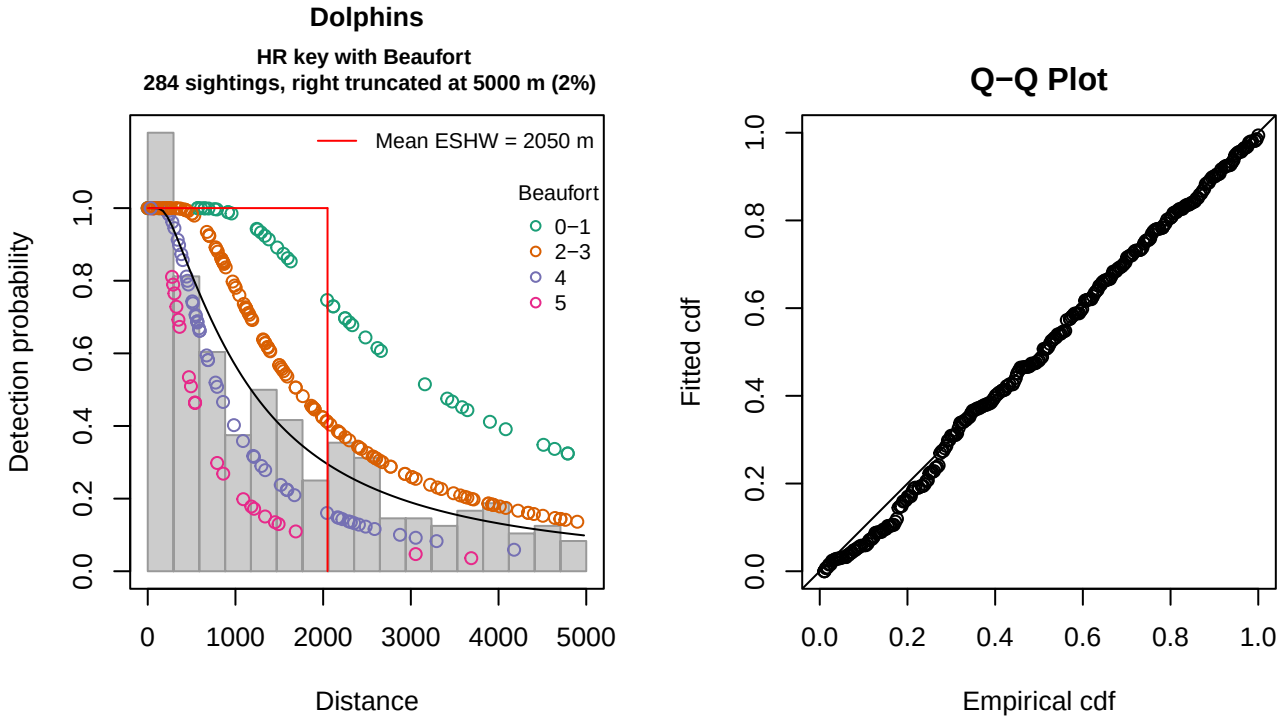

Figure 49: SEFSC AMAPPS detection function and Q-Q plot showing its goodness of fit.

Statistical output for this detection function:

```
Summary for ds object
Number of observations :  284
Distance range         :  0  -  5000
AIC                    :  4678.464

Detection function:
 Hazard-rate key function

Detection function parameters
Scale coefficient(s):
              estimate        se
(Intercept)  7.8386611 0.3487749
Beaufort2-3 -0.6450433 0.3816484
Beaufort4   -1.3990617 0.4441169
Beaufort5   -1.8689041 0.5186901
```

```
Shape coefficient(s):
             estimate        se
(Intercept) 0.3878689 0.1380351

                        Estimate           SE        CV
Average p               0.3478259   0.03965009 0.1139941
N in covered region 816.5004271 101.68622285 0.1245391

Distance sampling Cramer-von Mises test (unweighted)
Test statistic = 0.107898  p = 0.547527
```

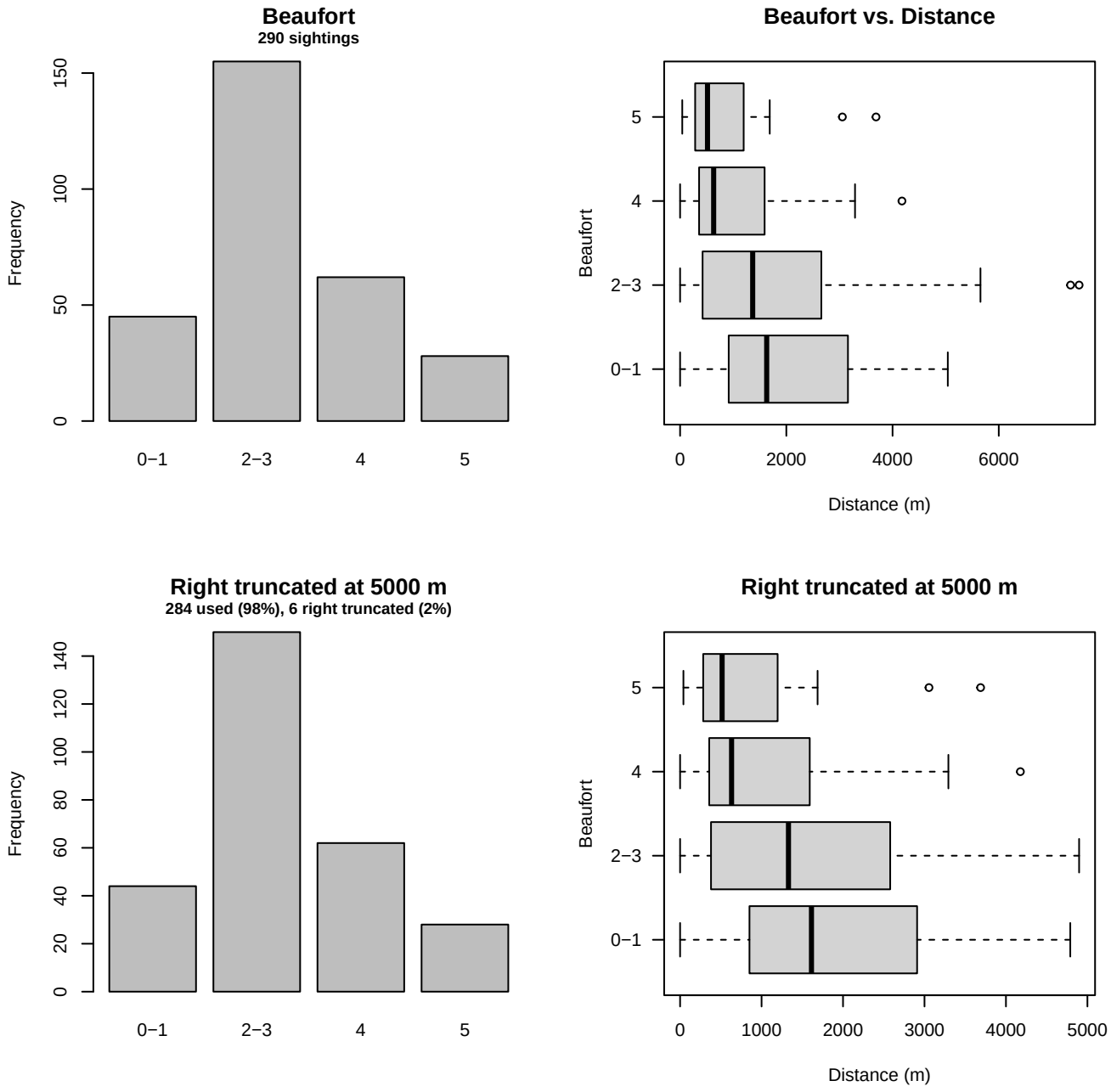

Figure 50: Distribution of the Beaufort covariate before (top row) and after (bottom row) observations were truncated to fit the SEFSC AMAPPS detection function.

2.2.2.3 NJ-DEP

After right-truncating observations greater than 3200 m, we fitted the detection function to the 175 observations that remained (Table 20). The selected detection function (Figure 51) used a hazard rate key function with no covariates.

Table 20: Observations used to fit the NJ-DEP detection function.

ScientificName	n
Delphinus delphis	19
Tursiops truncatus	156
Total	**175**

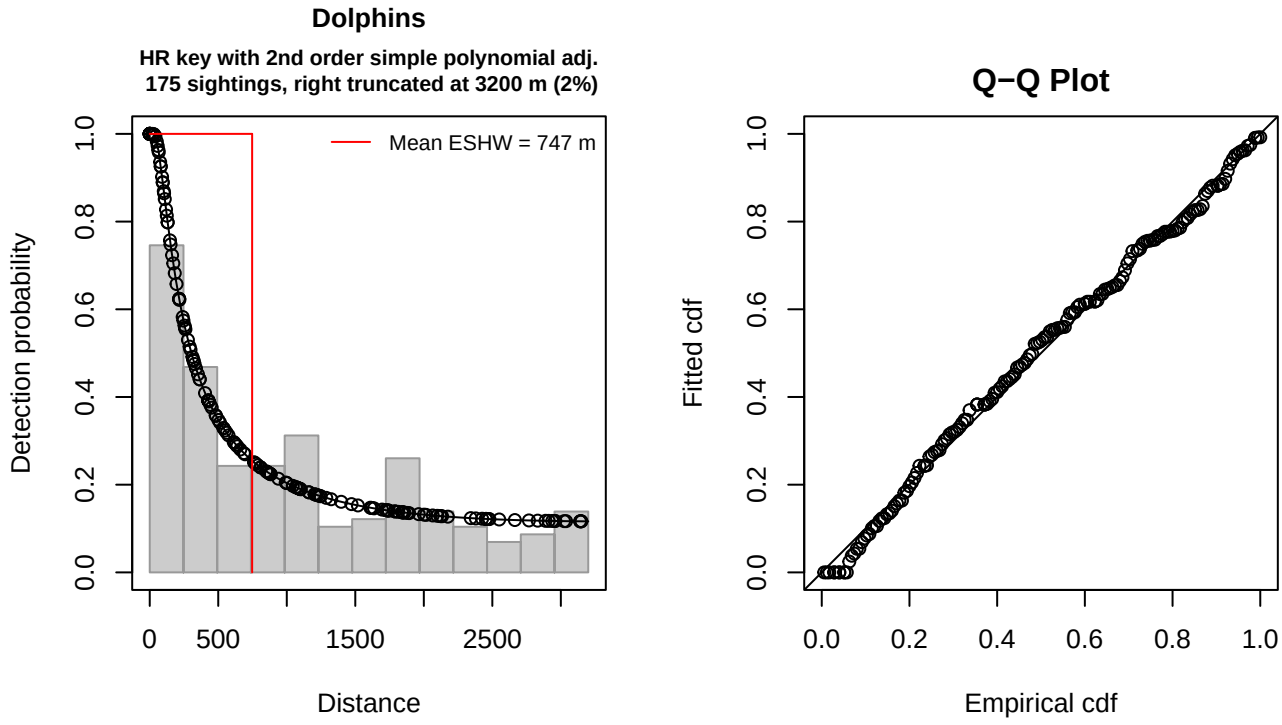

Figure 51: NJ-DEP detection function and Q-Q plot showing its goodness of fit.

Statistical output for this detection function:

```
Summary for ds object
Number of observations :  175
Distance range         :  0  -  3200
AIC                    :  2750.547

Detection function:
 Hazard-rate key function with simple polynomial adjustment term of order 2

Detection function parameters
Scale coefficient(s):
            estimate       se
(Intercept) 5.340225 0.502875

Shape coefficient(s):
                estimate        se
(Intercept) 2.663565e-07 0.3025183
```

```
Adjustment term coefficient(s):
               estimate       se
poly, order 2 0.8448098 1.306568


Monotonicity constraints were enforced.
                        Estimate           SE        CV
Average p              0.2335197   0.05159473 0.2209438
N in covered region 749.4013460 172.84391894 0.2306427

Monotonicity constraints were enforced.

Distance sampling Cramer-von Mises test (unweighted)
Test statistic = 0.069450  p = 0.754942
```

2.2.2.4 Large Vessels

After right-truncating observations greater than 1100 m, we fitted the detection function to the 36 observations that remained (Table 21). The selected detection function (Figure 52) used a half normal key function with no covariates.

Table 21: Observations used to fit the Large Vessels detection function.

ScientificName	n
Lagenorhynchus acutus	36
Total	**36**

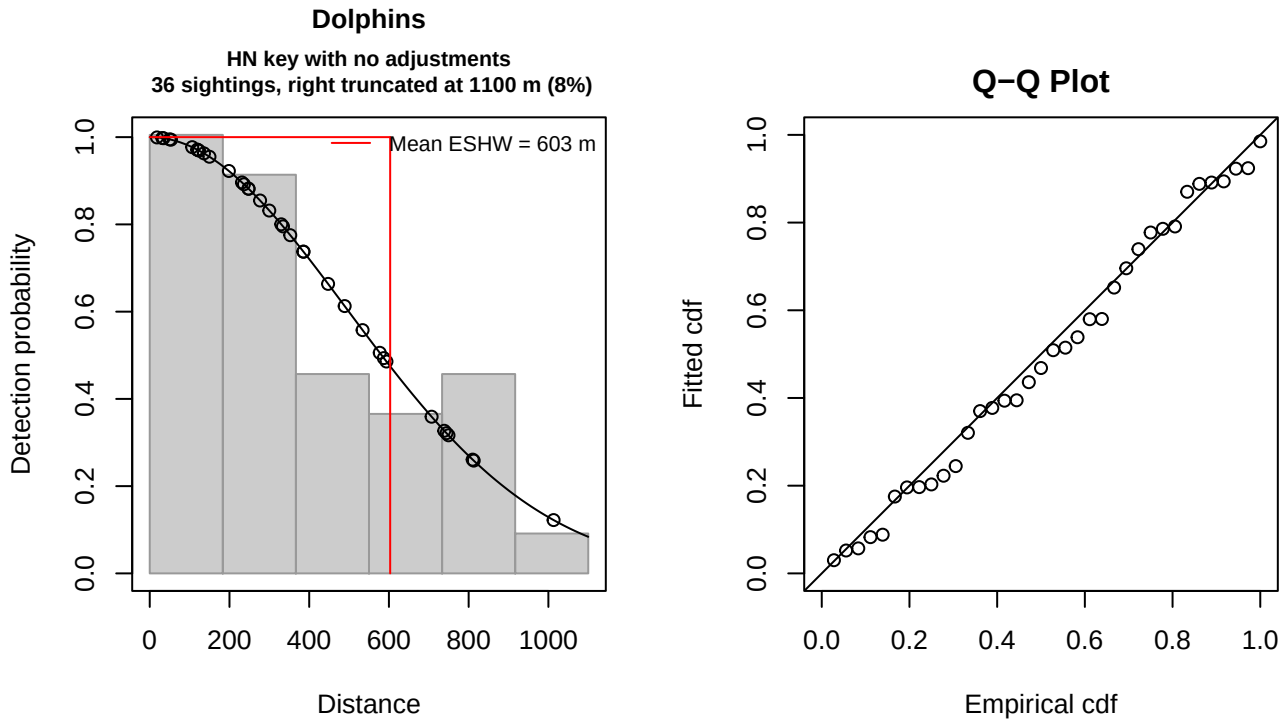

Figure 52: Large Vessels detection function and Q-Q plot showing its goodness of fit.

Statistical output for this detection function:

```
Summary for ds object
Number of observations :  36
Distance range         :  0  -  1100
```

```
AIC                    :  493.4472

Detection function:
 Half-normal key function

Detection function parameters
Scale coefficient(s):
            estimate        se
(Intercept) 6.202683 0.1646341

                       Estimate          SE        CV
Average p             0.5483057  0.07646146 0.1394504
N in covered region 65.6568085 11.74385160 0.1788672

Distance sampling Cramer-von Mises test (unweighted)
Test statistic = 0.026241  p = 0.986825
```

3 Bias Corrections

Density surface modeling methodology uses *distance sampling* (Buckland et al. 2001) to model the probability that an observer on a line transect survey will detect an animal given the perpendicular distance to it from the transect line. Distance sampling assumes that detection probability is 1 when perpendicular distance is 0. When this assumption is not met, detection probability is biased high, leading to an underestimation of density and abundance. This is known as the $g_0 < 1$ problem, where g_0 refers to the detection probability at distance 0. Modelers often try to address this problem by estimating g_0 empirically and dividing it into estimated density or abundance, thereby correcting those estimates to account for the animals that were presumed missed.

Two important sources of bias for visual surveys are known as *availability bias*, in which an animal was present on the transect line but impossible to detect, e.g. because it was under water, and *perception bias*, in which an animal was present and available but not noticed, e.g. because of its small size or cryptic coloration or behavior (Marsh and Sinclair 1989). Modelers often estimate the influence of these two sources of bias on detection probability independently, yielding two estimates of g_0, hereafter referred to as g_{0A} and g_{0P}, and multiply them together to obtain a final, combined estimate: $g_0 = g_{0A}.g_{0P}$.

Our overall approach was to perform this correction on a per-observation basis, to have the flexibility to account for many factors such as platform type, surveyor institution, group size, group composition (e.g. singleton, mother-calf pair, or surface active group), and geographic location (e.g. feeding grounds vs. calving grounds). The level of complexity of the corrections varied by species according to the amount of information available, with North Atlantic right whale having the most elaborate corrections, derived from a substantial set of publications documenting its behavior, and various lesser known odontocetes having corrections based only on platform type (aerial or shipboard), derived from comparatively sparse information. Here we document the corrections used for spinner dolphin.

3.1 Aerial Surveys

Only one aerial sighting was reported of this rare species, a mixed group of 70 spinner dolphins and 70 Clymene dolphins, sighted by UNCW in 2011 in the U.S. Navy's Cape Hatteras study area. To this sighting, we applied the perception bias correction factor of Carretta et al. (2000) for groups of more than 25 delphinids: $g_{0P} = 0.994$.

Our usual practice for estimating availability bias was to apply, on a per-sighting basis, the Laake et al. (1997) estimator, which requires the use of dive and surface intervals. We could find no intervals in the literature for spinner dolphin, but this was of little consequence because the next step was to apply the group availability estimator of McLellan et al. (2018). The group availability estimator assumes the individuals in the group dive asynchronously. Under this assumption, for a group of 70 animals, $g_{0A} > 0.99$, even for the longest diving animals, for which the single animal estimate might be $g_{0A} = 0.1$. As a proxy, we used the dive intervals for striped dolphin from Palka et al. (2017) and the resulting estimate for the group of 70 was $g_{0A} = 1$.

3.2 Shipboard Surveys

The four shipboard sightings of spinner dolphins available for analysis were reported by NEFSC and SEFSC on NOAA's broad scale abundance surveys that used high-power (25x150), pedestal-mounted binoculars. Palka et al. (2021) developed

perception bias corrections using two team, MRDS methodology (Burt et al. 2014) for high-power binocular surveys conducted in 2010-2017 by NEFSC and SEFSC during the AMAPPS program. Spinner dolphin was not included in the species modeled, so we used striped dolphin as a proxy (Table 22). We applied this correction to all high-power binocular sightings, including those prior to the AMAPPS program.

To account for the influence of large group sizes on perception bias, we followed Barlow and Forney (2007) and set the perception bias correction factor for sightings of more than 20 animals to $g_{0P} = 0.97$. Given that the dive interval of this species (Table 23) was short relative to the amount of time a given patch of water remained in view to shipboard observers, we assumed that no availability bias correction was needed ($g_{0A} = 1$).

Although we included the MCR Song of the Whale surveys that observed by naked eye, they reported no sightings so no corrections were needed under our methodology.

Table 22: Perception and availability bias corrections for spinner dolphin applied to shipboard surveys.

Surveys	Searching Method	Group Size	g_{0P}	g_{0P} Source	g_{0A}	g_{0A} Source
NEFSC	Binoculars	≤ 20	0.72	Palka et al. (2021): NEFSC: striped dolphin	1	Assumed
SEFSC	Binoculars	≤ 20	0.62	Palka et al. (2021): SEFSC: striped dolphin	1	Assumed
All	All	> 20	0.97	Barlow and Forney (2007)	1	Assumed

Table 23: Surface and dive intervals for spinner dolphin used to estimate availability bias corrections.

Surface Interval (s)	Dive Interval (s)	Source
44	59.4	Palka et al. (2017): striped dolphin

4 Geographic Strata

With so few sightings, it was not possible to fit a traditional density surface model that related density observed on survey segments to environmental covariates. Nor was it possible to make proper design-based abundance estimates using traditional distance sampling (Buckland et al. 2001), because the aggregate surveys provided very heterogeneous coverage that did not together constitute a proper systematic survey design.

To provide interested parties with at least rough estimates of density in ecologically relevant geographic strata, we first split the study area into six strata (Figure 1) at major habitat boundaries. We placed our first split at the continental shelf break, defined as the 100 meter isobath, separating the study area in into shelf and offshore regions. (We manually cut across the Northeast Channel of the Gulf of Maine, so that the Gulf was considered part of the shelf.) We then split the shelf region at Cape Hatteras, a location where the Gulf Stream separates from the continental shelf, which has previously been used to delineate community structure in marine mammals (Schick et al. 2011). We also split the shelf region at the Nantucket Shoals, which separate the Gulf of Maine from the New York Bight. We split off the bays and sounds of New York, Rhode Island, and southern Massachusetts, generally at the 10 m isobath, on the basis that these inshore areas are rarely visited by cetaceans of any species. Finally, we split the offshore region at the north wall of the Gulf Stream, starting at Cape Hatteras and extending along the north wall of the Gulf Stream, as defined with a long-term climatology of total kinetic energy, to the edge of the study area.

We then derived density estimates for each stratum by fitting a model with no covariates, under the assumption that density would be distributed uniformly within the stratum. This assumption, if true, would mean we would obtain similar density estimates for a given stratum under any sampling design, and therefore it would not matter if there was some heterogeneity in sampling within the stratum. However, we strongly caution that this assumption did not hold for the other, more-common species we successfully modeled with traditional density surface modeling, as evidenced by the non-uniform patterns in density predicted by those species' models. That said, when those results are viewed at a very coarse, ecoregional scale, the boundaries used here often correlate with boundaries or strong gradients in density in those models. Thus, for the much rarer species, such as spinner dolphin documented here, we offer this simplified approach as a rough-and-ready substitute for a full density surface model.

In this section, we present maps of each stratum that contained sightings, with tallies of effort and sightings that occurred.

4.1 Offshore North of Gulf Stream

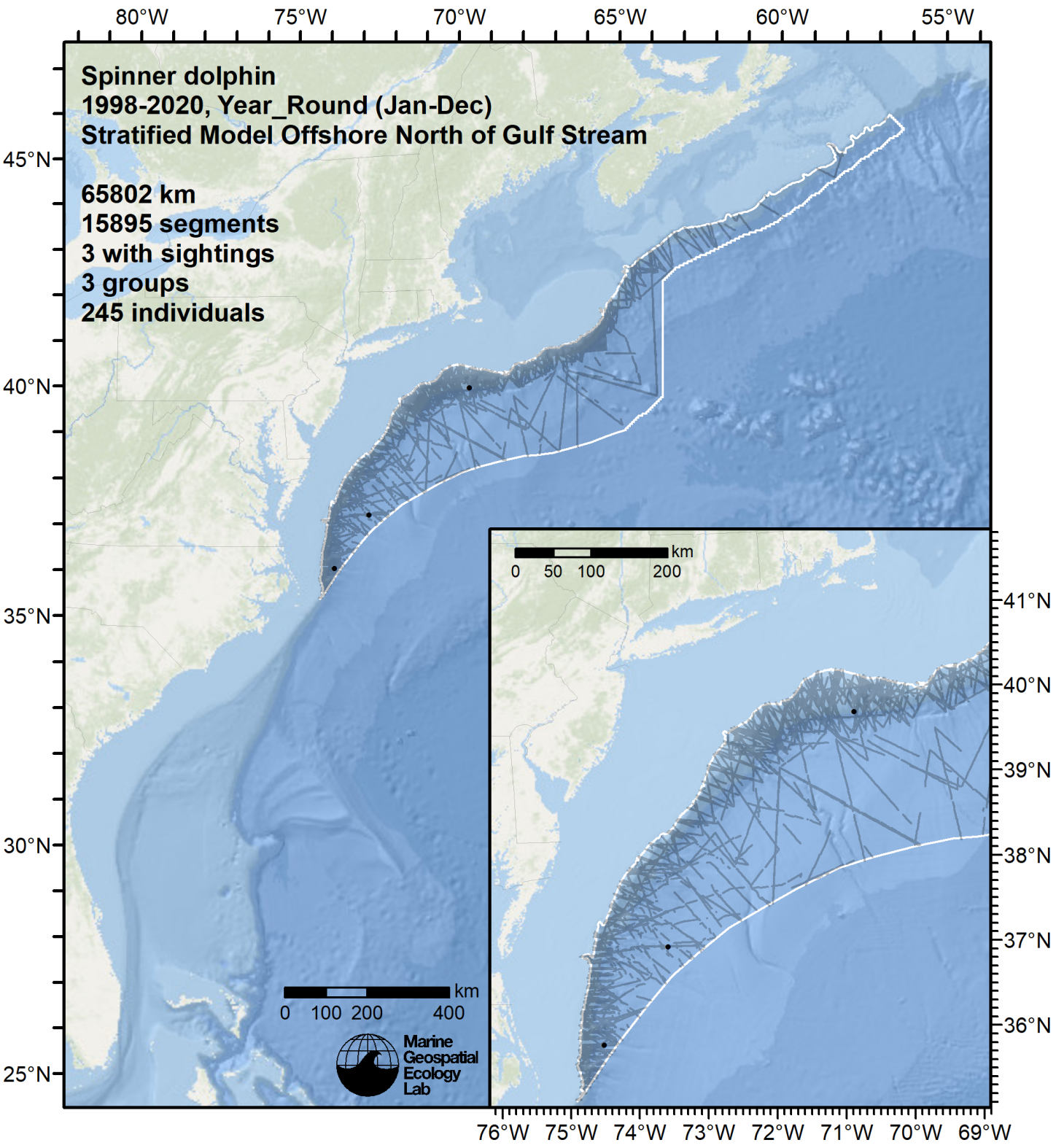

Figure 53: Survey segments and sightings used to estimate spinner dolphin density for the "Offshore North of Gulf Stream" region. Black points indicate segments with observations.

4.2 Offshore Gulf Stream and South

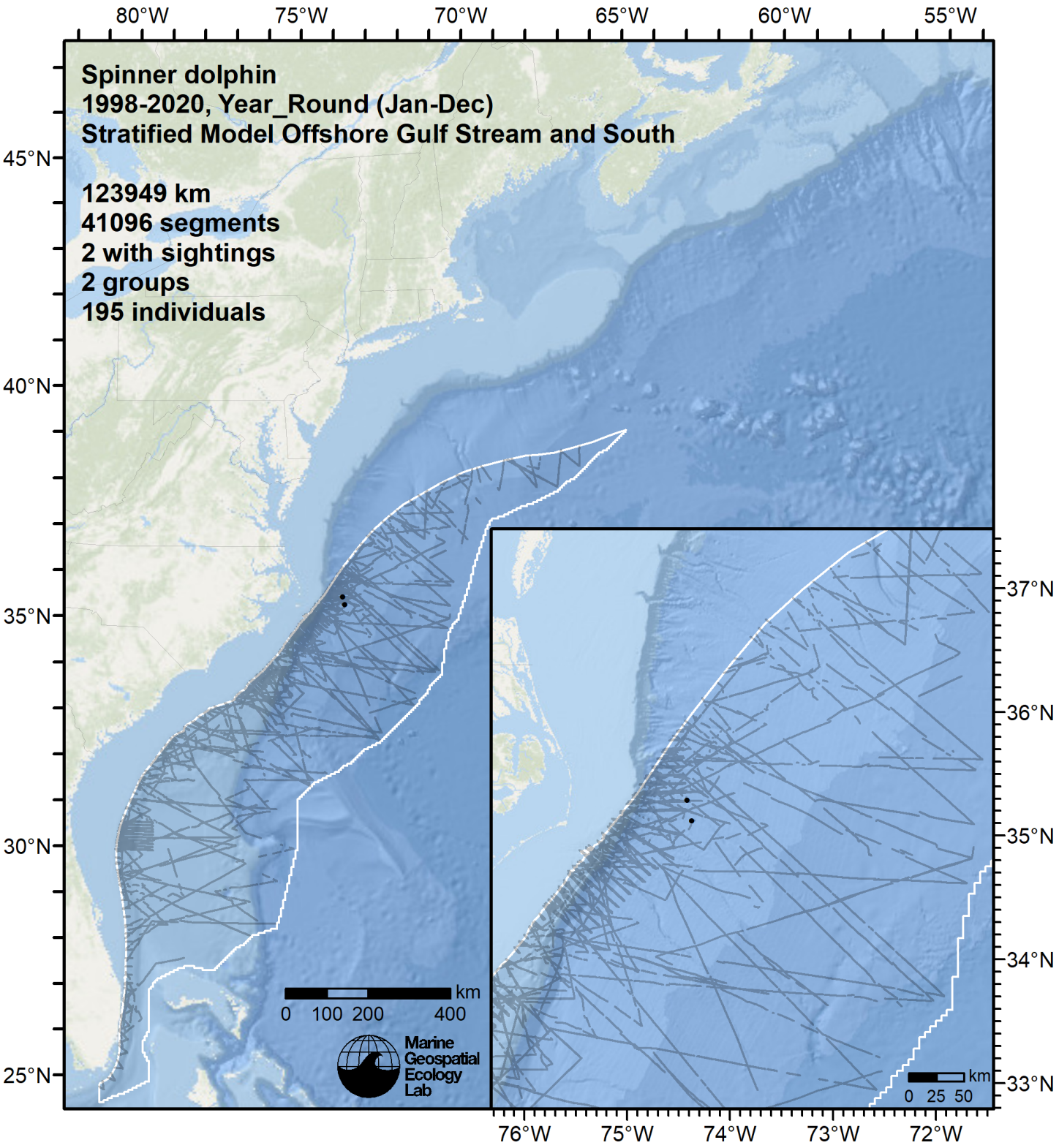

Figure 54: Survey segments and sightings used to estimate spinner dolphin density for the "Offshore Gulf Stream and South" region. Black points indicate segments with observations.

5 Predictions

5.1 Summarized Predictions

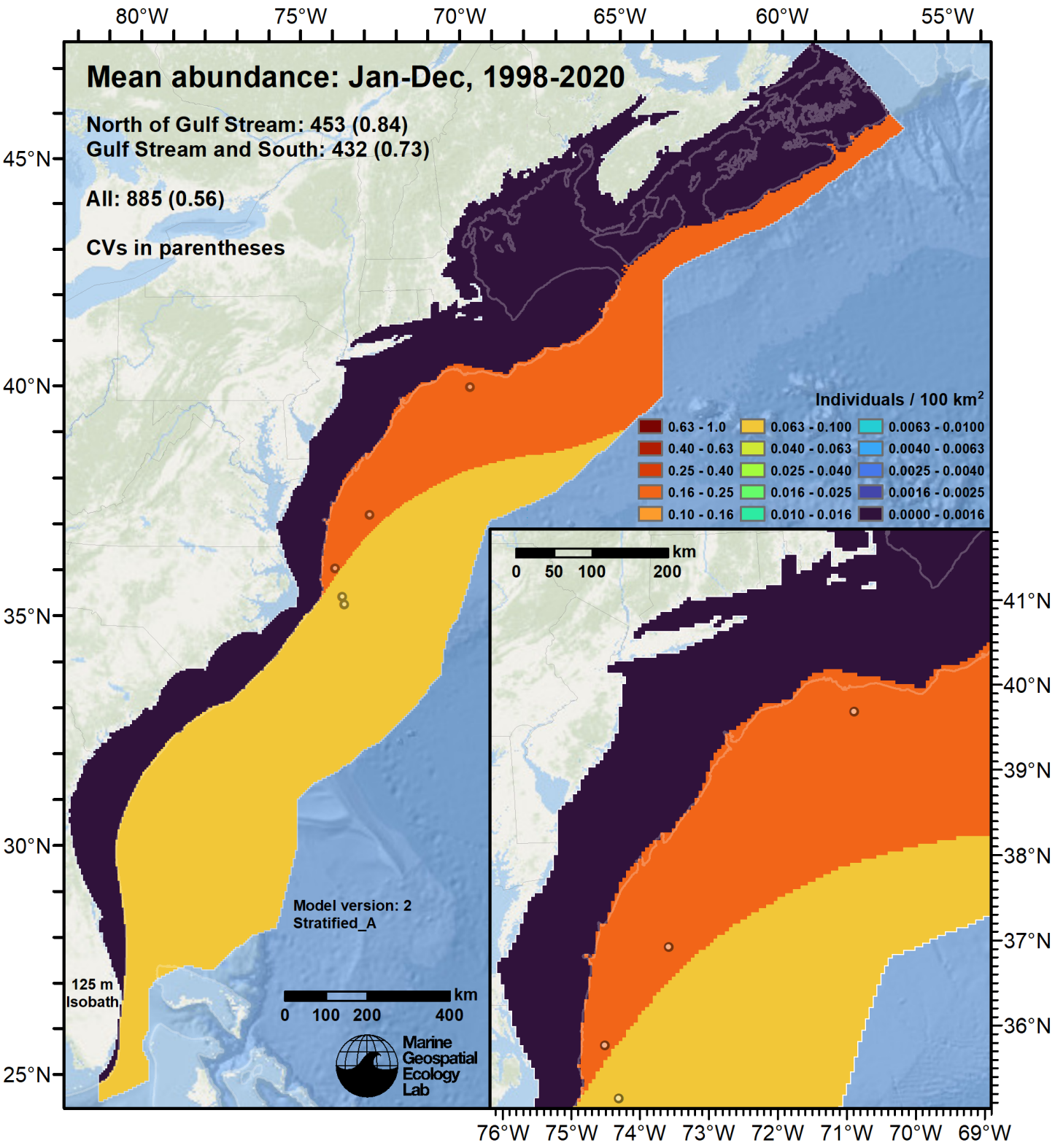

Figure 55: Spinner dolphin density estimated for the indicated period. Open circles indicate segments with observations. The abundance estimate and its coefficient of variation (CV) are given in the subtitle.

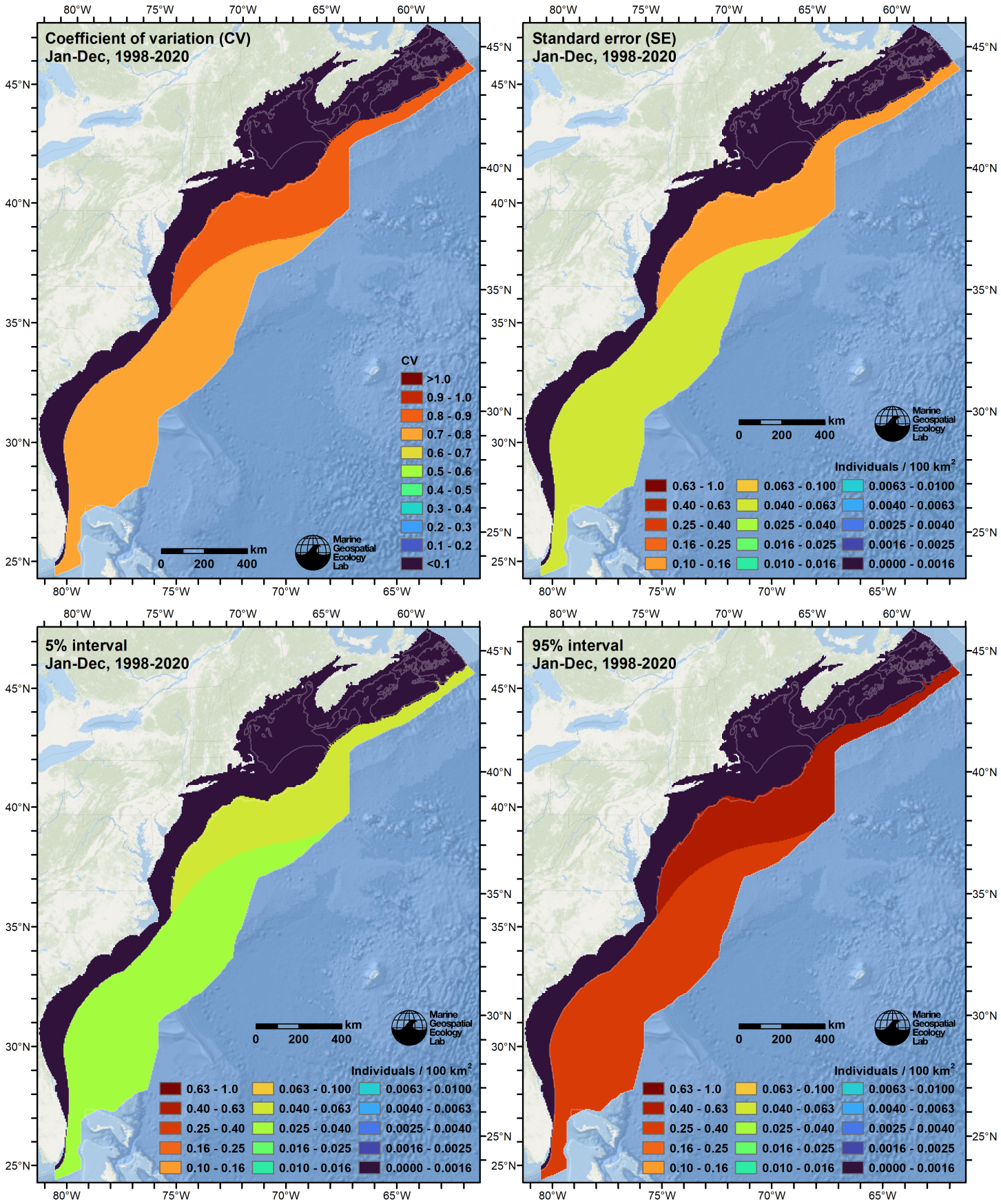

Figure 56: Uncertainty statistics for the spinner dolphin estimated density surface (Figure 55).

Table 24: Spinner dolphin abundance and density estimated for each stratum.

Region	Abundance	CV	95% Interval	Area (km^2)	Density (indiv. / 100 km^2)
Offshore Gulf Stream and South	432	0.727	121 - 1,550	499,300	0.087
Offshore North of Gulf Stream	453	0.838	108 - 1,894	253,575	0.179
Shelf Cape Hatt. to Nant. Shoals	0	0.000	0 - 0	104,425	0.000
Shelf North of Nantucket Shoals	0	0.000	0 - 0	302,025	0.000
Shelf South of Cape Hatteras	0	0.000	0 - 0	105,500	0.000
Sounds of NY, RI, and MA	0	0.000	0 - 0	8,600	0.000
Total	885	0.557	320 - 2,452	1,273,425	0.070

5.2 Abundance Comparisons

5.2.1 NOAA Stock Assessment Report

Table 25: Comparison of regional abundance estimates from the 2019 NOAA Stock Assessment Report (SAR) (Hayes et al. (2020)) to estimates from this density model extracted from roughly comparable zones (Figure 57 below). The SAR estimates were based on a single year of surveying, while the model estimates were taken from the multi-year mean density surfaces we provide to model users (Section 5.1).

2021 Stock Assessment Report			Density Model		
Month/Year	Area	N_{est}	Period	Zone	Abundance
Jun-Aug 2016	Central Virginia to lower Bay of Fundy[a]	160	Jan-Dec 1998-2020	NEFSC	387
Jun-Aug 2016	Florida to central Virginia[b]	3,942	Jan-Dec 1998-2020	SEFSC	419
Jun-Aug 2016			Jan-Dec 1998-2020	Canada	74
Jun-Aug 2016	Total	4,102	Jan-Dec 1998-2020	Total	880

[a] Estimate originally from Palka (2020).
[b] Estimate originally from Garrison (2020).

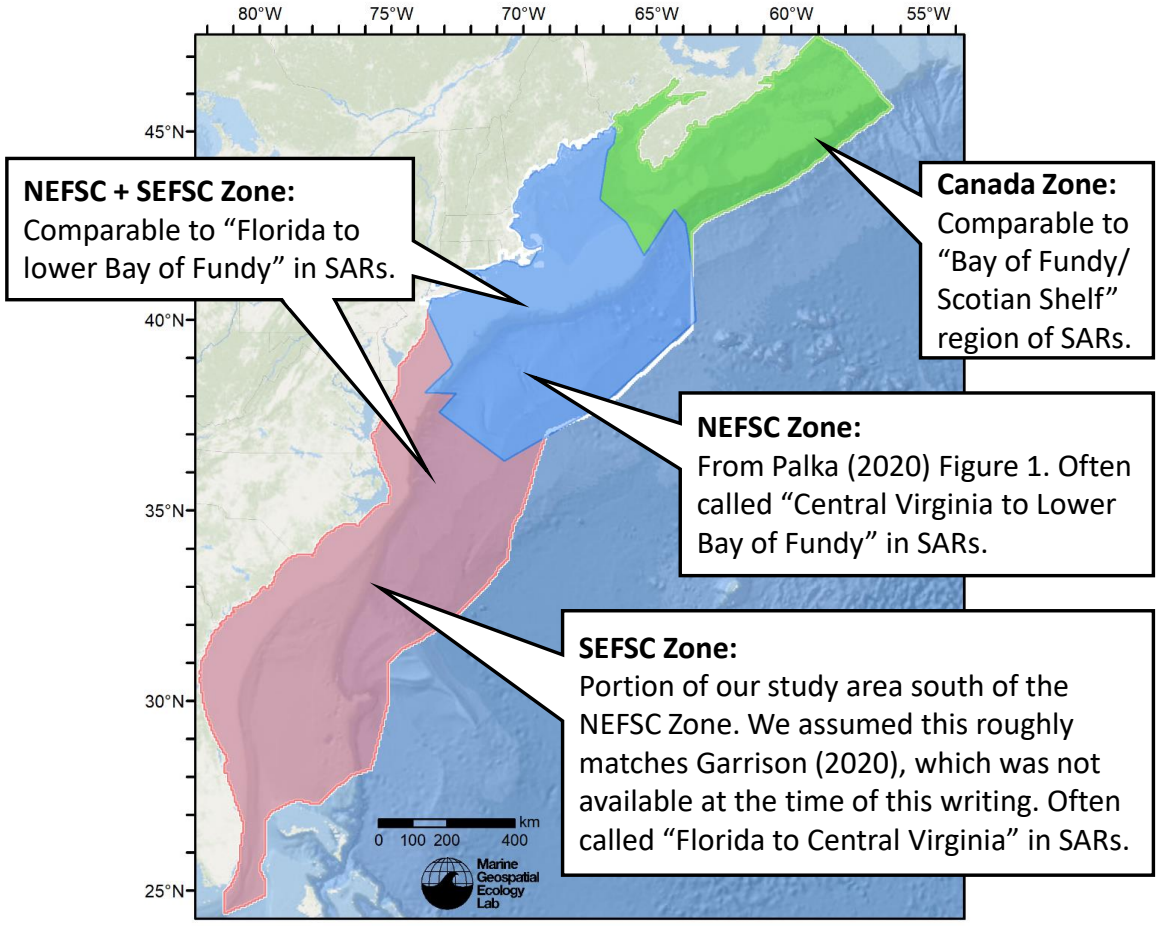

Figure 57: Zones for which we extracted abundance estimates from the density model for comparison to estimates from the NOAA Stock Assessment Report.

5.2.2 Previous Density Model

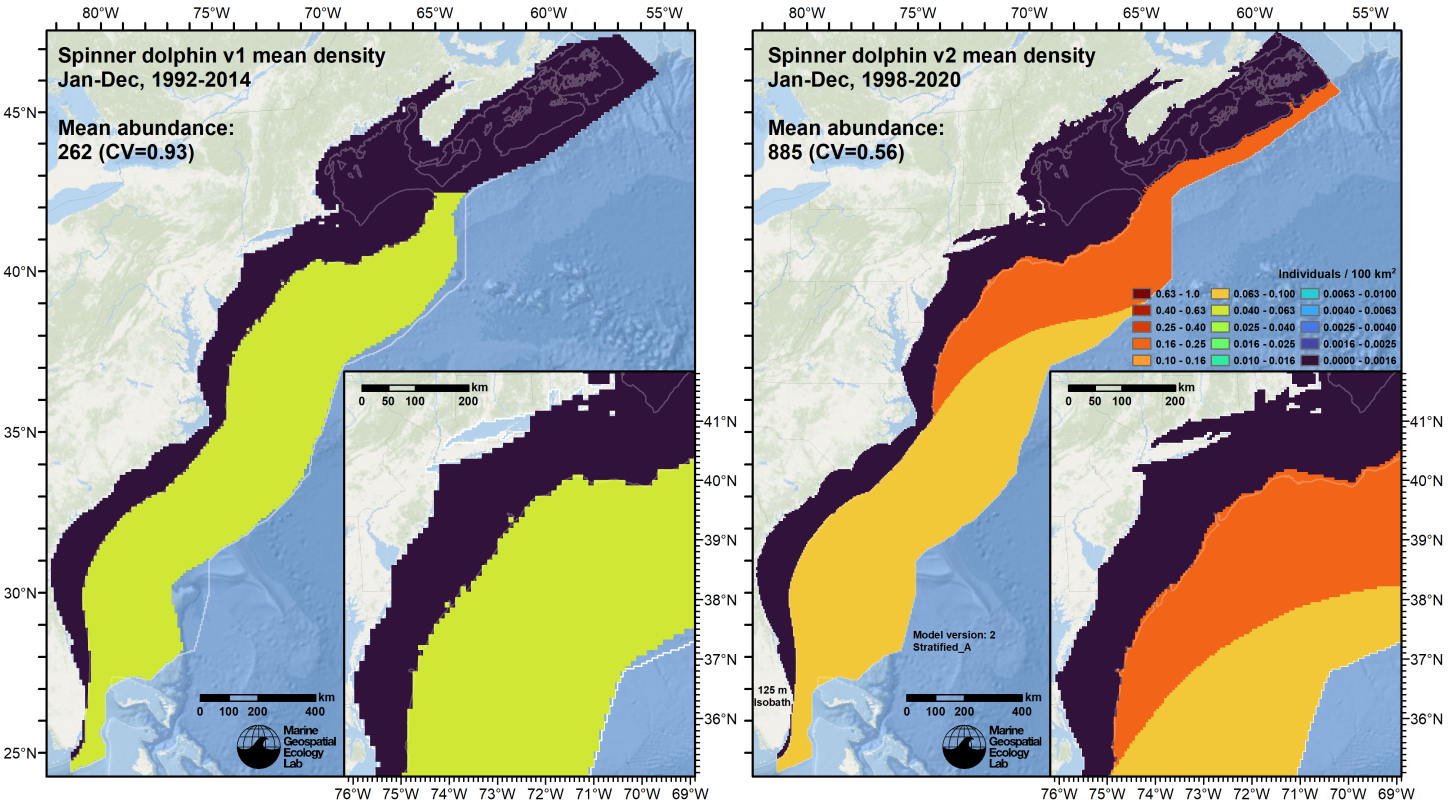

Figure 58: Comparison of the mean density predictions from the previous model (left) released by Roberts et al. (2016) to those from this model (right).

6 Discussion

Worldwide, the spinner dolphin occurs in both oceanic and coastal tropical waters. Presumably an offshore, deep-water species, its distribution in the Atlantic is very poorly known (Hayes et al. 2020).

In our east coast study area, the collaborators only reported five on-effort sightings over the analyzed period of 1998-2020. With insufficient sightings to model density from environmental predictors, we estimated density in six geographic strata with a simplified approach (Section 4). All of the sightings occurred in the two offshore strata, yielding a total abundance estimate of 885. The 2019 NOAA Stock Assessment Report previously estimated an abundance of 4102 from the 2016 AMAPPS campaign (Table 25). While NOAA's estimate was much higher than ours, we note that the 2019 SAR was the first SAR to ever provide an abundance estimate for the species, owing to the lack of sightings during earlier broad-scale survey campaigns. Given that we included all of NOAA's surveys back to 1998, we are not surprised that our multi-year estimate is lower than NOAA's the single year of 2016. However, we must reiterate that our stratified modeling approach does not fully correct for the heterogeneous distribution of sampling effort in space in time, which could have biased our abundance estimate (see Section 4).

Our new model estimated over three times higher abundance than our prior model (Figure 58); we attribute the larger abundance mainly to the increased number of sightings. Also, in our prior model, from the 2016 modeling cycle, we limited the extent of the zone for which the species was assumed to be present to waters south of 42 °N, on the basis of the northernmost known sightings (which were not utilizable in our model) occurring close to this latitude (Roberts et al. 2016). In the 2022 modeling cycle, we removed this limitation, allowing predictions to occur along the edge of the Scotian Shelf, based on evidence that odontocete distributions are shifting north in response to ocean warming in the region (Thorne et al. 2022). This decision should be considered speculative and precautionary until further surveying is conducted off the Scotian Shelf to better elucidate species distributions there. In any case, we anticipate the spinner dolphin will remain overall a rare inhabitant of our study area.

References

Barco SG, Burt L, DePerte A, Digiovanni R Jr. (2015) Marine Mammal and Sea Turtle Sightings in the Vicinity of the Maryland Wind Energy Area July 2013-June 2015, VAQF Scientific Report #2015-06. Virginia Aquarium & Marine Science Center Foundation, Virginia Beach, VA

Barlow J, Forney KA (2007) Abundance and population density of cetaceans in the California Current ecosystem. Fishery Bulletin 105:509–526.

Buckland ST, Anderson DR, Burnham KP, Laake JL, Borchers DL, Thomas L (2001) Introduction to Distance Sampling: Estimating Abundance of Biological Populations. Oxford University Press, Oxford, UK

Burt ML, Borchers DL, Jenkins KJ, Marques TA (2014) Using mark-recapture distance sampling methods on line transect surveys. Methods in Ecology and Evolution 5:1180–1191. doi: 10.1111/2041-210X.12294

Carretta JV, Lowry MS, Stinchcomb CE, Lynn MS, E. CR (2000) Distribution and abundance of marine mammals at San Clemente Island and surrounding offshore waters: Results from aerial and ground surveys in 1998 and 1999. NOAA Administrative Report LJ-00-02. NOAA National Marine Fisheries Service, Southwest Fisheries Center, La Jolla, CA

Cole T, Gerrior P, Merrick RL (2007) Methodologies of the NOAA National Marine Fisheries Service Aerial Survey Program for Right Whales (Eubalaena glacialis) in the Northeast U.S., 1998-2006. U.S. Department of Commerce, Woods Hole, MA

Cotter MP (2019) Aerial Surveys for Protected Marine Species in the Norfolk Canyon Region: 2018–2019 Final Report. HDR, Inc., Virginia Beach, VA

Foley HJ, Paxton CGM, McAlarney RJ, Pabst DA, Read AJ (2019) Occurrence, Distribution, and Density of Protected Species in the Jacksonville, Florida, Atlantic Fleet Training and Testing (AFTT) Study Area. Duke University Marine Lab, Beaufort, NC

Garrison LP (2020) Abundance of cetaceans along the southeast U.S. East coast from a summer 2016 vessel survey. PRD Contribution # PRD-2020-04. NOAA National Marine Fisheries Service, Southeast Fisheries Science Center, Miami, FL

Garrison LP, Martinez A, Maze-Foley K (2010) Habitat and abundance of cetaceans in Atlantic Ocean continental slope waters off the eastern USA. Journal of Cetacean Research and Management 11:267–277.

Geo-Marine, Inc. (2010) New Jersey Department of Environmental Protection Baseline Studies Final Report Volume III: Marine Mammal and Sea Turtle Studies. Geo-Marine, Inc., Plano, TX

Hayes SA, Josephson E, Maze-Foley K, Rosel PE, Byrd B, Chavez-Rosales S, Cole TV, Garrison LP, Hatch J, Henry A, Horstman SC, Litz J, Lyssikatos MC, Mullin KD, Orphanides C, Pace RM, Palka DL, Powell J, Wenzel FW (2020) US Atlantic and Gulf of Mexico Marine Mammal Stock Assessments - 2019. NOAA National Marine Fisheries Service, Northeast Fisheries Science Center, Woods Hole, MA

Laake JL, Calambokidis J, Osmek SD, Rugh DJ (1997) Probability of Detecting Harbor Porpoise From Aerial Surveys: Estimating g(0). Journal of Wildlife Management 61:63–75. doi: 10.2307/3802415

Mallette SD, Lockhart GG, McAlarney RJ, Cummings EW, McLellan WA, Pabst DA, Barco SG (2014) Documenting Whale Migration off Virginia's Coast for Use in Marine Spatial Planning: Aerial and Vessel Surveys in the Proximity of the Virginia Wind Energy Area (VA WEA), VAQF Scientific Report 2014-08. Virginia Aquarium & Marine Science Center Foundation, Virginia Beach, VA

Mallette SD, Lockhart GG, McAlarney RJ, Cummings EW, McLellan WA, Pabst DA, Barco SG (2015) Documenting Whale Migration off Virginia's Coast for Use in Marine Spatial Planning: Aerial Surveys in the Proximity of the Virginia Wind Energy Area (VA WEA) Survey/Reporting Period: May 2014 - December 2014, VAQF Scientific Report 2015-02. Virginia Aquarium & Marine Science Center Foundation, Virginia Beach, VA

Mallette SD, McAlarney RJ, Lockhart GG, Cummings EW, Pabst DA, McLellan WA, Barco SG (2017) Aerial Survey Baseline Monitoring in the Continental Shelf Region of the VACAPES OPAREA: 2016 Annual Progress Report. Virginia Aquarium & Marine Science Center Foundation, Virginia Beach, VA

Marsh H, Sinclair DF (1989) Correcting for Visibility Bias in Strip Transect Aerial Surveys of Aquatic Fauna. The Journal of Wildlife Management 53:1017. doi: 10.2307/3809604

McAlarney R, Cummings E, McLellan W, Pabst A (2018) Aerial Surveys for Protected Marine Species in the Norfolk Canyon Region: 2017 Annual Progress Report. University of North Carolina Wilmington, Wilmington, NC

McLellan WA, McAlarney RJ, Cummings EW, Read AJ, Paxton CGM, Bell JT, Pabst DA (2018) Distribution and abundance of beaked whales (Family Ziphiidae) Off Cape Hatteras, North Carolina, U.S.A. Marine Mammal Science. doi: 10.1111/mms.12500

Mullin KD, Fulling GL (2003) Abundance of cetaceans in the southern U.S. North Atlantic Ocean during summer 1998. Fishery Bulletin 101:603–613.

Palka D (2020) Cetacean Abundance in the US Northwestern Atlantic Ocean Summer 2016. Northeast Fish Sci Cent Ref Doc. 20-05. NOAA National Marine Fisheries Service, Northeast Fisheries Science Center, Woods Hole, MA

Palka D, Aichinger Dias L, Broughton E, Chavez-Rosales S, Cholewiak D, Davis G, DeAngelis A, Garrison L, Haas H, Hatch J, Hyde K, Jech M, Josephson E, Mueller-Brennan L, Orphanides C, Pegg N, Sasso C, Sigourney D, Soldevilla M, Walsh H (2021) Atlantic Marine Assessment Program for Protected Species: FY15 – FY19 (OCS Study BOEM 2021-051). U.S. Deptartment of the Interior, Bureau of Ocean Energy Management, Washington, DC

Palka DL (2006) Summer abundance estimates of cetaceans in US North Atlantic navy operating areas (NEFSC Reference Document 06-03). U.S. Department of Commerce, Northeast Fisheries Science Center, Woods Hole, MA

Palka DL, Chavez-Rosales S, Josephson E, Cholewiak D, Haas HL, Garrison L, Jones M, Sigourney D, Waring G, Jech M, Broughton E, Soldevilla M, Davis G, DeAngelis A, Sasso CR, Winton MV, Smolowitz RJ, Fay G, LaBrecque E, Leiness JB, Dettloff K, Warden M, Murray K, Orphanides C (2017) Atlantic Marine Assessment Program for Protected Species: 2010-2014 (OCS Study BOEM 2017-071). U.S. Deptartment of the Interior, Bureau of Ocean Energy Management, Washington, DC

Read AJ, Barco S, Bell J, Borchers DL, Burt ML, Cummings EW, Dunn J, Fougeres EM, Hazen L, Hodge LEW, Laura A-M, McAlarney RJ, Peter N, Pabst DA, Paxton CGM, Schneider SZ, Urian KW, Waples DM, McLellan WA (2014) Occurrence, distribution and abundance of cetaceans in Onslow Bay, North Carolina, USA. Journal of Cetacean Research and Management 14:23–35.

Roberts JJ, Best BD, Mannocci L, Fujioka E, Halpin PN, Palka DL, Garrison LP, Mullin KD, Cole TVN, Khan CB, McLellan WA, Pabst DA, Lockhart GG (2016) Habitat-based cetacean density models for the U.S. Atlantic and Gulf of Mexico. Scientific Reports 6:22615. doi: 10.1038/srep22615

Roberts JJ, Yack TM, Halpin PN (2023) Marine mammal density models for the U.S. Navy Atlantic Fleet Training and Testing (AFTT) study area for the Phase IV Navy Marine Species Density Database (NMSDD), Document Version 1.3. Duke University Marine Geospatial Ecology Lab, Durham, NC

Ryan C, Boisseau O, Cucknell A, Romagosa M, Moscrop A, McLanaghan R (2013) Final report for trans-Atlantic research passages between the UK and USA via the Azores and Iceland, conducted from R/V Song of the Whale 26 March to 28 September 2012. Marine Conservation Research International, Essex, UK

Schick R, Halpin P, Read A, Urban D, Best B, Good C, Roberts J, LaBrecque E, Dunn C, Garrison L, Hyrenbach K, McLellan W, Pabst D, Palka D, Stevick P (2011) Community structure in pelagic marine mammals at large spatial scales. Marine Ecology Progress Series 434:165–181. doi: 10.3354/meps09183

Thorne LH, Heywood EI, Hirtle NO (2022) Rapid restructuring of the odontocete community in an ocean warming hotspot. Global Change Biology gcb.16382. doi: 10.1111/gcb.16382

Torres LG, Mclellan WA, Meagher E, Pabst DA (2005) Seasonal distribution and relative abundance of bottlenose dolphins, Tursiops truncatus, along the US mid-Atlantic coast. Journal of Cetacean Research and Management 7:153.

Whitt AD, Powell JA, Richardson AG, Bosyk JR (2015) Abundance and distribution of marine mammals in nearshore waters off New Jersey, USA. Journal of Cetacean Research and Management 15:45–59.